THE POTENTIAL ROLE OF ERK1/2 MAP KINASES IN THE REGULATION OF NEUROMUSCULAR JUNCTION INTEGRITY AND BONE MORPHOGENETIC PROTEIN SIGNALING

A Dissertation

by

SHUO WANG

Submitted to the Office of Graduate and Professional Studies of
Texas A&M University
in partial fulfillment of the requirements for the degree of

DOCTOR OF PHILOSOPHY

Chair of Committee,	Mendell Rimer
Committee Members,	Rajesh C. Miranda
	Wesley Thompson
	Mark Harlow
Head of Program,	Warren Zimmer

May 2018

Major Subject: Biomedical Sciences

ABSTRACT

It is known that extracellular signal-regulated kinases 1 and 2 (ERK1/2) play important roles in development and maintenance of skeletal muscles *in vitro* and *in vivo*. However, it is not clear whether muscle ERK1/2 can regulate neuromuscular junction (NMJ) structure and function and (or) have unique substrates and downstream pathways in skeletal muscle. Previously, we generated an ERK 1/2 double knockout (DKO) mouse line using germ line *Erk1* mutation and *Cre-loxP* deletion of *Erk2*. Those DKO animals were viable after birth but displayed stunted postnatal growth, muscle weakness, and shorter lifespan. Next, two typical fast-twitch muscles, the sternomastoid (STN) and the tibialis anterior (TA), were examined. A mixture of fiber loss and mild muscle atrophy was found, and STN but not TA underwent partial denervation. To explore the role of ERK1/2 in slow-twitch, type 1 muscle fibers, we studied the mutant soleus muscle (SOL) in the aspect of morphology, expression of denervation and synaptic markers, and mitochondrial function. Next, we examined the status of bone morphogenetic (BMP) signaling in mutant SOL and myotubes by measuring mRNA and phosphorylation level of several BMP components.

It is shown that young adult mutant SOL was drastically wasted, with highly atrophied type 1 fibers, denervation at most synaptic sites, induction of "fetal" acetylcholine receptor (AChRγ) subunit, reduction of "adult" AChRε subunit, and impaired mitochondrial function. In weanlings, fiber morphology and mitochondrial markers were normal, yet AChRγ upregulation and AChRε downregulation were

observed. In mutant weanlings, most of the fetal AChRs appeared at NMJs on type1 muscle fibers. These results suggest that: (1) ERK1/2 are critical for slow-twitch fiber growth; (2) a defective γ/ε-AChR subunit switch, preferentially at synapses on slow fibers, precedes denervation and wasting of mutant SOL; (3) the neuromuscular synapse is a primary subcellular target for muscle ERK1/2 function *in vivo*.

It is shown that mutant SOL exhibited alterations in the BMP pathway: decreased expression of *Bmpr1b*, unchanged expression of the target gene *Id-1*, the negative regulator *Noggin* and the intracellular kinase *Smad6*, and unchanged phosphorylation level of Smad1/5/8. These experiments suggest that unlike normal muscle, BMP signaling is not activated in mutant SOL after denervation. However, *Bmpr1b* expression and Smad1/5/8 phosphorylation were not altered in BMP-treated myotubes subjected to pharmacological inhibition of ERK1/2 activation. These results suggest that ERK1/2 regulate BMP signaling in SOL through an indirect mechanism.

ACKNOWLEDGEMENTS

I would like to thank my committee chair, Dr. Mendell Rimer, and my committee members, Dr. Miranda, Dr. Thompson, Dr. Harlow for their guidance and support throughout the course of this research.

Thanks also go to my friends and colleagues and the department faculty and staff for making my time at Texas A&M University a great experience.

Finally, thanks to my mother and father for their encouragement and to my wife for her patience and love.

CONTRIBUTORS AND FUNDING SOURCES

Contributors

This work was supervised by a thesis (or) dissertation committee consisting of Professors Mendell Rimer and Rajesh C. Miranda of the Department of Neuroscience and Experimental Therapeutics and Professors Wesley Thompson and Mark Harlow of the Department

All work for the thesis (or) dissertation was completed by the student, under the advisement of Mendell Rimer of the Department of Neuroscience and Experimental Therapeutics.

Funding Sources

This work was made possible in part by NIH under Grant Number R21NS077177.

ABBREVIATIONS

αBTX	α-Bungarotoxin
AChE	Acetylcholinesterase
AChR	Acetylcholine Receptor
AD	Alzheimer's Diseases
ALS	Amyotrophic Lateral Sclerosis
ARIA	Acetylcholine Receptor Inducing Activity
BDNF	Brain-Derived Neurotrophic Factor
BMK1	Big Mitogen-activated Protein Kinase 1
BMP	Bone Morphogenetic Protein
CNS	Central Nervous System
DGC	Dystrophin Glycoprotein Complex
DMD	Duchenne Muscular Dystrophy
DKO	Double Knockout
4EBP1	4E-Binding Protein 1
ECM	Extracellular Matrix
EDMD	Autosomal Emery-Dreifuss Muscular Dystrophy
EGF	Epidermal Growth Factor
EIF4E	Eukaryotic translation Initiation Factor 4E
ERK1/2	Extracellular Signal-Regulated Protein Kinase 1 and 2
FGF	Fibroblast Growth Factor

GABP	GA-Binding Protein
GDF	Growth Differentiation Factor
GDNF	Glial Derived-Neurotrophic Factor
GEF	RasGTPase Exchange Factor
GRB2	Growth factor Receptor-Bound protein 2
HD	Huntington Diseases
HDAC4	Histone Deacetylase 4
HGF	Hepatocyte Growth Factor
HNC	polypeptide Hormone Neurotransmitter and Chemokine
IGF	Insulin-like Growth Factor
JNK	c-Jun N-terminal Kinases
LMNA	Lamin A/C gene
LRP4	Low-density lipoprotein Receptor-related Protein 4
LTD	Long Term Depression
LS	Leopard Syndrome
LTP	Long Term Potentiation
MAPKs	Mitogen-Activated Protein Kinases
MEK	Mitogen-activated protein kinase Kinase
MHC	Myosin Heavy Chain
mTOR	Mechanistic Target Of Rapamycin
MuSK	Muscle-Specific Kinase
NFAT3	Nuclear Factor of Activated T-cells 3

NMJ	Neuromuscular Junction
PDGF	Platelet-derived Growth Factor
PEA3	Polyomavirus Enhancer Activator 3
PI3K	Phosphoinositide 3-Kinase
PKB	Protein Kinase B
PTEN	Phosphatase and Tensin homolog
PTPN11	Tyrosine-Protein Phosphatase Non-receptor type 11
RSK2	Ribosomal S6 Kinase 2
RTK	Receptor Tyrosine Kinase
SH2	Src Homology 2
SMA	Spinal Muscular Atrophy
SMN	Survival Motor Neuron
SOD1	Superoxide Dismutase 1
SOL	Soleus
SOS	Son of Sevenless
STN	Sternomastoid
TA	Tibialis Anterior
TGFβ	Transforming growth factorβ
tSC	terminal Schwann Cell

TABLE OF CONTENTS

Page

LIST OF FIGURES

Page

LIST OF TABLES

Page

CHAPTER I

INTRODUCTION

1.1 Overview

The Neuromuscular Junction (NMJ) is a specific synapse formed by a tripartite cellular structure in the peripheral nervous system: the nerve terminal of motor neurons, the skeletal muscle fiber cell membrane (a.k.a. sarcolemma) and surrounding terminal Schwann cells[1]. When an action potential arrives to the presynaptic terminal of motor neurons, the voltage-dependent calcium channels open and the influx calcium binds to Synaptotagmin, triggering neurotransmitter release into the synaptic cleft. Next, the NMJ-specific neurotransmitter, acetylcholine (ACh), binds to nicotinic acetylcholine receptors (nAChRs) on the sarcolemma and induces depolarization of the muscle fiber, causing a cascade that eventually leads to muscle contraction[1]. Neurotransmission is terminated by the hydrolysis of ACh by the enzyme acetylcholinesterase (AChE), which accumulates in the synaptic cleft, the extracellular space between the presynaptic terminal and the postsynaptic membrane. The NMJ develops, functions and is maintained by numerous small molecules. For example, the binding of Agrin (a proteoglycan, secreted from nerve terminal) to LRP4 (low-density lipoprotein receptor-related protein 4) and Musk (the muscle-specific kinase, residing on the sarcolemma) initiates the formation of acetylcholine receptors (AchR) clusters [2]; the proteins in the active zone (the site of ACh release) keep synaptic vesicles in place nearby the presynaptic membrane and mediate synaptic vesicle fusion[3]. Dysfunction of any of those

"synaptic molecules" can impair the integrity of the NMJ and eventually cause neuromuscular disease.

Neuromuscular disease (NMD) is a very comprehensive term that includes many illnesses that impair the functional ability of muscles caused by either direct pathology of muscle or indirect pathology of nerve. In the latter situation, some diseases are derived from the central nervous system in the brain, such as Parkinson's disease, Huntington's disease. Some disorders have lower motor neuron problems, such as Spinal Muscular Atrophy. The remaining are mixed upper and lower motoneuron problems, like Amyotrophic Lateral Sclerosis (a.k.a. Lou Gehrig's disease).

On the other hand, many muscle disorders induce NMD as well. Acquired myasthenia gravis is an NMD caused by auto-immune responses to the acetylcholine receptor (AChR), which binds to neurotransmitter acetylcholine at neuromuscular junctions (NMJs) [4]. In Duchenne's and Becker's muscular dystrophy, patients genetically lose the ability to produce normal dystrophin, a sizable rod-like protein that maintains the stability of the sarcolemma and NMJs[5].These diseases have relatively clear pathological mechanisms while others do not. The lamins are a group of proteins that are components of the nuclear envelope. Emery–Dreifuss muscular dystrophy is an NMD caused by mutation of these genes. The nuclear envelope regulates the movement of many molecules in and out of nuclei, which is important for the activity of many cell signaling pathways. For example, the Ras-Extracellular signal-Regulated Kinase 1 and 2 (ERK1/2) pathway is dysregulated in the autosomal type of Emery–Dreifuss muscular dystrophy[6], however, the correlation between Ras-ERK dysregulation in muscle and

pathology of the disease is largely unknown. Rasopathies, rare syndromes of genetic origin with accompanying skeletal muscle abnormalities, are caused by germline mutation of genes that alter Ras-ERK pathways[7].

Mitogen-Activated Protein Kinases (MAPKs), a group of intracellular signaling pathways, control multiple biological processes, including cellular proliferation, differentiation, apoptosis, adhesion, etc.[8] Each MAPK pathway contains a three-tiered kinase cascade: a MAPK Kinase Kinase (MAP3Ks), a MAPK Kinase (MAP2Ks) and a MAPK[8]. Extracellular signal-Regulated Kinase1 and 2 (ERK1/2) is one member of this family and respond to several growth factors and are activated through Ras-Raf (MAP3Ks) - MEK1/2(MAP2Ks)-ERK1/2(MAPK) cascade[9]. ERK1/2 can either translocate into the nucleus and phosphorylate substrates, like transcriptional factors, or activate other substrates within the cytosol[10].

It has been known that ERK1/2 play important roles in development and maintenance of skeletal muscles. In cell culture, ERK 1/2 is implicated in the regulation of myoblast proliferation[11], and ERK2 is reported to promote myocyte fusion and survival[12]. Work from the Rimer lab showed that ERK 1/2 seem to be in a feedback loop that suppresses AChR clustering induced by the proteoglycan Agrin[13]. Besides, it has been shown that ERK1/2 maintain skeletal muscle mass in adults[14] and control both the slow-twitch (a.k.a. type1) [15] and fast-twitch muscle fiber phenotypes (a.k.a. type2) [16].

However, it is not clear whether muscle ERK1/2 can interact with specific synaptic molecules and eventually regulate NMJ function just like dystrophin. In addition, ERK1/2 is a universally expressed protein kinase in mammalian cells but may

have unique features and functions in skeletal muscle. Until now, no muscle-specific ERK1/2 substrate and pathway have been identified. Lastly, in terms of disease, the exact mechanism of the correlation between dysfunction of ERK1/2 and the pathology of Emery–Dreifuss muscular dystrophy and Rasopathies related muscle atrophy is not fully understood.

To begin answering those questions, previously[17], for the first time, we generated an ERK 1/2 double knockout (DKO) mouse line using germ line *Erk1* mutation and Cre-loxP deletion of *Erk2*. Those DKO animals were viable after-birth but displayed stunted postnatal growth, muscle weakness, and shorter lifespan. Next, two typical fast twitch muscles, the sternomastoid (STN) and the tibialis anterior (TA), were examined at 9-14 weeks of age. A mixture of fiber loss and mild muscle atrophy was found with minimal changes in fiber type composition. In STN, but not TA, terminal axonal sprouting and upregulation of the fetal AChR γ-subunit mRNA were seen, documenting evidence of partial denervation. In addition, NMJs in both mutant muscles showed fragmentation.

In chapter II, we continue studying the phenotype in ERK1/2 DKO Soleus (SOL), a typical slow twitch muscle. Young adult mutant soleus was drastically wasted, with highly atrophied type 1 fIbers, denervation at most synaptic sites, induction of "fetal" AChRγ, reduction of "adult" AChRε, and impaired mitochondrial biogenesis and function. In weanlings, fiber morphology and mitochondrial markers were mostly normal, yet AChRγ upregulation and AChRε downregulation were observed. Synaptic sites with fetal AChRs in weanling muscle were ~3% in control and ~40% in mutants, with most of the latter on type 1 fibers. These results suggest that: (1) ERK1/2 are

critical for slow-twitch fiber growth; (2) a defective γ/ε-AChR subunit switch, preferentially at synapses on slow fibers, precedes wasting of mutant soleus; (3) denervation is likely to drive this wasting, and (4) the neuromuscular synapse is a primary subcellular target for muscle ERK1/2 function in vivo.

BMP signaling is activated after nerve transection-induced denervation[18], and we found ERK1/2 DKO SOL has the cardinal signs of denervation. In chapter III, we examined the status of BMP signaling in ERK1/2 DKO SOL. We found increased expression of *Gdf5 (a.k.a. BMP14), Gdf6 (a.k.a. BMP13),* decreased expression of *Bmpr1b,* unchanged expression of *Id-1*, *Noggin* and *Smad6,* and unchanged phosphorylation level of Smad1/5/8 in ERK1/2 DKO SOL. However, *Bmpr1b* expression and Smad1/5/8 phosphorylation were not altered in BMP-treated myotubes subjected to pharmacological inhibition of ERK1/2 activation. We conclude that: (1) ERK1/ 2 regulate denervation induced- BMP signaling activation in skeletal muscle, at least in SOL; (2) Reduced expression of *Bmpr1b*, unchanged expression of *Noggin* and *Smad6,* are potential factors that account for inefficient BMP activation in ERK1/2 DKO skeletal muscle; (3) ERK1/2-regulated BMP activation probably depends on changes of ERK1/2 downstream gene expression rather than direct interaction through kinase activity.

1.2 NMJ

1.2.1 Structure, function and development

As early as 19th century, after he examined many species, Wilhelm Friedrich Kühne firstly described NMJ as the communication site between motor neurons and

multinucleated muscle cells, myofibers[19] He proposed the function of NMJ is to transmit signals from nerve to skeletal muscle[20]. Motor neurons, skeletal muscle fibers, and terminal Schwann cells (tSC) are the three major components of NMJ and kranocytes is probably the fourth component at NMJ[20, 21] (also see Fig 1.1). At the NMJ of an adult, each myofiber is only innervated by one motor axon. However, axonal branching from a single motor neuron can innervate multiple myofibers. This motor neuron and all the myofibers it innervates are called one motor unit[22]. The terminal Schwann cells surround the nerve terminal tightly and are considered to be critical to many aspects of NMJ, such as formation, regeneration, synaptic transmission and long-term maintenance[20, 23, 24]. The nerve terminal usually becomes larger for neurotransmitter release. The synaptic vesicle is tiny lipid layer structure that contains neurotransmitter inside[25]. Many synaptic vesicles tethering firmly to the surface of the presynaptic membrane along with concentrated proteins related to neurotransmitter release is named active zone. The postsynaptic membrane, or so-called Sarcolemma, folds up and down to increase the surface, tightly aligns with presynaptic terminals, positions directly across the active zones and has most of their neurotransmitter receptors at the crests, allowing for efficient synaptic transmission[19]. The space between presynaptic terminal and sarcolemma is the synaptic cleft, which contains numerous synaptic molecules that facilitate NMJ function, such as AChE[26].

Sir Henry Hallett Dale in 1914 discovered the first neurotransmitter ACh, which is the dominant neurotransmitter type at vertebrate'NMJs[27]. When synaptic transmission happens, voltage-gated calcium channels sense the action potential at nerve terminal and

open for calcium influx. The high concentration of calcium in cytoplasm triggers synaptic vesicle fusion onto the presynaptic membrane and eventually neurotransmission release (Ach) through exocytosis[20]. The neurotransmitter receptors on the postsynaptic membrane at NMJ are classified as nicotinic, but they actually bind nicotine very weakly[28].They bind strongly to components of certain types of snake venom, such as a-bungarotoxin (BTX). The skeletal muscle AChR is a heteropentamer that contains 2 α, 1β, 1γ and 1δ subunits (In an adult, the γ subunit will be gradually replaced by the ε subunit[29]). ACh binds to the α subunits at their interfaces with neighboring γ (ε) and δ subunits, allowing for a short opening time of the cation channel and the influx of sodium[30].

This cation flow generates "synaptic potential," followed by a series of reactions and eventually leads to muscle contraction. Again, the normal function of NMJ is ensured by the specialized structure at both pre and post-synaptic membrane: (1) enlarged nerve terminal contains enough synaptic vesicle within the active zone: (2) the dense AChR clustering reside on the crest of "junction folds" and align with the active zone.

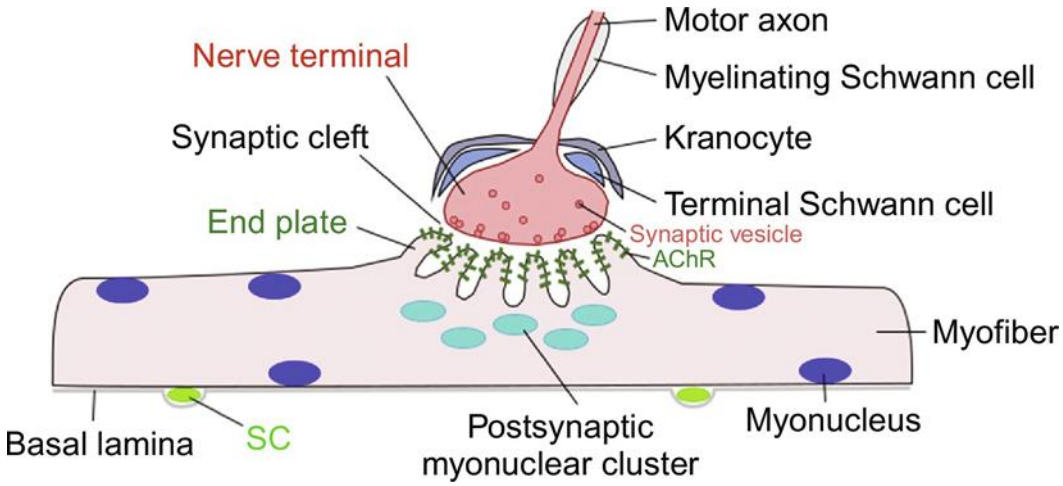

Figure 1.1. Cellular components of an NMJ.
The NMJ is comprised of three elements: presynaptic motor nerve terminal, postsynaptic membrane (sarcolemma) and terminal Schwann cells. Kranocytes, the possible forth component at NMJ, is also shown. Adapted with permission from Current Topics in Developmental Biology by Wenxuan Liu,Joe V. Chakkalakal, 2018, Elsevier, Amsterdam, Netherlands. Copyright [2018] by Elsevier[159].

How does the skeletal muscle get innervated? Before the motor axon arrives, primitive AChR clusters appear in the central region of myotubes in a nerve-independent manner known as pre-patterning. This muscle self-regulation process suggests that muscle have a vital role in the initial development of NMJs[31]. Motor axons reach some, of the pre-patterned AChR clusters and innervate them but also generate other AChR clusters *de novo*. Then the innervated clusters become large while the un-innervated ones eventually disappear[32]. In the beginning, these immature AChR clusters are multi-innervated by motor axons. Later, the redundant axonal input will be removed by a process called synaptic elimination[33] so that each myofiber is innervated by only one axon. As the NMJ becomes mature, the postsynaptic membrane invaginates to create junctional folds where AChRs begin to accumulate. As a result, NMJ is shaped from a

"plaque" like look to a typical "pretzel" like appearance[34]. Certainly, AChR complete subunit composition changes at the same period. Remarkably, the density of AChR in the synaptic regions increase from 1000/ μm^2 to 10000/ μm^2 and that in the extra-synaptic sites drop to as low as < 10/μm^2. This postsynaptic AChR rearrangement largely depends on the key molecular mechanism: the agrin – Lrp4 - Musk axis. Agrin, a proteoglycan, is secreted mostly by the motor neurons and crucial for stabilizing and redistributing AChR clusters at synaptic domains[35]. The binding of neuronal agrin to the transmembrane protein Lrp4 activates the Muscle specific kinase, Musk[36, 37]. Then active Musk results in AChR clustering at the synaptic sites through Rapsyn, a peripheral membrane protein that binds both to cytoskeletal proteins and AChRs [38]. Conversely, ACh induces depolarization of the myofibers, suppressing AChR gene expression and speeding up AChR degradation in other regions of the myofiber[39, 40]. During NMJ maturation, the presynaptic terminal changes as well. Active zone's numbers increases and the density of neurotransmission-related protein goes up. This presynaptic differentiation is partly induced by the "retrograde signals" from myofibers. For example, some types of fibroblast growth factors (e.g., FGF7) participate in synaptic vesicle accumulation and presynaptic differentiation[41]. Glial cell-derived neurotrophic factor (GDNF) and brain-derived neurotrophic factor (BDNF) also mediate presynaptic maturation and synapse elimination[42, 43]. Furthermore, tSC secretes molecules such as transforming growth factor β (TGFβ) to promote NMJ maturation[44]. Lastly, Lrp4, the critical transmembrane protein for postsynaptic AChR clustering, is also suggested to be

necessary for presynaptic differentiation by binding to motor axons and inducing clustering of synaptic-vesicle and active-zone proteins in a Musk independent manner[45].

1.2.2 Regeneration & muscle re-innervation

After peripheral nerve lesion, the distal end of axon undergoes a process called Wallerian degeneration. The cell membrane, cytoskeleton, and organelles of axon quickly disrupt and the myelin sheath peels off from the axon[46]. Next, the myelinating Schwan cells transform to a proliferative status, phagocytose axons/myelin debris and secrete cytokines/chemokines to recruit macrophages. The resident macrophages and recruited macrophages together clean the remaining myelin debris and produce molecules that assist axon regeneration[47]. Active Schwann cells form a cellular conduit named Bands of Büngner to provide guidance for axon regeneration and release neurotrophic factors to promote axon outgrowth as well[48, 49]. When the proximal axon grows closer to the distal end plate, terminal Schwann cells take over the job to continue to guide the axon until the targeted synaptic site is re-innervated[5]. The previously denervated synaptic site will be re-innervated by the regenerating axon when the damage is not severe; significant nerve injury could lead to re-innervation of a remodeled synaptic region[50]. Axons from the neighboring NMJs, growing on terminal Schwann cell processes, could extend to nearby denervated synaptic sites before the regenerating axon grows back. As a result, terminal Schwann cells facilitate nerve sprouting and reinnervation[23]. Lastly, kranocytes (a.k.a. NMJ-capping cells) exist outside the basal lamina but form caps over NMJs during synaptic development. These cells are believed

to be critical for muscle re-innervation, because they activate, proliferate and spread following denervation in advance of terminal Schwann cell sprouting[51].

It has been noticed that without myofibers, the regenerating NMJ could be maintained for a short period due to the presence of basal lamina. However, this NMJ eventually disappeared[52], suggesting muscle itself is important for regeneration and maintenance of NMJ. Besides, NMJ regeneration depends on appropriate signaling from skeletal muscle. For example, in the absence of muscle-derived microRNA-206, delayed re-innervation occurred after nerve injury[53]. It has been reported that muscle-derived GDNF facilitate NMJ regeneration by promoting the retrograde signals[42]. Satellite cells, the primary source for the nuclei of myofibers, are critical for skeletal muscle regeneration[54]. Recently, a study revealed that increased Satellite cell activity and fusion of Satellite cells to myofibers were observed nearby the regenerating NMJs. Furthermore, loss of Satellite cells results in defective NMJ re-innervation, abnormality in postsynaptic morphology, and reduced number of postsynaptic myonuclei, suggesting a role for Satellite cells in the regeneration of NMJs[55].

1.2.3 Maintenance

It is easy to understand that mutation of any NMJ component can lead to destabilization of NMJ and eventually degeneration[56]. Moreover, those scaffold proteins within muscle cytosol and extracellular matrix (ECM), such as dystrophin-glycoprotein complex, ensure NMJ stability, although they are not required for NMJ formation. For example, the absence of components of the complex, including α-syntrophin and α-dystrobrevin result in unstable NMJ[57], probably through increased AChR turnover[58]. As

we know, the agrin-Lrp4-Musk axis is required for NMJ formation[35-38]. It turns out Agrin signaling is also indispensable for the long-term maintenance of NMJ. For instance, NMJ stability was lost when Musk was knocked out in adult mice[59]. Moreover, ErbB kinases can maintain a high density of AChR attached to the synaptic sites by phosphorylating α-dystrobrevin 1[60]. Besides, muscarinic AChR and sympathetic inputs to the synapse appear also required for NMJ maintenance[61].

1.2.4 Example of neuromuscular diseases

The autoimmune disease myasthenia gravis is a neuromuscular disorder caused by an antibody against AChR and in rare cases, Agrin, MuSK, and Lrp4[62]. Suffering patients may have localized eye muscle weakness, impaired voluntary muscles movement. AChE inhibitors usually are involved in the treatment of myasthenia gravis to protect Ach from breakdown. In addition, immune-suppressors are also used[63].

Duchenne muscular dystrophy (DMD) is a progressive, severe myopathy induced by mutations in the DMD gene encoding the dystrophin protein[64]. Dystrophin is a main component of the dystrophin-glycoprotein complex (DGC), which provides mechanical strength at the plasma membrane[65]. Dystrophin-deficient muscle fibers have weak bonds that cause long-term accumulative injury, resulting in muscle dysfunction[66]. There is no cure for the DMD. Available medications in clinics include corticosteroids, other immune-suppressors[67]. However, they do not ultimately address its original cause[68]. Stem cell transplantation[69], gene delivery[70,] and genome editing[71] have been applied to research using different animal models in the pre-clinic stage, shedding light on the therapeutic strategy to this severe disease.

Besides to these muscle-derived neuromuscular diseases, alteration of structure and functional feature at NMJ can be observed in various disorders, such as those affecting motoneurons, including amyotrophic lateral sclerosis (ALS), characterized by progressive motor neuron death and atrophy of denervated muscles[72] and spinal muscular atrophy (SMA), a neuromuscular disease caused by mutations in the survival motor neuron gene (SMN)[73] ; disorders of the Schwann cells, including Charcot-Marie-Tooth disease and Guillain-Barre syndrome.

1.3 ERK1/2 pathway

1.3.1 Components, signal transduction & substrates

Protein kinases are one of the largest protein families in mammalian cells[74]. Dysfunction of protein kinases play key roles in human disease and a variety of drugs have been developed to target protein kinase for therapy. Belonging to serine and threonine protein kinases, mitogen-activated protein kinases (MAPKs) are composed of a family of protein kinases regulating a wide range of biological processes, including cell proliferation and differentiation, mitosis and meiosis, cell survival and apoptosis, and angiogenesis[75,76]. The traditional MAP kinase family comprise three subfamilies: extracellular signal-regulated kinase (ERK1/2, are mainly activated by growth factors), c-Jun N-terminal kinase (JNK1/2/3, are mainly induced by cellular stress) and p38-MAP kinase (α, β, δ, and γ). In addition, ERK5 (a.k.a. BMK1) is a relatively novel MAP kinase and can be activated by both growth factor and cellular stress[77]. Certainly, other MAP kinases exist[78-81]. However they are either not authentic MAP kinases or not within the MAP kinase cascade. The MAP kinase signaling has a three-tiered cascade: a MAP

kinase is activated by a MAP kinase kinase (MKK or MAP2K), which is in turn activated by a MAP kinase kinase kinase (MEKK or MAP3K) [82]. Until now, in mammalian cells, 12 MAP kinases, 7 MAP2Ks, and 20 MAP3Ks have been found.

ERK1 and ERK2 share 83% of the structure and the main difference is that ERK1 contains a 17-amino-acid-residue insertion in its N-terminal extension so as to provide signal specificity. However, the core protein kinase domains are identical in ERK1/2[83]. ERK1/2 is universally expressed in all tissue types. In the classical ERK activation (Fig 1.2), growth factors (such as Fibroblast growth factor, epidermal growth factor and platelet growth factor) bind receptor tyrosine kinase (RTK) to induce autophosphorylation of RTK's cytoplasmic domain, generating binding sites for the src homology 2 (SH2) domain of the GRB2 (Growth factor receptor-bound protein 2). GRB2 has two SH3 domains which recruit the Ras guanyl-nucleotide exchange factor (SOS) and the RasGTPase exchange factor (GEF) to the membrane. SOS catalyzes Ras GTP exchange and Ras-GTP then recruits Raf (the MAP3K) to the membrane, where it is phosphorylated[84]. In the *de novo* activation (Fig 1.2), polypeptide hormone neurotransmitter and chemokine (HNC) is able to activate protein Kinase C (PKC), which also promotes ERK activation[85]. Cell-permeable phorbol esters such as PMA bind and activate PKC by mimicking the natural PKC ligand diacylglycerol. The mechanism of PKC-activated ERK is not fully understood and could be through activation of SOS or Raf. Raf activates MEK (the MAP2K) and MEK activates ERK (the MAPK) via phosphorylation. ERK1/2 preferentially phosphorylates substrates that contain the consensus sequence Pro-Xaa-Ser/Thr-Pro[86]. Distinct signals induce activation of

ERK1/2, resulting in the phosphorylation of different substrates. For now, more than 150 substrates of ERK1/2 have been identified. These substrates can be classified as transcription factors, protein kinases, protein phosphatases, cytoskeletal proteins, scaffolding proteins, receptors, signaling molecules, apoptosis-related proteins, as well as other types of proteins[87] (also see Table 1.1).

1.3.2 ERK1/2 and neurological diseases

ERK1/2 have been suggested to have a crucial role in the regulation of physiological brain functions. Synaptic plasticity is essential to information processing in the brain and measurement of long-term potentiation (LTP) and long-term depression (LTD) is the best way to study synaptic plasticity. English and Sweatt firstly observed activation of ERK1/2 in rat hippocampal area CA1 after high-frequency stimulation, which can induce LTP[88]. Later, the role of ERK1/2 in NMDA receptor-independent LTP in the hippocampus was confirmed by Kanterewicz's group[89]. Considering ERK1/2 play a role in cell proliferation and differentiation, Samuels' group found that increased ERK1/2 activity can result in macrocephaly while decreased ERK1/2 activity can result in microcephaly, suggesting that the ERK1/2 regulate neural progenitor cells population[90]. In addition, it has been found ERK1/2 mediated the generation of astrocytes from radial progenitors in the developing cortex[91]. Furthermore, ERK1/2 pathway dominantly regulates oligodendrocyte differentiation and myelination[92, 93]. Experiments have suggested that ERK1/2 facilitate the inflammatory response in microglia[94] and astrocytes[95]. A variety of evidence indicates that by suppressing the

ERK1/2 pathway, many drugs can reduce neuroinflammation in stroke and intracranial infections[96, 97].

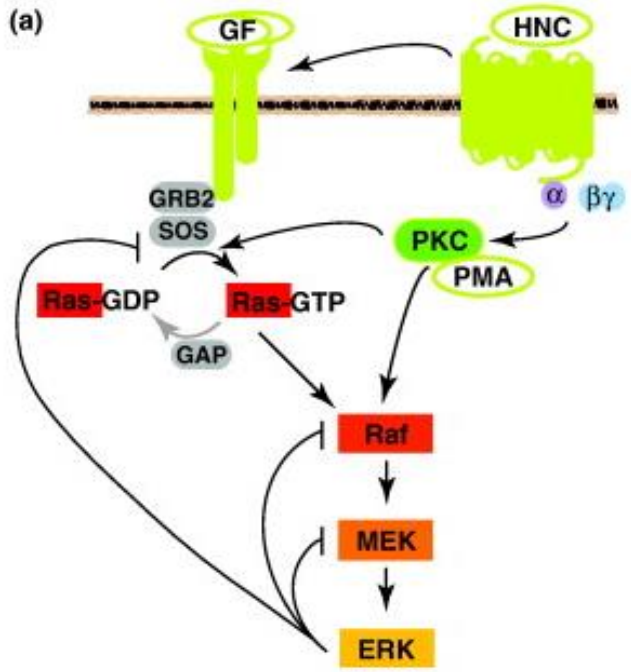

Figure 1.2. The Ras-ERK-MAPK Pathway.
The growth factor triggered-ERK activation (up left) and the polypeptide hormone neurotransmitter and chemokine (HNC) induced-ERK activation (up right). Adapted with permission from The Ras-ERK and PI3K-mTOR pathways: cross-talk and compensation by Michelle C et al., 2011, Trends in Biochemical Sciences, 36(6), 320-328. Copyright [2018] by Elsevier[160].

Transcription factors	Kinases and phosphatases	Cytoskeletal proteins	Signaling proteins	Apoptotic proteins and proteinases	Other proteins
RUNX1 Androgen receptor ATF2 BCL6 BMAL1 CBP C/EBPβ CRY1/2 E47 Elk1 ER81 ERF Estrogen receptor c-Fos Fra1 GATA1/2 HIF1α HSF1 ICER c-Jun Microphthalmia c-Myc N-Myc Net (Sap2) NFATc4 NF-IL6 NGFI-B/TR3/Nur77 Pax6 PPARγ P53 Progesterone receptor RNA Pol. II PUNX2 Sap1 Smad1 Smad2/3 SP1 SRC1 SREBP1/2 STAT1/3 STAT5a TAL1/SCL TFII-I TFIIIB TGIF TIF1A Tob UBF	DAPK ERK1/2 FAK1 GRK2 Inhibitor-2 Lck MAPKAP3 MAPKAP5 MEK1/2 MKP1/2 MKP3 MKP7 MLCK MNK1/2 MSK1/2 PAK1 PTP2C Raf1 B-Raf RSK1-4 S6K Syk	Annexin XI Caldesmon Calnexin CENP-E Connexin-43 Cortactin Crystallin DOC1R Dystrophin Lamin B2 MAP1 MAP2 MAP4 MISS NF-H NF-M Paxillin Stathmin SWI/SNF Synapsin 1 Tau Vinexin b	EGFR ENaCβ/γ Fe65 FRS2 Gab1 Gab2 GAIP Grb10 IRS1 LAT LIFR MARCKS Naf1α PDE4 PLCβ PLCγ Potassium channel Kv 4.2 KSR1 Rab4 SH2-B ShcA Sos1 Spin90 TSC2	Bad Bim-EL Calpain Caspase 9 EDD IEX1 MCL-1 TIS2 TNFR CD120a	Amphiphysin 1 CPSII/CAD CR16 GRASP55 GRASP65 HABP1 Histone H HnRNP-K KIP MBP PHAS-I (4E-BP1) CPLA2 Rb SAP90/PSD95 Spinophilin Topoisomerase II Tpr TTP (Nup47) Tyrosine hydroxylase Vif Vpx

Table 1.1. ERK1/2 targets.
ERK1/2 targeted transcription factors, kinase and phosphatases, cytoskeletal proteins, signaling proteins, apoptosis-related proteins, as well as other types of proteins. Adapted with from[87].

The ERK1/2 signaling pathway is involved in the pathology of many CNS diseases. Inhibition of ERK1/2 activation usually protect neurons from apoptosis and inflammation and reduces damage after stroke[98]. Feng showed that ERK signals participate in the neuronal apoptosis observed in the hippocampus in early post-subarachnoid hemorrhage brain injury[99]. The oxidative stress response that occurs in microglia is mediated by the activation of ERK1/2. Recent studies have shown that the oxidative stress response in microglia plays a central role in the etiology of Parkinson's disease? (PD) [100]. Therefore, the ERK1/2 pathway plays a regulatory role in PD-related cellular processes. Mutant superoxide dismutase 1 (SOD1) is one of the genetic factors that cause ALS. It has been suggested that phosphorylated ERK1/2 was found increased in the hippocampus and cerebellum in SOD1 G93A transgenic mice[101]. Abnormality of ERK1/2 was also observed in other neurological diseases, such as Huntington's disease (HD) [102]and Alzheimer's disease (AD) [103].

1.3.3 ERK1/2 and neuromuscular diseases

It has been proposed that the role of ERK1/2 in NMJ formation is the regulator for the Neuregulin-mediated transcription of synaptic genes, including AchRδ and ε. Koike[104]and Duclert[105] identified a single six-base pair element named the N box, which is required for synapse-specific expression of the reporter gene. In the N box mutated transgenic mice, the expression of a reporter gene in adult muscle was completely abolished[106]. Nichols discovered that a point mutation within the N box of AchRε promoter region could induce congenital myasthenia[107]. In cultured muscle cells, Schaeffer found a heterodimer composed of 58 and 43 kDa polypeptides that specifically

interact with the N box sequence[108], which was known to be the Ets-related transcription factor GABP. The 58 kDa GABP α subunit binds DNA through its Ets domain. The 43 kDa GABP β subunit does not directly interact with DNA but has ankyrin repeats that mediate its interaction with GABP α, strengthening the interaction of the α subunit with DNA[109]. Indeed, mutation of GABP α or β inhibits N box-regulated transcription from the AChRδ and ε promoters in cultured myotubes[110].

In 1933, Falls extracted a protein from the chicken brain, found it was able to stimulate AchR expression in cultured myotubes and named this protein ARIA (acetylcholine receptor inducing activity) [110]. ARIA is 42 kDa protein belonging to the neuregulin 1 family, a group of 14 proteins that are generated from the alternative splicing of a single gene[111]. Neuregulins receptors belong to the same family as the EGF receptor: the erbB family of tyrosine kinase receptors. Neuregulins can interact a variety of dimers of ErbB subunits. However, only ErbB2 and ErbB4 are localized in the muscle postsynaptic membrane[112].

As early as in 1998, it had been reported that in breast cancer cells, neuregulins were able to upregulate the transcriptional activity of the Ets factor PEA3 through the ERK and JNK signaling pathways[113]. The activated signaling pathways in response to neuregulins have been tested in muscle cells as well. Addition of Neuregulin leads to the phosphorylation of their erbB tyrosine kinase receptors and subsequent activation of the cyclin-dependent kinase cdk5[114]. Active ErbB receptors synergize with cdk5 and activate both the MAP kinase and JNK pathways via Ras[115]. Ras activation triggers the activation of the MAP kinase and JNK pathways. Inhibiting the MAP kinase or JNK

pathways is enough to block neuregulin dependent transcriptional activation[115]. In vivo, injection of dominant-negative mutants of ras, raf, and MEK inhibits the expression of a reporter gene driven by the AChRε promoter[115]. Importantly, it has been proved that ERK1/2 is able to phosphorylate GABP directly *in vitro*[116]. However, the theory of Neuregulin regulated AChR expression was challenged due to the emerging evidence later *in vivo*. Escher et al. showed that NMJ was able to form normally when the ErbB2 and ErbB4 were specifically knocked out in mice skeletal muscle, suggesting Neuregulin is not required for AChR formation[117]. This finding is consistent with the hypothesis that AChR formation is directly induced by Agrin-Lrp4-Musk axis[118], although further experiments are needed to test it.

Autosomal Emery-Dreifuss muscular dystrophy (EDMD) is induced by mutations in the lamin A/C gene (LMNA) encoding A-type nuclear lamins, which are intermediate filament proteins of the nuclear envelope[119, 120]. It has been reported that over-activated ERK signaling pathway was found in both cardiac and skeletal muscle of $Lmna^{H222P/H222P}$ mice, which is the model for human EDMD[121, 6]. Moreover, treatment with selumetinib, a MEK1/2 inhibitor, was able to alleviate myopathy, reduce serum creatine phosphokinase and increase skeletal function[6]. However, the mechanism that links abnormal ERK pathway to EDMD is still unknown.

A class of developmental diseases called the “RASopathies”, is caused by germline mutations in genes that encode components of ERK 1/2 pathway. Although any component of the ERK1/2 pathway can be affected, they all induce ERK dysfunction and therefore numerous overlapping phenotypes between the syndromes, including

characteristic facial features, cardiac defects, cutaneous abnormalities, neurocognitive delay and more importantly, myopathy and muscle dystrophy[122, 123]. The majority of these syndromes are caused by gain of function in ERK pathway, however, LEOPARD syndrome (LS), a rare autosomal dominant disorder, is due to reduced catalytic activity of SHP-2 (a.k.a. PTPN11) [124] which is critical for ERK signaling transduction, suggesting loss of ERK is a pathological factor for skeletal muscle atrophy.

1.3.4 ERK and myogenesis

In primary muscle cell culture, ERK pathway has been suggested to promote myoblast proliferation[125]. This increased ERK activity can be achieved by adding a variety of growth factors, including FGF[126], hepatocyte growth factor (HGF) [127], insulin-like growth factor (IGF) [128] and platelet-derived growth factor (PDGF) [129]. The role of ERK in myoblast proliferation is probably preventing cell cycle exit and promoting entry into S phase[130, 131]. However, how does ERK accomplish these functions is totally unknown.

ERK1/2 pathway inhibits myoblast differentiation by preventing the nuclear accumulation of MEF2[132], and reducing the expression of a myogenic factor, MyoD[133], the CDK inhibitor p21[134]and other transcriptional regulatory proteins[135]. In addition, during differentiation, expression of FGF receptors are reduced[136] and the activity of ERK decreases[137]. Again, the exact mechanism that accounts for the inhibitory effect of ERK pathway during differentiation is largely unknown. ERK activity return as differentiation continues and myocytes are ready to fuse into myotubes. At least ERK2 is critical for myocyte fusion and survival[138]. ERK is able to phosphorylate the 90-kDa

ribosomal S6 kinase 2 (RSK2), which promotes myocyte fusion via phosphorylation and transcriptional activation of nuclear factor of activated T cell 3 (NFAT3)[139].

Myoblasts/myocytes have a unique bi-phasic requirement for ERK activity (Fig 1.3). ERK1/2 is needed for myoblast proliferation, inhibitory to myoblast differentiation, and later required for myocyte fusion. Until now, no ERK muscle- specific targets have been identified.

1.3.5 Muscle fiber types and transition

Skeletal muscle is a heterogeneous tissue composed of a variety of fast and slow fiber types (Type1, 2A, 2B, and X) (Table 1.2) Major differences between muscle fiber types relate to their specific combinations of myosin chains (isoforms of myosin light and heavy chains) [140]. Myosin heavy chain (MHC) isoforms represent the most proper markers for fiber type. According to this, pure fiber types are characterized by the expression of a single MHC isoform, whereas hybrid fiber types express two or more MHC isoforms. Moreover, muscle fibers are capable of adjusting their phenotypic properties in response to altered functional demands[140]. Under certain conditions, changes can be induced in MHC isoform expression heading in the direction of either fast-to-slow or slow-to-fast. Increased neuromuscular activity[141] and mechanical loading[142] induce fast-to-slow transitions, whereas reduced neuromuscular activity and mechanical unloading, result in slow-to-fast transition. In addition, small molecules[143] or genetic regulation of signaling pathway[144] could also lead to muscle fiber type transition.

1.4 The role of TGFβ and BMP signaling in muscle mass maintenance

The balance between rates of protein synthesis and degradation is critical to muscle health. Myofiber size increase, a process termed hypertrophy, occurs when the rates of protein synthesis exceed rates of protein degradation. The insulin-like growth factor 1 (IGF1)–phosphoinositide 3-kinase (PI3K)–Akt/protein kinase B (PKB)–mammalian target of rapamycin (mTOR) signaling axis is believed to be the key regulator of protein synthesis in muscle, mainly through controlling S6, a ribosomal protein, and factor 4E-binding protein 1 (4EBP1), an inhibitor of the ribosomal eukaryotic translation initiator factor 4E (eIF4E) [145]. In contrast to this, reduction of muscle mass and atrophy of myofibers is due to loss of proteins, organelles, and cytoplasm. The main cellular degradation pathways, including the ubiquitin-proteasome and the autophagy-lysosome systems, contribute to this process[146]. Atrogenes are atrophy-related genes that activate those two pathways[147]. Firstly, deactivation of Akt releases the inhibitory effect of atrogenes. Next, atrogenes will encode two most-induced muscle-specific ubiquitin ligases, atrogin1 (a.k.a. MAFbx) and MuRF1 (a.k.a.Trim63). Lastly, these two ligases will target proteins to the proteasome for degradation. Other atrogenes also encode proteins that are critical for the activity of the autophagy-lysosome system[148].

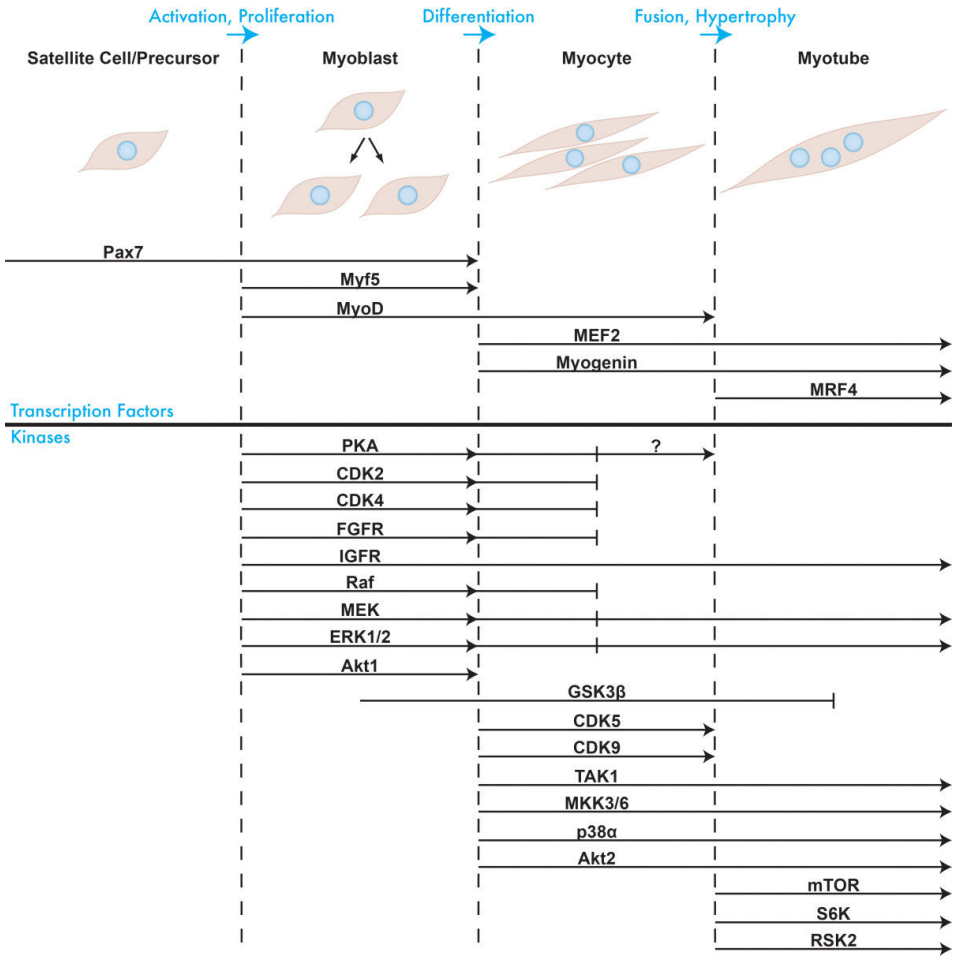

Figure 1.3. The regulation of the different stages of myogenesis by transcription factors and kinases.
The upper part of the figure shows transcription factors required for the processes of myoblast proliferation, differentiation and myocyte fusion into myotubes, respectively. The lower part shows the protein kinases and the stages that they regulate. Adapted with permission from[161].

	Type I fibers	Type II a fibers	Type II x fibers	Type II b fibers
Contraction time	Slow	Moderately Fast	Fast	Very fast
Resistance to fatigue	High	Fairly high	Moderate	Low
Activity Used for	Aerobic activity	Long-term anaerobic activity	Short-term anaerobic activity	Short-term anaerobic activity
Maximum duration of use	Hours	Less than 30 minutes	Less than 5 minutes	Less than 1 minute
Power produced	Low	Medium	High	Very high
Mitochondrial density	Very High	High	Medium	Low
Capillary density	High	Intermediate	Low	Low
Oxidative capacity	High	High	Moderate	Low
Major storage fuel	Triglycerides	Creatine phosphate, glycogen	ATP, Creatine phosphate, glycogen (little)	ATP, Creatine phosphate
Properties	Consumes lactic acid	Produce lactic acid and Creatine phosphate	Consume Creatine phosphate	Consume Creatine phosphate

Table 1.2. Differences in skeletal muscle fiber types.
Adapted from http://musclewanted.com/muscle-fiber-types/

In the TGFβ superfamily, more than 30 ligands selectively bind to specific receptor subtypes. Different combinations of ligands and receptors result in distinct biological actions (Fig 1.4). The accomplishment of TGFβ signaling transduction depends on the recruitment of the Smad transcription regulators or so-called Receptor Smads. For example, Activins and some growth and differentiation factors (GDFs) (e.g., GDF8, GDF11) promote the activity of Smad2/3. In contrast to this, other GDF ligands and the bone morphogenetic proteins (BMPs) utilize Smad1/5/8 to regulate target genes. The ligands of TGFβ and BMP pathway bind to TGFb/BMP type II receptors (TGFβ and BMP have their own type I and II subtypes) and recruit TGFβ/BMP type I[148] to phosphorylate their Rsmads, leading to the formation of Rsmads- Smad4 complex and transcriptional regulation of other genes[149]. Smad4 is also called Co-smad. Some

molecules are able to modulate the TGFβ and BMP pathways by blocking Type I receptor-mediated activation of Smad1/5/8 and Smad2/3, such as Smad6, 7 (a.k.a. inhibitory-smads)[150, 151].

Evidence from a variety of experiments suggests the TGFβ pathway negatively controls muscle mass. For example, myostatin is a TGFβ pathway ligand that is expressed predominantly in skeletal muscle and functions as a negative regulator of muscle growth. Deletion of myostatin gene resulted in muscle hypertrophy in animals[152]. The Smad2/3 is able to activate atrogin1[153]and inhibit the IGF1/Akt/mTOR pathway[154]. To be specific, Smad3 inhibits the expression of two miRNAs, miRNA-29 and miRNA-486, both of which target phosphatase and tensin homolog (PTEN), leading to increased activity of Akt[155]. In addition, Smad3 is able to regulate Akt directly in other system[156].

Conversely, BMP signaling promotes muscle hypertrophy. The first evidence is that Smad4 knockout in mice induced slight muscle atrophy instead of hypertrophy[18]. Moreover, these Smad4$^{-/-}$ mice displayed dramatically severe muscle atrophy after denervation[18]. Secondly, the BMP antagonist Noggin reverted the hypertrophic phenotype of myostatin$^{-/-}$ mice, suggesting a dominant role of BMP pathway in muscle mass regulation. Furthermore, BMP7 overexpression was sufficient to induce muscle growth and to mitigate muscle atrophy after denervation[18, 157]. Lastly, denervation-induced muscle atrophy was worse if GDF5 (a.k.a. BMP14) was deleted or Smad6 was overexpressed[18, 157]. It seems that BMP pathway regulates muscle hypertrophy probably via Akt/mTOR pathways because interruption of Akt/mTOR pathway is sufficient to block the hypertrophic effect from BMP pathway[157]. Moreover, Smad1/5/8 can

negatively regulate atrogin1, Murf1, and another novel atrogene, MUSA1 (a.k.a. Fbxo30)[157]. Specific blocking of MUSA1 is able to revert the atrophic phenotype found in Smad4$^{-/-}$ mice. In addition, overexpression of *Smad6* can upregulate histone deacetylase 4 (HDAC4) and subsequently myogenin. This pathway has been proposed as a key process to trigger muscle atrophy[158]. It is true that inhibition of HDAC4 is able to downregulate atrogin1, Murf1[158].

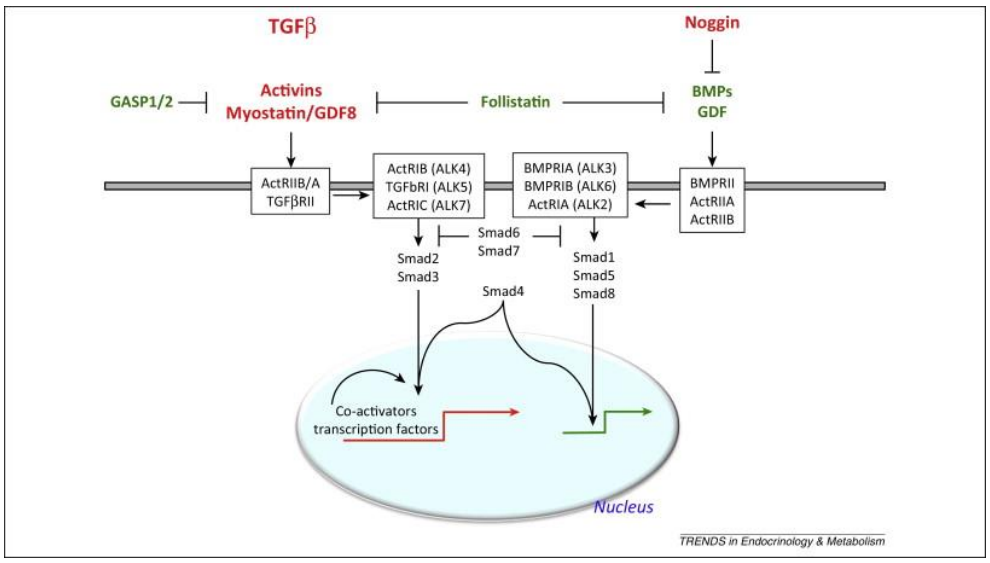

Figure 1.4. Signaling and crosstalk between TGFβ and BMP pathways.
The transcriptional event that negatively controls muscle mass is depicted in red and the one that promotes muscle growth in green. The different ligands bind to type II receptors that are partially shared by the two pathways. Type II receptors recruit different type I receptors, which activate the downstream R-Smad transcription factors. Adapted with permission from TGFβ and BMP signaling in skeletal muscle: potential significance for muscle-related disease by Roberta Sartori et al., 2014, Trends in Endocrinology & Metabolism, 25(9), 464-471. Copyright [2018] by Elsevier[162].

1.5 References

1. Levitan, I. B., & Kaczmarek, L. K. (2015). The neuron: cell and molecular biology. Oxford: Oxford University Press.

2. Zong, Y., & Jin, R. (2012). Structural mechanisms of the agrin–LRP4–MuSK signaling pathway in neuromuscular junction differentiation. Cellular and Molecular Life Sciences, 70(17), 3077-3088. doi:10.1007/s00018-012-1209-9

3. Kittel, R. J., & Heckmann, M. (2016). Synaptic vesicle proteins and active zone plasticity. Frontiers in Synaptic Neuroscience, 8. doi:10.3389/fnsyn.2016.00008

4. Hohlfeld, R., Wekerle, H., & Marx, A. (2012). The immunopathogenesis of Myasthenia Gravis. Myasthenia Gravis and Myasthenic Disorders, 60-89. doi:10.1093/med/9780199738670.003.0003

5. Flanigan, K. M. (2014). Duchenne and Becker Muscular Dystrophies. Neurologic Clinics, 32(3), 671-688. doi:10.1016/j.ncl.2014.05.002

6. Muchir, A., Kim, Y., Reilly, S. A., Wu, W., Choi, J. C., & Worman, H. J. (2013). Inhibition of extracellular signal-regulated kinase 1/2 signaling has beneficial effects on skeletal muscle in a mouse model of Emery-Dreifuss muscular dystrophy caused by lamin A/C gene mutation. Skeletal Muscle, 3(1), 17. doi:10.1186/2044-5040-3-17

7. Tidyman, W. E., & Rauen, K. A. (2009). The RASopathies: developmental syndromes of Ras/MAPK pathway dysregulation. Current Opinion in Genetics & Development, 19(3), 230-236. doi:10.1016/j.gde.2009.04.001

8. Yoon, S., & Seger, R. (2006). The extracellular signal-regulated kinase: Multiple substrates regulate diverse cellular functions. Growth Factors, 24(1), 21-44. doi:10.1080/02699050500284218

9. Rimer, M. (2011). Emerging roles for MAP kinases in agrin signaling. Communicative & Integrative Biology, 4(2), 143-146. doi:10.4161/cib.4.2.14357

10. Osborne, J. K., Zaganjor, E., & Cobb, M. H. (2011). Signal control through Raf: in sickness and in health. Cell Research, 22(1), 14-22. doi:10.1038/cr.2011.193

11. Jones, N. C., Fedorov, Y. V., Rosenthal, R. S., & Olwin, B. B. (2001). ERK1/2 is required for myoblast proliferation but is dispensable for muscle gene expression and cell fusion. Journal of Cellular Physiology, 186(1), 104-115. doi:10.1002/1097-4652(200101)186:1<104::aid-jcp1015>3.3.co;2-s

12. Knight, J. D., & Kothary, R. (2011). The myogenic kinome: protein kinases critical to mammalian skeletal myogenesis. Skeletal Muscle, 1(1), 29. doi:10.1186/2044-5040-1-29

13. Rimer, M. (2010). Modulation of Agrin-induced acetylcholine receptor clustering by Extracellular Signal-regulated Kinases 1 and 2 in Cultured Myotubes. Journal of Biological Chemistry, 285(42), 32370-32377. doi:10.1074/jbc.m110.144774

14. Shi, H., Scheffler, J. M., Zeng, C., Pleitner, J. M., Hannon, K. M., Grant, A. L., & Gerrard, D. E. (2009). Mitogen-activated protein kinase signaling is necessary for the maintenance of skeletal muscle mass. American Journal of Physiology-Cell Physiology, 296(5). doi:10.1152/ajpcell.00475.2008

15. Shi, H., Scheffler, J. M., Pleitner, J. M., Zeng, C., Park, S., Hannon, K. M., . . . Gerrard, D. E. (2008). Modulation of skeletal muscle fiber type by mitogen-activated protein kinase signaling. The FASEB Journal, 22(8), 2990-3000. doi:10.1096/fj.07-097600

16. Murgia, M., Serrano, A. L., Calabria, E., Pallafacchina, G., Lømo, T., & Schiaffino, S. (2000). Ras is involved in nerve-activity-dependent regulation of muscle genes. Nature Cell Biology, 2(3), 142-147. doi:10.1038/35004013

17. Seaberg, B., Henslee, G., Wang, S., Paez-Colasante, X., Landreth, G. E., & Rimer, M. (2015). Muscle-derived extracellular signal-regulated kinases 1 and 2 are required for the maintenance of adult myofibers and their Neuromuscular Junctions. Molecular and Cellular Biology, 35(7), 1238-1253. doi:10.1128/mcb.01071-14

18. Sartori, R., Schirwis, E., Blaauw, B., Bortolanza, S., Zhao, J., Enzo, E., . . . Sandri, M. (2013). BMP signaling controls muscle mass. Nature Genetics, 45(11), 1309-1318. doi:10.1038/ng.2772

19. Sanes, J. R., & Lichtman, J. W. (1999). Development of the vertebrate neuromuscular junction. Annual Review of Neuroscience, 22(1), 389-442. doi:10.1146/annurev.neuro.22.1.389

20. Hong, I. H., & Etherington, S. J. (2011). Neuromuscular Junction. Chichester : John Wiley & Sons, Ltd . doi:DOI: 10.1002/9780470015902.a0023202

21. Griffin, J. W., & Thompson, W. J. (2008). Biology and pathology of nonmyelinating Schwann cells. Glia, 56(14), 1518-1531. doi:10.1002/glia.20778

22. Larsson, L., & Ansved, T. (1995). Effects of ageing on the motor unit. Progress in Neurobiology, 45(5), 397-458. doi:10.1016/0301-0082(95)98601-z

23. Kang, H., Tian, L., Mikesh, M., Lichtman, J. W., & Thompson, W. J. (2014). Terminal Schwann Cells Participate in Neuromuscular Synapse Remodeling during Reinnervation following Nerve Injury. Journal of Neuroscience, 34(18), 6323-6333. doi:10.1523/jneurosci.4673-13.2014

24. Barik, A., Li, L., Sathyamurthy, A., Xiong, W., & Mei, L. (2016). Schwann Cells in Neuromuscular Junction Formation and Maintenance. Journal of Neuroscience, 36(38), 9770-9781. doi:10.1523/jneurosci.0174-16.2016

25. Squire, L. R., Berg, D., Bloom, F. E., Lac, S. D., Ghosh, A., & Spitzer, N. C. (2013). Neurotransmitters. In Fundamental neuroscience (4th ed.) (pp. 117-138). San Diego: Academic Press.

26. Fagerlund, M., & Eriksson, L. (2009). Current concepts in neuromuscular transmission. British Journal of Anaesthesia, 103(1), 108-114. doi:10.1093/bja/aep150

27. Dale, H. H. (1914). The action of certain esters and ethers of choline, and their relation to muscarine. Journal of Pharmacology and Experimental Therapeutics, 6(2), 147-190.

28. Xiu, X., Puskar, N. L., Shanata, J. A., Lester, H. A., & Dougherty, D. A. (2009). Nicotine binding to brain receptors requires a strong cation–π interaction. Nature, 458(7237), 534-537. doi:10.1038/nature07768

29. Mishina, M., Takai, T., Imoto, K., Noda, M., Takahashi, T., Numa, S., . . . Sakmann, B. (1986). Molecular distinction between fetal and adult forms of muscle acetylcholine receptor. Nature, 321(6068), 406-411. doi:10.1038/321406a0

30. Unwin, N., & Fujiyoshi, Y. (2012). Gating Movement of Acetylcholine Receptor Caught by Plunge-Freezing. Journal of Molecular Biology, 422(5), 617-634. doi:10.1016/j.jmb.2012.07.010

31. Kummer, T. T., Misgeld, T., & Sanes, J. R. (2006). Assembly of the postsynaptic membrane at the neuromuscular junction: paradigm lost. Current Opinion in Neurobiology, 16(1), 74-82. doi:10.1016/j.conb.2005.12.003

32. Vock, V. M., Ponomareva, O. N., & Rimer, M. (2008). Evidence for muscle-dependent neuromuscular synaptic site determination in mammals. Journal of Neuroscience, 28(12), 3123-3130. doi:10.1523/jneurosci.5080-07.2008

33. Thompson, W. (1983). Synapse elimination in neonatal rat muscle is sensitive to pattern of muscle use. Nature, 302(5909), 614-616. doi:10.1038/302614a0

34. Sanes, J. R., & Lichtman, J. W. (2001). Development: Induction, assembly, maturation and maintenance of a postsynaptic apparatus. Nature Reviews Neuroscience, 2(11), 791-805. doi:10.1038/35097557

35. Mcmahan, U. (1990). The Agrin hypothesis. Cold Spring Harbor Symposia on Quantitative Biology, 55(0), 407-418. doi:10.1101/sqb.1990.055.01.041

36. Kim, N., Stiegler, A. L., Cameron, T. O., Hallock, P. T., Gomez, A. M., Huang, J. H., . . . Burden, S. J. (2008). Lrp4 is a receptor for Agrin and forms a complex with MuSK. Cell, 135(2), 334-342. doi:10.1016/j.cell.2008.10.002

37. Apel, E. D., Glass, D. J., Moscoso, L. M., Yancopoulos, G. D., & Sanes, J. R. (1997). Rapsyn is required for MuSK signaling and recruits synaptic components to a MuSK-containing scaffold. Neuron, 18(4), 623-635. doi:10.1016/s0896-6273(00)80303-7

38. Gautam, M., Noakes, P., Mudd, J., Nichol, M., Chu, G., Sanes, J. R., & Merlie, J. (1995). Failure of postsynaptic specialization to develop at neuromuscular junctions of rapsyn-deficient mice. Nature, 377(6546), 232-236. doi:10.1038/377232a0

39. Lin, W., Dominguez, B., Yang, J., Aryal, P., Brandon, E. P., Gage, F. H., & Lee, K. (2005). Neurotransmitter acetylcholine negatively regulates neuromuscular synapse formation by a Cdk5-dependent mechanism. Neuron, 46(4), 569-579. doi:10.1016/j.neuron.2005.04.002

40. Misgeld, T., Burgess, R. W., Lewis, R. M., Cunningham, J. M., Lichtman, J. W., & Sanes, J. R. (2002). Roles of neurotransmitter in synapse formation. Neuron, 36(4), 635-648. doi:10.1016/s0896-6273(02)01020-6

41. Fox, M. A., Sanes, J. R., Borza, D., Eswarakumar, V. P., Fässler, R., Hudson, B. G., . . . Umemori, H. (2007). Distinct target-derived signals organize formation, maturation, and maintenance of motor nerve terminals. Cell, 129(1), 179-193. doi:10.1016/j.cell.2007.02.035

42. Baudet, C., Pozas, E., Adameyko, I., Andersson, E., Ericson, J., & Ernfors, P. (2008). Retrograde signaling onto ret during motor nerve terminal maturation. Journal of Neuroscience, 28(4), 963-975. doi:10.1523/jneurosci.4489-07.2008

43. Nguyen, Q. T. (1998). Hyperinnervation of neuromuscular junctions caused by GDNF overexpression in muscle. Science, 279(5357), 1725-1729. doi:10.1126/science.279.5357.172543.

44. Feng, Z., & Ko, C. (2008). Schwann cells promote synaptogenesis at the neuromuscular junction via transforming growth factor- 1. Journal of Neuroscience, 28(39), 9599-9609. doi:10.1523/jneurosci.2589-08.200844.

45. Yumoto, N., Kim, N., & Burden, S. J. (2012). Lrp4 is a retrograde signal for presynaptic differentiation at neuromuscular synapses. Nature, 489(7416), 438-442. doi:10.1038/nature11348

46. Gillingwater, T. H., & Ribchester, R. R. (2001). Compartmental neurodegeneration and synaptic plasticity in the Wldsmutant mouse. The Journal of Physiology, 534(3), 627-639. doi:10.1111/j.1469-7793.2001.00627.x

47. Chen, P., Piao, X., & Bonaldo, P. (2015). Role of macrophages in Wallerian degeneration and axonal regeneration after peripheral nerve injury. Acta Neuropathologica, 130(5), 605-618. doi:10.1007/s00401-015-1482-4

487. O. Büngner Ueber die (1890). Degenerations- und Regeneration svorgänge am Nerven nach Verletzungen Universität Marburg, Marburg, Germany

49. Heumann, R. (1987). Changes of nerve growth factor synthesis in nonneuronal cells in response to sciatic nerve transection. The Journal of Cell Biology, 104(6), 1623-1631. doi:10.1083/jcb.104.6.1623

50. Nguyen, Q. T., Sanes, J. R., & Lichtman, J. W. (2002). Pre-existing pathways promote precise projection patterns. Nature Neuroscience, 5(9), 861-867. doi:10.1038/nn905

51. Court, F. A., Gillingwater, T. H., Melrose, S., Sherman, D. L., Greenshields, K. N., Morton, A. J., . . . Ribchester, R. R. (2008). Identity, developmental restriction and reactivity of extralaminar cells capping mammalian neuromuscular junctions. Journal of Cell Science, 121(23), 3901-3911. doi:10.1242/jcs.031047

52. Sanes, J. R. (1978). Reinnervation of muscle fiber basal lamina after removal of myofibers. Differentiation of regenerating axons at original synaptic sites. The Journal of Cell Biology, 78(1), 176-198. doi:10.1083/jcb.78.1.176

53. Williams, A. H., Valdez, G., Moresi, V., Qi, X., Mcanally, J., Elliott, J. L., . . . Olson, E. N. (2009). MicroRNA-206 delays ALS progression and promotes regeneration of neuromuscular synapses in mice. Science, 326(5959), 1549-1554. doi:10.1126/science.1181046

54. Brack, A., & Rando, T. (2012). Tissue-specific stem cells: lessons from the skeletal muscle satellite cell. Cell Stem Cell, 10(5), 504-514. doi:10.1016/j.stem.2012.04.001

55. Liu, W., Wei-Lapierre, L., Klose, A., Dirksen, R. T., & Chakkalakal, J. V. (2015). Inducible depletion of adult skeletal muscle stem cells impairs the regeneration of neuromuscular junctions. ELife, 4. doi:10.7554/elife.09221

56. Couesnon, A., Offner, N., Bernard, V., Chaverot, N., Backer, S., Dimitrov, A., . . . Bloch-Gallego, E. (2013). CLIPR-59: a protein essential for neuromuscular junction

stability during mouse late embryonic development. Development, 140(11), 2444-2444. doi:10.1242/dev.098160

57. Valenzuela, I. M., Mouslim, C., Pires-Oliveira, M., Adams, M. E., Froehner, S. C., & Akaaboune, M. (2011). Nicotinic acetylcholine receptor stability at the NMJ deficient in -Syntrophin In vivo. Journal of Neuroscience, 31(43), 15586-15596. doi:10.1523/jneurosci.4038-11.2011

58. Aittaleb, M., Valenzuela, I. M., & Akaaboune, M. (2017). Spatial distribution and molecular dynamics of dystrophin glycoprotein components at the neuromuscular junction in vivo. Journal of Cell Science, 130(10), 1752-1759. doi:10.1242/jcs.198358

59. Hesser, B. A., Henschel, O., & Witzemann, V. (2006). Synapse disassembly and formation of new synapses in postnatal muscle upon conditional inactivation of MuSK. Molecular and Cellular Neuroscience, 31(3), 470-480. doi:10.1016/j.mcn.2005.10.020

60. Schmidt, N., Akaaboune, M., Gajendran, N., Valenzuela, I. M., Wakefield, S., Thurnheer, R., & Brenner, H. R. (2011). Neuregulin/ErbB regulate neuromuscular junction development by phosphorylation of α-dystrobrevin. The Journal of Cell Biology, 195(7), 1171-1184. doi:10.1083/jcb.201107083

61. Khan, M. M., Lustrino, D., Silveira, W. A., Wild, F., Straka, T., Issop, Y., . . . Rudolf, R. (2016). Sympathetic innervation controls homeostasis of neuromuscular junctions in health and disease. Proceedings of the National Academy of Sciences, 113(3), 746-750. doi:10.1073/pnas.1524272113

62. Berrih-Aknin, S., Frenkian-Cuvelier, M., & Eymard, B. (2014). Diagnostic and clinical classification of autoimmune myasthenia gravis. Journal of Autoimmunity, 48-49, 143-148. doi:10.1016/j.jaut.2014.01.003

63. Gilhus, N. E., & Verschuuren, J. J. (2015). Myasthenia gravis: subgroup classification and therapeutic strategies. The Lancet Neurology, 14(10), 1023-1036. doi:10.1016/s1474-4422(15)00145-3

64. Souza, P. V., Naylor, F. G., Wladimir Bocca Vieira De Rezende Pinto, & Oliveira, A. S. (2017). Duchenne muscular dystrophy: classical and new therapeutic purposes and future perspectives. Arquivos de Neuro-Psiquiatria, 75(8), 495-496. doi:10.1590/0004-282x20170086

65. Guiraud, S., Aartsma-Rus, A., Vieira, N. M., Davies, K. E., Ommen, G. B., & Kunkel, L. M. (2015). The Pathogenesis and therapy of muscular dystrophies. Annual Review of Genomics and Human Genetics, 16(1), 281-308. doi:10.1146/annurev-genom-090314-025003

66. Lapidos, K. A. (2004). The Dystrophin glycoprotein complex: signaling strength and integrity for the sarcolemma. Circulation Research, 94(8), 1023-1031. doi:10.1161/01.res.0000126574.61061.25

67. Moxley, R. T., Pandya, S., Ciafaloni, E., Fox, D. J., & Campbell, K. (2010). Change in natural history of Duchenne muscular dystrophy with long-term corticosteroid treatment: implications for management. Journal of Child Neurology, 25(9), 1116-1129. doi:10.1177/0883073810371004

68. Ricotti, V., Manzur, A., Scott, E., & Muntoni, F. (2011). P4.5 Benefits and adverse effects of glucocorticoids in boys with Duchenne muscular dystrophy. Neuromuscular Disorders, 21(9-10), 705-706. doi:10.1016/j.nmd.2011.06.970

69. Robinson-Hamm, J. N., & Gersbach, C. A. (2016). Gene therapies that restore dystrophin expression for the treatment of Duchenne muscular dystrophy. Human Genetics, 135(9), 1029-1040. doi:10.1007/s00439-016-1725-z

70. Wang, B., Li, J., & Xiao, X. (2000). Adeno-associated virus vector carrying human minidystrophin genes effectively ameliorates muscular dystrophy in mdx mouse model. Proceedings of the National Academy of Sciences, 97(25), 13714-13719. doi:10.1073/pnas.240335297

71. Duan, D. (2011). Duchenne muscular dystrophy gene therapy: lost in translation? Research and Reports in Biology, 31. doi:10.2147/rrb.s13463

72. Logroscino, G., Tortelli, R., Rizzo, G., Marin, B., Preux, P. M., & Malaspina, A. (2015). Amyotrophic lateral sclerosis: an aging-related disease. Current Geriatrics Reports, 4(2), 142-153. doi:10.1007/s13670-015-0127-8

73. Boido, M., & Vercelli, A. (2016). Neuromuscular Junctions as Key Contributors and Therapeutic Targets in Spinal Muscular Atrophy. Frontiers in Neuroanatomy, 10. doi:10.3389/fnana.2016.00006

74. Manning, G. (2002). The protein kinase complement of the human genome. Science, 298(5600), 1912-1934. doi:10.1126/science.1075762

75. Chen, Z., Gibson, T. B., Robinson, F., Silvestro, L., Pearson, G., Xu, B., . . . Cobb, M. H. (2001). MAP kinases. Chemical Reviews, 101(8), 2449-2476. doi:10.1021/cr000241p

76. Platanias, L. C. (2003). Map kinase signaling pathways and hematologic malignancies. Blood, 101(>12), 4667-4679. doi:10.1182/blood-2002-12-3647

77. Lee, J., Ulevitch, R., & Han, J. (1995). Primary structure of BMK1: a new mammalian MAP kinase. Biochemical and Biophysical Research Communications, 213(2), 715-724. doi:10.1006/bbrc.1995.2189

78. Boulton, T. G., Nye, S. H., Robbins, D. J., Ip, N. Y., Radzlejewska, E., Morgenbesser, S. D., . . . Yancopoulos, G. D. (1991). ERKs: A family of protein-serine/threonine kinases that are activated and tyrosine phosphorylated in response to insulin and NGF. Cell, 65(4), 663-675. doi:10.1016/0092-8674(91)90098-j

79. Gonzalez, F. A., Raden, D. L., Rigby, M. R., & Davis, R. J. (1992). Heterogeneous expression of four MAP kinase isoforms in human tissues. FEBS Letters, 304(2-3), 170-178. doi:10.1016/0014-5793(92)80612-k

80. Abe, M. K., Kuo, W., Hershenson, M. B., & Rosner, M. R. (1999). Extracellular Signal-Regulated Kinase 7 (ERK7), a Novel ERK with a C-Terminal Domain That Regulates Its Activity, Its Cellular Localization, and Cell Growth. Molecular and Cellular Biology, 19(2), 1301-1312. doi:10.1128/mcb.19.2.1301

81. Abe, M. K., Saelzler, M. P., Espinosa, R., Kahle, K. T., Hershenson, M. B., Beau, M. M., & Rosner, M. R. (2002). ERK8, a New Member of the Mitogen-activated Protein

Kinase Family. Journal of Biological Chemistry, 277(19), 16733-16743. doi:10.1074/jbc.m112483200

82. Chang, L., & Karin, M. (2001). Mammalian MAP kinase signalling cascades. Nature, 410(6824), 37-40. doi:10.1038/35065000

83. Roskoski, R. (2012). ERK1/2 MAP kinases: Structure, function, and regulation. Pharmacological Research, 66(2), 105-143. doi:10.1016/j.phrs.2012.04.005

84. Mckay, M. M., & Morrison, D. K. (2007). Integrating signals from RTKs to ERK/MAPK. Oncogene, 26(22), 3113-3121. doi:10.1038/sj.onc.1210394

85. Rozengurt, E. (2012). Signaling pathways induced by G-protein-coupled receptors. Physiology of the Gastrointestinal Tract, 75-96. doi:10.1016/b978-0-12-382026-6.00004-x

86. Gonzalez, F. A., Raden, D. L., & Davis, R. J. (1991). Identification of substrate recognition determinants for human ERK1 and ERK2 protein kinases. The Journal of Biological Chemistry, 266(33), 22159-22163.

87. Yoon, S., & Seger, R. (2006). The extracellular signal-regulated kinase: Multiple substrates regulate diverse cellular functions. Growth Factors, 24(1), 21-44. doi:10.1080/02699050500284218

88. English, J. D., & Sweatt, J. D. (1997). A requirement for the mitogen-activated protein kinase cascade in hippocampal long term potentiation. Journal of Biological Chemistry, 272(31), 19103-19106. doi:10.1074/jbc.272.31.19103

89. Gallagher, S. M. (2004). Extracellular signal-regulated protein kinase activation is required for metabotropic glutamate receptor-dependent long-term depression in

hippocampal area CA1. Journal of Neuroscience, 24(20), 4859-4864. doi:10.1523/jneurosci.5407-03.2004

90. Samuels, I. S., Saitta, S. C., & Landreth, G. E. (2009). MAPing CNS development and cognition: an ERKsome process. Neuron, 61(2), 160-167. doi:10.1016/j.neuron.2009.01.001

91. Li, X., Newbern, J. M., Wu, Y., Morgan-Smith, M., Zhong, J., Charron, J., & Snider, W. D. (2012). MEK is a key regulator of aliogenesis in the developing brain. Neuron, 75(6), 1035-1050. doi:10.1016/j.neuron.2012.08.031

92. Fyffe-Maricich, S. L., Karlo, J. C., Landreth, G. E., & Miller, R. H. (2011). The ERK2 mitogen-activated protein kinase regulates the timing of oligodendrocyte differentiation. Journal of Neuroscience, 31(3), 843-850. doi:10.1523/jneurosci.3239-10.2011

93. Fyffe-Maricich, S. L., Schott, A., Karl, M., Krasno, J., & Miller, R. H. (2013). Signaling through ERK1/2 controls myelin thickness during myelin repair in the adult central nervous system. Journal of Neuroscience, 33(47), 18402-18408. doi:10.1523/jneurosci.2381-13.2013

94. Kim, S., Lee, M., Lee, B., Gwon, W., Joung, E., Yoon, N., & Kim, H. (2014). Anti-inflammatory effects of sargachromenol-rich ethanolic extract of myagropsis myagroides on lipopolysaccharide-stimulated BV-2 cells. BMC Complementary and Alternative Medicine, 14(1). doi:10.1186/1472-6882-14-231

95. Park, G. H., Jeon, S. J., Ryu, J. R., Choi, M. S., Han, S., Yang, S., . . . Ko, K. H. (2009). Essential role of mitogen-activated protein kinase pathways in protease activated

receptor 2-mediated nitric-oxide production from rat primary astrocytes. Nitric Oxide, 21(2), 110-119. doi:10.1016/j.niox.2009.05.007

96. Wang, Y., Zheng, Y., Lu, J., Chen, G., Wang, X., Feng, J., . . . Sun, Q. (2010). Purple sweet potato color suppresses lipopolysaccharide-induced acute inflammatory response in mouse brain. Neurochemistry International, 56(3), 424-430. doi:10.1016/j.neuint.2009.11.016

97. Xia, Q., Hu, Q., Wang, H., Yang, H., Gao, F., Ren, H., . . . Wang, G. (2015). Induction of COX-2-PGE2 synthesis by activation of the MAPK/ERK pathway contributes to neuronal death triggered by TDP-43-depleted microglia. Cell Death and Disease, 6(3). doi:10.1038/cddis.2015.69

98. Namura, S., Iihara, K., Takami, S., Nagata, I., Kikuchi, H., Matsushita, K., . . . Alessandrini, A. (2001). Intravenous administration of MEK inhibitor U0126 affords brain protection against forebrain ischemia and focal cerebral ischemia. Proceedings of the National Academy of Sciences, 98(20), 11569-11574. doi:10.1073/pnas.181213498

99. Feng, D., Wang, B., Ma, Y., Shi, W., Tao, K., Zeng, W., . . . Qin, H. (2015). The Ras/Raf/Erk pathway mediates the subarachnoid hemorrhage-induced apoptosis of hippocampal neurons through phosphorylation of p53. Molecular Neurobiology, 53(8), 5737-5748. doi:10.1007/s12035-015-9490-x

100. Qian, L., Tan, K. S., Wei, S., Wu, H., Xu, Z., Wilson, B., . . . Flood, P. M. (2007). Microglia-mediated neurotoxicity is inhibited by morphine through an opioid receptor-independent reduction of NADPH oxidase activity. The Journal of Immunology, 179(2), 1198-1209. doi:10.4049/jimmunol.179.2.1198

101. Chung, Y. H., Joo, K. M., Lim, H. C., Cho, M. H., Kim, D., Lee, W. B., & Cha, C. I. (2005). Immunohistochemical study on the distribution of phosphorylated extracellular signal-regulated kinase (ERK) in the central nervous system of SOD1G93A transgenic mice. Brain Research, 1050(1-2), 203-209. doi:10.1016/j.brainres.2005.05.060

102. Apostol, B. L., Illes, K., Pallos, J., Bodai, L., Wu, J., Strand, A., . . . Thompson, L. M. (2005). Mutant huntingtin alters MAPK signaling pathways in PC12 and striatal cells: ERK1/2 protects against mutant huntingtin-associated toxicity. Human Molecular Genetics, 15(2), 273-285. doi:10.1093/hmg/ddi443

103. Ferrer, I., Blanco, R., Carmona, M., Ribera, R., Goutan, E., Puig, B., . . . Ribalta, T. (2006). Phosphorylated MAP kinase (ERK1, ERK2) expression is associated with early Tau deposition in neurones and glial cells, but not with increased nuclear DNA vulnerability and cell death, in Alzheimer disease, picks disease, progressive supranuclear palsy and corticobasal degeneration. Brain Pathology,11(2), 144-158. doi:10.1111/j.1750-3639.2001.tb00387.x

104. Koike, S., Schaeffer, L., & Changeux, J. P. (1995). Identification of a DNA element determining synaptic expression of the mouse acetylcholine receptor delta-subunit gene. Proceedings of the National Academy of Sciences, 92(23), 10624-10628. doi:10.1073/pnas.92.23.10624

105. Duclert, A., Savatier, N., Schaeffer, L., & Changeux, J. (1996). Identification of an element crucial for the sub-synaptic expression of the acetylcholine receptor ϵ-subunit gene. Journal of Biological Chemistry, 271(29), 17433-17438. doi:10.1074/jbc.271.29.17433

106. Fromm, L., & Burden, S. J. (1998). Synapse-specific and neuregulin-induced transcription require an Ets site that binds GABPalpha /GABPbeta. Genes & Development, 12(19), 3074-3083. doi:10.1101/gad.12.19.3074

107. Nichols, P., Croxen, R., Vincent, A., Rutter, R., Hutchinson, M., Newsom-Davis, J., & Beeson, D. (1999). Mutation of the acetylcholine receptor ε-subunit promoter in congenital myasthenic syndrome. Annals of Neurology, 45(4), 439-443. doi:10.1002/1531-8249(199904)45:4<439::aid-ana4>3.3.co;2-n

108. Schaeffer, L. (1998). Implication of a multisubunit Ets-related transcription factor in synaptic expression of the nicotinic acetylcholine receptor. The EMBO Journal, 17(11), 3078-3090. doi:10.1093/emboj/17.11.3078

109. Batchelor, A. H. (1998). The Structure of GABP/: an ETS domain- ankyrin repeat heterodimer bound to DNA. Science, 279(5353), 1037-1041. doi:10.1126/science.279.5353.1037

110. Falls, D. (1993). ARIA, a protein that stimulates acetylcholine receptor synthesis, is a member of the neu ligand family. Cell, 72(5), 801-813. doi:10.1016/0092-8674(93)90407-h

111. Burden, S. J. (1998). The formation of neuromuscular synapses. Genes & Development, 12(2), 133-148. doi:10.1101/gad.12.2.133

112. Trinidad, J. C., Fischbach, G. D., & Cohen, J. B. (2000). The agrin/MuSK signaling pathway is spatially segregated from the neuregulin/erbB receptor signaling pathway at the neuromuscular junction. Journal of Neuroscience, 20(23), 8762-8770.

113. Ohagan, R. C., & Hassell, J. A. (1998). The PEA3 Ets transcription factor is a downstream target of the HER2/Neu receptor tyrosine kinase. Oncogene, 16(3), 301-310. doi:10.1038/sj.onc.1201547

114. Fu, A. K., Fu, W., Cheung, J., Tsim, K. W., Ip, F. C., Wang, J. H., & Ip, N. Y. (2001). Cdk5 is involved in neuregulin-induced AChR expression at the neuromuscular junction. Nature Neuroscience, 4(4), 374-381. doi:10.1038/86019

115. Si, J., Wang, Q., & Mei, L. (1999). Essential roles of c-JUN and c-JUN N-terminal kinase (JNK) in neuregulin-increased expression of the acetylcholine receptor epsilon-subunit. The Journal of Neuroscience, 19(19), 8498-8508.

116. Fromm, L., & Burden, S. J. (2001). Neuregulin-1-stimulated phosphorylation of GABP in skeletal muscle cells†. Biochemistry, 40(17), 5306-5312. doi:10.1021/bi002649m

117. Escher, P. (2005). Synapses form in skeletal muscles lacking neuregulin receptors. Science, 308(5730), 1920-1923. doi:10.1126/science.1108258

118. Li, L., Xiong, W. C., & Mei, L. (2018). Neuromuscular junction formation, aging, and disorders. Annual Reviews of Physiology, 80, 159-188.

119. Mckeon, F. D., Kirschner, M. W., & Caput, D. (1986). Homologies in both primary and secondary structure between nuclear envelope and intermediate filament proteins. Nature, 319(6053), 463-468. doi:10.1038/319463a0

120. Fisher, D. Z., Chaudhary, N., & Blobel, G. (1986). CDNA sequencing of nuclear lamins A and C reveals primary and secondary structural homology to intermediate

filament proteins. Proceedings of the National Academy of Sciences, 83(17), 6450-6454. doi:10.1073/pnas.83.17.6450

121. Muchir, A., Pavlidis, P., Decostre, V., Herron, A. J., Arimura, T., Bonne, G., & Worman, H. J. (2007). Activation of MAPK pathways links LMNA mutations to cardiomyopathy in Emery-Dreifuss muscular dystrophy. Journal of Clinical Investigation, 117(5), 1282-1293. doi:10.1172/jci29042

122. Tidyman, W. E., Lee, H. S., & Rauen, K. A. (2011). Skeletal muscle pathology in Costello and cardio-facio-cutaneous syndromes: Developmental consequences of germline Ras/MAPK activation on myogenesis. American Journal of Medical Genetics Part C: Seminars in Medical Genetics, 157(2), 104-114. doi:10.1002/ajmg.c.30298

123. Stevenson, D. A., Allen, S., Tidyman, W. E., Carey, J. C., Viskochil, D. H., Stevens, A., . . . Rauen, K. A. (2012). Peripheral muscle weakness in RASopathies. Muscle & Nerve, 46(3), 394-399. doi:10.1002/mus.23324

124. Kontaridis, M. I., Swanson, K. D., David, F. S., Barford, D., & Neel, B. G. (2005). PTPN11 (Shp2) Mutations in LEOPARD syndrome have dominant negative, not activating, effects. Journal of Biological Chemistry, 281(10), 6785-6792. doi:10.1074/jbc.m513068200

125. Volonte, D., Liu, Y., & Galbiati, F. (2005). The modulation of caveolin-1 expression controls satellite cell activation during muscle repair. The FASEB Journal, 19(2), 237-239. doi:10.1096/fj.04-2215fje

126. Miralles, F., Ron, D., Baiget, M., Félez, J., & Muñoz-Cánoves, P. (1998). Differential regulation of urokinase-type plasminogen activator expression by basic

fibroblast growth factor and serum in myogenesis. Journal of Biological Chemistry, 273(4), 2052-2058. doi:10.1074/jbc.273.4.2052

127. Volonte, D., Liu, Y., & Galbiati, F. (2005). The modulation of caveolin-1 expression controls satellite cell activation during muscle repair. The FASEB Journal, 19(2), 237-239. doi:10.1096/fj.04-2215fje

128. Adi, S. (2002). Early stimulation and late inhibition of extracellular signal-regulated kinase 1/2 phosphorylation by IGF-I: A potential mechanism mediating the switch in IGF-1 action on skeletal muscle cell differentiation. Endocrinology, 143(2), 511-516. doi:10.1210/en.143.2.511

129. Lawlor, M. A., Feng, X., Everding, D. R., Sieger, K., Stewart, C. E., & Rotwein, P. (2000). Dual control of muscle cell survival by distinct growth factor-regulated signaling pathways. Molecular and Cellular Biology, 20(9), 3256-3265. doi:10.1128/mcb.20.9.3256-3265.2000

130. Jones, N. C., Fedorov, Y. V., Rosenthal, R. S., & Olwin, B. B. (2000). ERK1/2 is required for myoblast proliferation but is dispensable for muscle gene expression and cell fusion. Journal of Cellular Physiology, 186(1), 104-115. doi:10.1002/1097-4652(200101)186:1<104::aid-jcp1015>3.0.co;2-0

131. Lathrop, B. (1985). Control of myogenic differentiation by fibroblast growth factor is mediated by position in the G1 phase of the cell cycle. The Journal of Cell Biology, 101(6), 2194-2198. doi:10.1083/jcb.101.6.2194

132. Dorman, C. M., & Johnson, S. E. (1999). Activated Raf inhibits avian myogenesis through a MAPK-dependent mechanism. Oncogene, 18(37), 5167-5176. doi:10.1038/sj.onc.1202907

133. Vaidya, T. B., Rhodes, S. J., Taparowsky, E. J., & Konieczny, S. F. (1989). Fibroblast growth factor and transforming growth factor beta repress transcription of the myogenic regulatory gene MyoD1. Molecular and Cellular Biology, 9(8), 3576-3579. doi:10.1128/mcb.9.8.3576

134. Rommel, C. (1999). Differentiation stage-specific inhibition of the Raf-MEK-ERK pathway by Akt. Science, 286(5445), 1738-1741. doi:10.1126/science.286.5445.1738

135. Sternberg, E. A., Spizz, G., Perry, M. E., & Olson, E. N. (1989). A ras-dependent pathway abolishes activity of a muscle-specific enhancer upstream from the muscle creatine kinase gene. Molecular and Cellular Biology, 9(2), 594-601. doi:10.1128/mcb.9.2.594

136. Olwin, B. B. (1988). Cell surface fibroblast growth factor and epidermal growth factor receptors are permanently lost during skeletal muscle terminal differentiation in culture. The Journal of Cell Biology, 107(2), 761-769. doi:10.1083/jcb.107.2.761

137. Hamilton, D. L., Philp, A., Mackenzie, M. G., & Baar, K. (2010). Prolonged activation of S6K1 does not suppress IRS or PI-3 kinase signaling during muscle cell differentiation. BMC Cell Biology, 11(1), 37. doi:10.1186/1471-2121-11-37

138. Sarbassov, D. D. (1998). Insulin receptor substrate-1 and phosphatidylinositol 3-kinase regulate extracellular signal-regulated kinase-dependent and -independent

signaling pathways during myogenic differentiation. Molecular Endocrinology, 12(12), 1870-1878. doi:10.1210/me.12.12.1870

139. Cho, Y., Yao, K., Bode, A. M., Bergen, H. R., Madden, B. J., Oh, S., . . . Dong, Z. (2007). RSK2 mediates muscle cell differentiation through regulation of NFAT3. Journal of Biological Chemistry, 282(11), 8380-8392. doi:10.1074/jbc.m611322200

140. Schiaffino, S., & Reggiani, C. (2011). Fiber types in mammalian skeletal muscles. Physiological Reviews, 91(4), 1447-1531. doi:10.1152/physrev.00031.2010

141. Schuler, M., & Pette, D. (1996). Fiber transformation and replacement in low-frequency stimulated rabbit fast-twitch muscles. Cell and Tissue Research, 285(2), 297-303. doi:10.1007/s004410050647

142. Pette, D., & Staron, R. S. (2000). Myosin isoforms, muscle fiber types, and transitions. Microscopy Research and Technique, 50(6), 500-509. doi:10.1002/1097-0029(20000915)50:6<500::aid-jemt7>3.3.co;2-z

143. Lynch, C. J., Xu, Y., Hajnal, A., Salzberg, A. C., & Kawasawa, Y. I. (2015). RNA sequencing reveals a slow to fast muscle fiber type transition after olanzapine infusion in rats. Plos One, 10(4). doi:10.1371/journal.pone.0123966

144. Miyazaki, M., Hitomi, Y., Kizaki, T., Ohno, O., Haga, S., & Takemasa, T. (2004). Contribution of the calcineurin signaling pathway to overload-induced skeletal muscle fiber-type transition. Journal of Physiology and Pharmacology, 55(4), 751-764.

145. Laplante, M., & Sabatini, D. M. (2013). Regulation of mTORC1 and its impact on gene expression at a glance. Journal of Cell Science, 126(8), 1713-1719. doi:10.1242/jcs.125773

146. Sandri, M. (2013). Protein breakdown in muscle wasting: Role of autophagy-lysosome and ubiquitin-proteasome. The International Journal of Biochemistry & Cell Biology, 45(10), 2121-2129. doi:10.1016/j.biocel.2013.04.023

147. Lecker, S. H., Jagoe, R. T., Gilbert, A., Gomes, M., Baracos, V., Bailey, J., . . . Goldberg, A. L. (2004). Multiple types of skeletal muscle atrophy involve a common program of changes in gene expression. The FASEB Journal, 18(1), 39-51. doi:10.1096/fj.03-0610com

148. Massagué, J. (2012). TGFβ signalling in context. Nature Reviews Molecular Cell Biology, 13(10), 616-630. doi:10.1038/nrm3434

149. Massague, J. (2005). Smad transcription factors. Genes & Development, 19(23), 2783-2810. doi:10.1101/gad.1350705

150. Imamura, T., Takase, M., Nishihara A, A., Oeda, E., Hanai J, J., Kawabata, M., & Miyazono, K. (1997). Smad6 inhibits signalling by the TGF-beta superfamily. Nature, 389(6651), 622-626. doi:10.1038/39355

151. Hayashi, H., Abdollah, S., Qiu, Y., Cai, J., Xu, Y., Grinnell, B. W., . . . Falb, D. (1997). The MAD-related protein Smad7 associates with the TGFβ receptor and functions as an antagonist of TGFβ signaling. Cell, 89(7), 1165-1173. doi:10.1016/s0092-8674(00)80303-7

152. Mcpherron, A. C., Lawler, A. M., & Lee, S. (1997). Regulation of skeletal muscle mass in mice by a new TGF-p superfamily member. Nature, 387(6628), 83-90. doi:10.1038/387083a0

153. Lokireddy , S., McFarlane, C., Ge, X., Zhang, H., Sze, S. K., Sharma, M., & Kambadur, R. (2011). Myostatin induces degradation of sarcomeric proteins through a Smad3 signaling mechanism during skeletal muscle wasting. Molecular Endocrinology, 25(11), 1936-1949. doi:10.1210/me.2011-1124

154. Trendelenburg, A. U., Meyer, A., Rohner, D., Boyle, J., Hatakeyama, S., & Glass, D. J. (2009). Myostatin reduces Akt/TORC1/p70S6K signaling, inhibiting myoblast differentiation and myotube size. American Journal of Physiology-Cell Physiology, 296(6). doi:10.1152/ajpcell.00105.2009

155. Hitachi, K., Nakatani, M., & Tsuchida, K. (2014). Myostatin signaling regulates Akt activity via the regulation of miR-486 expression. The International Journal of Biochemistry & Cell Biology, 47, 93-103. doi:10.1016/j.biocel.2013.12.003

156. Conery, A. R., Cao, Y., Thompson, E. A., Townsend, C. M., Ko, T. C., & Luo, K. (2004). Akt interacts directly with Smad3 to regulate the sensitivity to TGF-β-induced apoptosis. Nature Cell Biology, 6(4), 366-372. doi:10.1038/ncb1117

157. Winbanks, C. E., Chen, J. L., Qian, H., Liu, Y., Bernardo, B. C., Beyer, C., . . . Gregorevic, P. (2013). The bone morphogenetic protein axis is a positive regulator of skeletal muscle mass. The Journal of Cell Biology, 203(2), 345-357. doi:10.1083/jcb.201211134

158. Moresi, V., Williams, A. H., Meadows, E., Flynn, J. M., Potthoff, M. J., Mcanally, J., . . . Olson, E. N. (2010). Myogenin and class II HDACs control neurogenic muscle atrophy by inducing E3 ubiquitin ligases. Cell, 143(1), 35-45. doi:10.1016/j.cell.2010.09.004

159. Liu, W., & Chakkalakal, J. V. (2017). The Composition, development, and regeneration of neuromuscular junctions. Current Topics in Developmental Biology, 126, 99-124. doi:10.1016/bs.ctdb.2017.08.005

160. Mendoza, M. C., Er, E. E., & Blenis, J. (2011). The Ras-ERK and PI3K-mTOR pathways: cross-talk and compensation. Trends in Biochemical Sciences, 36(6), 320-328. doi:10.1016/j.tibs.2011.03.006

161. Knight, J. D., & Kothary, R. (2011). The myogenic kinome: protein kinases critical to mammalian skeletal myogenesis. Skeletal Muscle, 1(1), 29. doi:10.1186/2044-5040-1-29

162. Sartori, R., Gregorevic, P., & Sandri, M. (2014). TGFβ and BMP signaling in skeletal muscle: potential significance for muscle-related disease. Trends in Endocrinology & Metabolism, 25(9), 464-471. doi:10.1016/j.tem.2014.06.002

CHAPTER II

MANUSCRIPT#1[*]

2.1 Overview

To test the role of extracellular signal-regulated kinases 1 and 2 (ERK1/2) in slow-twitch, type 1 skeletal muscle fibers, we studied the soleus muscle in mice genetically deficient for myofiber ERK1/2. Young adult mutant soleus was drastically wasted, with highly atrophied type 1 fibers, denervation at most synaptic sites, induction of "fetal" acetylcholine receptor gamma subunit (AChRγ), reduction of "adult" AChRε, and impaired mitochondrial biogenesis and function. In weanlings, fiber morphology and mitochondrial markers were mostly normal, yet AChRγ upregulation and AChRε downregulation were observed. Synaptic sites with fetal AChRs in weanling muscle were ~3% in control and ~40% in mutants, with most of the latter on type 1 fibers. These results suggest that: (1) ERK1/2 are critical for slow-twitch fiber growth; (2) a defective γ/ε-AChR subunit switch, preferentially at synapses on slow fibers, precedes wasting of mutant soleus; (3) denervation is likely to drive this wasting, and (4) the neuromuscular synapse is a primary subcellular target for muscle ERK1/2 function in vivo.

[*] This chapter is re-printed from Defective Acetylcholine Receptor Subunit Switch Precedes Atrophy of Slow-Twitch Skeletal Muscle Fibers Lacking ERK1/2 Kinases in Soleus Muscle by Shuo Wang et al., 2016 Scientific Reports, 6, 38745, Springer Nature, Australia. Copyright [2018] by Springer Nature. This is an open access article distributed under the terms of the Creative Commons CC BY license, which permits unrestricted use, distribution, and reproduction in any medium, provided the original work is properly cited.

2.2 Introduction

Developmental switches in the subunit composition of ligand-gated ion channels that serve as neurotransmitter receptors at glutamatergic, GABAergic, and cholinergic synapses are important for structural and functional synaptic maturation throughout the nervous system. The subunit composition of acetylcholine receptors (AChRs) in the postsynaptic apparatus at developing neuromuscular junctions (NMJ) in the mammalian embryo is $\alpha_2\beta\gamma\delta$. As the synapses mature neonatally, these "fetal" AChRs are gradually replaced by "adult" receptors composed of $\alpha_2\beta\delta\varepsilon$, which have different channel conductance properties[1, 2]. Germline deletion of *Chrne*[3–5], the gene encoding AChRε , yields mice that survive embryonic development but harbor NMJs with much lower AChR density that retain AChRγ . These animals have defective neuromuscular transmission, display gradual muscle weakness and atrophy, and die by 2–3 months after birth. Thus the γ /ε -AChR subunit switch is essential for normal skeletal muscle development. Extracellular signal-regulated kinases 1 and 2 (ERK1/2), the prototypical mitogen-activated protein kinases, mediate a multitude of responses to growth factors and cytokines in cellular proliferation, differentiation, senescence, apoptosis, and survival[6]. ERK1/2 have been implicated in the maintenance of adult skeletal muscle mass[7] and, seemingly paradoxically, in the control of both the fast-twitch (type 2)[8] and the slow-twitch (type 1)[9] fiber type phenotypes. Previously[10], we generated mice genetically deficient in myofiber ERK1/2. These animals survived development but displayed stunted postnatal growth, muscle weakness and shorter lifespan. We studied

two fast-twitch muscles in young adult mice, the sternomastoid (STN) and the tibialis anterior (TA), and found that in both mutant muscles NMJs became fragmented and had reduced *Chrne* expression. In STN, but not TA, we documented morphological and molecular evidence of partial denervation (e.g. terminal axonal sprouting and induction of the fetal AChRγ -subunit mRNA, respectively). Both muscles also displayed a mixture of fiber loss and mild atrophy, but minimal changes in fiber-type composition. These results were consistent with a role for ERK1/2 in the maintenance of muscle mass, but not of the fast-twitch fiber phenotype, and demonstrated an important role for ERK1/2 in keeping the structural integrity of the mature NMJ in vivo. In our previous experiments[10], we did not study the effects of lack of ERK1/2 on predominantly slow-twitch muscles, nor could we discern whether the phenotypes observed were primarily derived from synaptic or extrasynaptic functions of myofiber ERK1/2. Here we focused our studies mainly on the soleus (SOL), a prototypical slow-twitch muscle, which unlike the STN and TA has abundant type 1 fibers, rich in mitochondria and highly dependent on oxidative metabolism[11, 12]. ERKs are most active in type 1 fibers[9]. Thus it is important to determine the consequences that develop for these cells when these kinases are absent. We found that fiber morphology in mutant SOL in young adults (9–14 weeks of age) was much more affected than in either the STN or TA. Type 1 fibers in the SOL, in particular, were very atrophied at this age. We also found fragmented NMJs with low levels of AChR expression and evidence of extensive denervation in these muscles. Moreover, defective mitochondrial function and/or biogenesis were part of the phenotype in mutant SOL in young adults. The striking severity and rapidity in the

development of this phenotype facilitated the examination of muscles at different postnatal times. While, at three weeks after birth, control and mutant muscles were similar in fiber morphology, we found evidence of nascent denervation and a defective γ /ε -AChR subunit switch predominantly at NMJs on type 1 fibers. This suggests synaptic instability precedes extrasynaptic changes in myofibers lacking ERK1/2 in SOL. These results also support the notion that the synapse is a primary subcellular target for muscle ERK1/2 function in vivo.

2.3 Results

We combined a germ line *Erk1* mutation with conditional Cre-loxP *Erk2* inactivation in skeletal muscle to produce mice lacking both ERK1/2 selectively in skeletal myofibers (hereafter DKO mice). *Cre* was driven by the human α -skeletal muscle actin (*Hsa*) promoter, which is expressed only in myofibers, and not in other cells in the muscle tissue, starting around embryonic day 9.5[13–15]. In the fast-twitch STN and TA we measured a ~90% reduction in ERK2 levels in mutants relative to control[10]. In DKO SOL, ERK2 levels were ~70% lower than in control (Fig. 2.1). In our initial characterization of these animals, we found they could be divided into two groups according to how fast they lost weight[10]. "Severe" animals lost weight quickly starting at about 7 weeks of age, while "mild" double mutants were able to keep their weight at that age but clearly failed to keep up with controls. Severe and mild DKO mice were generated at about 1:1 ratio, and displayed similar signs of muscle weakness (e.g. forelimb grip strength normalized to body weight) between 7–11 weeks of age[10]. The difference in weight progression between mild and severe DKO mice seemed

unexplained by lower ERK2 in the latter, as residual ERK2 levels were similar between mild and severe DKO muscle ($p = 0.32$; Fig. 2.1). We do not know the reason for these mild/ severe differences but we propose they could be related to undetermined differences in genetic background. For the experiments below all the mutant mice that were 9 weeks or older were DKO mild, while those younger could not be distinguished as mild or severe before that age.

2.3.1. Effects on Fiber Number, Fiber Type Composition, and Preferential Atrophy of Type 1 Fibers

We cut frozen cross sections of SOL muscles from young adults (9–14 weeks old), and stained for dystrophin to mark the cell surface of the myofibers. While control SOL showed a homogenous distribution of fiber sizes, SOL muscle from DKO mice showed a clear reduction in muscle cross-sectional area suggesting fiber loss, with many atrophied and hypertrophied fibers among the remaining myofibers (Fig. 2.2**a**). Although we detected fiber loss in DKO STN, such dramatic heterogeneity in fiber size was not observed in DKO STN or TA of the same age[10]. Next, we used immunostaining for the four canonical adult myosin heavy chains (MyHC types 1, 2A, 2B and 2X) [11] at different postnatal times: 3 (weaning), 5–6, 9, and 14 weeks of age. We followed a protocol that allowed simultaneous staining for all isoforms on the same section; types 1, 2A and 2B by positive staining, 2X by the absence of any staining[16]. Muscles in DKO weanlings appeared similar to controls in cross-sectional area and variability of fiber size (Supplementary Fig. 1), while in young adult DKO, type 1 fibers, in particular, were very atrophied (Fig. 2.2**b**,**c**). We then determined fiber numbers and fiber type

composition in controls and DKOs from such stained cross sections. DKO SOL had slightly fewer fibers than control at weaning, but by 5 weeks of age, DKO SOL had many fewer fibers than control, reaching a ~40% reduction relative to control by 9 weeks (Fig. 2.2**d**). In 9–14 week-old young adults, controls had 835.8 ± 40.2 fibers on average (n = 4), while DKOs had 493.8 ± 44.3 fibers (n = 5). This was a statistically significant reduction (p = 0.0007; t-test). These data suggested a clear postnatal loss of fibers in the DKO SOL. The inset in Fig. 2.2**d** shows representative muscles for control and DKO at 14 weeks and illustrates the extent of wasting at the whole muscle level. Muscle wet weight was consistent with the above data as 14 week-old DKO SOL weighed ~40% less than control (DKO: 9.45 ± 1.21 mg; n = 4 muscles. Control: 14.72 ± 0.88 mg; n = 6 muscles; p = 0.007). The loss in DKO SOL mass was not simply a reflection of the loss of body weight[10], as even after normalization to body weight, muscle weights remained lower in mutants than in controls (DKO: 0.44 ± 0.07 mg/g, n = 2 animals. Control: 0.58 ± 0.05 mg/g, n = 3 animals). Interestingly, fiber type composition remained largely unchanged, with relative percentages of the most abundant fiber types (1, 2A and 2X) in mutant muscle being similar to those in age-matched control (Fig. 2.2**e**). Nevertheless, some changes in fiber composition that affected rare fiber types in the SOL were observed in DKO muscle. Thus, type 2B fibers, which were a very variable ~4% in control at 3 weeks, were absent in DKO at this age. However, type 2B fibers in control SOL reached the same very low levels in DKO by 5–6 weeks (Fig. 2.2**e**). Type1 + 2A hybrid fibers (Fig. 2.2**c**), which were less than ~0.2% in control, were present at ~5% at 9 weeks or later (Fig. 2.2**e**). When fiber counts were sorted by

fiber type (Supplementary Fig. 2), type 1, 2A and 2X fibers in young adult (9–14 week-old) DKO were all reduced relative to age-matched control. Thus, cell loss affected all major fiber types and started after 3 weeks of age. At 9 weeks, we also analyzed fiber type composition by measuring mRNA levels for the genes encoding the myosin heavy chains (*Myh1*, *Myh2*, *Myh4*, *Myh7*) [11] by real-time PCR. In DKO SOL, a statistically significant ~3-fold reduction of *Myh7* (type 1) mRNA ($p = 0.004$), and a tendency toward reduction in *Myh4* (type 2B) transcript (Fig. 2.3**a**) were observed. In the fast-twitch DKO STN and TA muscles, no statistically significant changes in expression of myosin heavy chain genes were detected, even though a tendency toward decrease was seen for *Myh7* (Supplementary Fig. 3). Our results are better interpreted in the context of the normal levels of *Myh7* expression in each of the muscle groups. *Myh7* expression in control SOL was ~30-fold higher than in STN and TA (Supplementary Fig. 3). Thus, because of higher control levels, the 70% reduction in *Myh7* mRNA expression in DKO SOL is much more meaningful than a similar tendency in TA or STN, where *Myh7* expression is normally very low (i.e. there are very few type 1 fibers in these muscles). The reduction in *Myh7* mRNA levels in the DKO SOL was associated with the preferential atrophy of these fibers (Fig. 2.2**b**,**c**) and not with fiber switching, as relative fiber type composition was largely similar between control and DKO SOL (Fig. 2.2**e**). Indeed, a histogram of fiber areas showed that ~70% of type 1 fibers in 14 week DKO SOL were smaller than 750 μm^2, while almost no fibers that small were found in controls (Fig. 2.3**b**). On the other hand, very small (< 750 μm^2) and very large (> 3000 μm^2) 2A and 2X fibers were much more abundant in DKO SOL than in control (Fig. 2.3**c**,

d), suggesting that these fast-twitch fibers undergo both atrophy and hypertrophy. At 5–6 weeks, average area for all major fiber types was statistically larger in DKO SOL than in control (Supplementary Fig. 4). This result suggests that fibers in DKO SOL may hypertrophy before atrophy ensues, perhaps as a compensation for fiber loss.

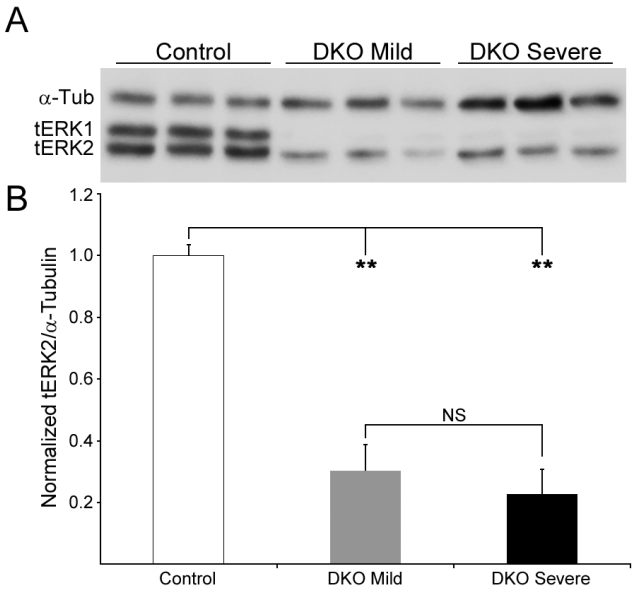

Figure 2.1. ERK1/2 levels in control and DKO 9 week-old SOL.
(**a**) Lysates from 3 separate SOL muscles from Control, DKO mild and DKO severe were probed simultaneously for total ERK1/2 (tERK1/2) and for α –tubulin (α -Tub) to check for loading differences. In DKO muscle, ERK1 was completely eliminated and ERK2 was sharply reduced. (**b**) Normalization to α -Tub showed ERK2 levels were 0.30 ± 0.08 –fold and 0.23 ± 0.08 –fold control levels in DKO mild mice and in DKO severe mice, respectively. Values are mean + SD. **p < 0.01; NS, no significant.

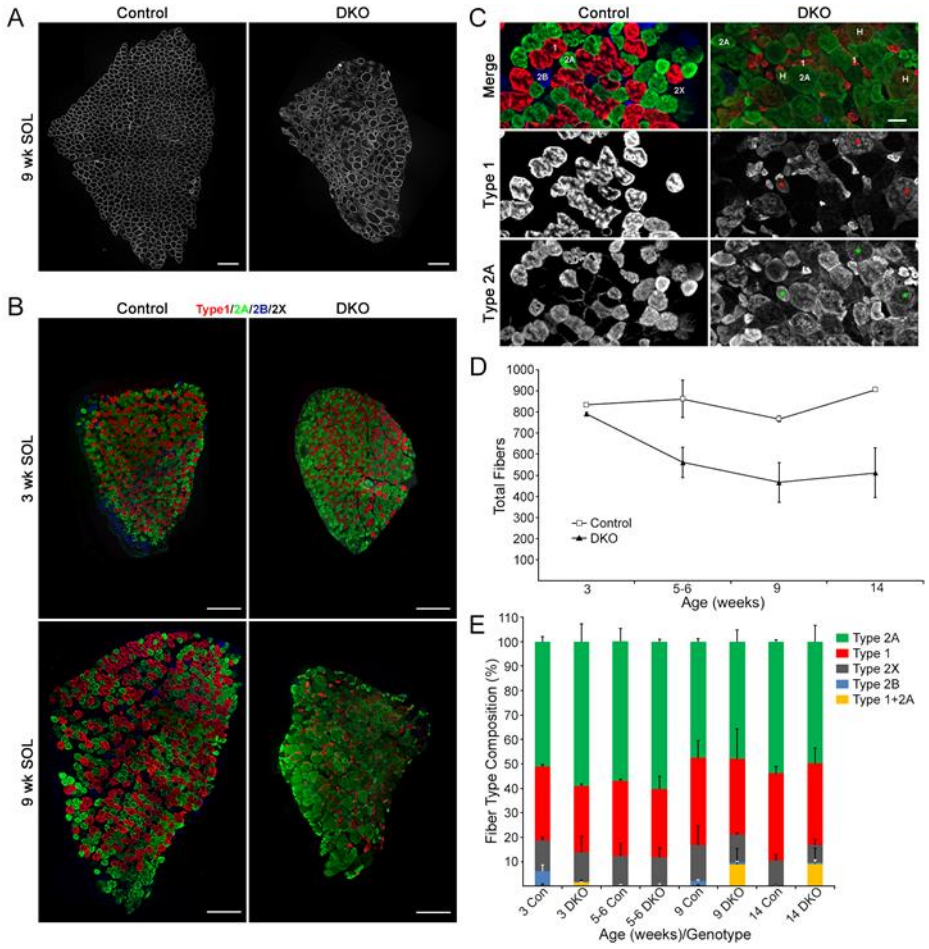

Figure 2.2. Dramatic wasting of the young adult DKO SOL.
(**a**) Cross sections of SOL from 9-week-old control and DKO females stained for dystrophin. Notice reduction in muscle cross-sectional area and dramatic heterogeneity of fiber size in the DKO SOL. Scale bar: 200 μ m. (**b**) Simultaneous immunostaining for MyHC types in SOL. Types 1, 2A, and 2B were positively stained, while type 2X was identified by the absence of staining. At 3 weeks, control and DKO SOL were similar in cross sectional area. Note small size of most type 1 fibers in 9 week DKO. Scale bar: 200 μ m. (**c**) Higher magnification field for MyHC staining at 9 weeks. Examples of hybrid (H, 1 + 2A) fibers are highlighted with asterisks (*). Scale bar: 50 μ m. (**d**) Fiber numbers per cross section in control and DKO SOL at different postnatal times. N = 2–3 muscles per time point/genotype. Values are mean ± SD. Inset shows control (top) and DKO (bottom) representative muscles at 14-weeks (females). Scale bar: 2 mm. (**e**) Fiber type composition in control (CON) and DKO SOL at different postnatal times.
N = 2–3 muscles per time point/genotype. Values are mean + SD.

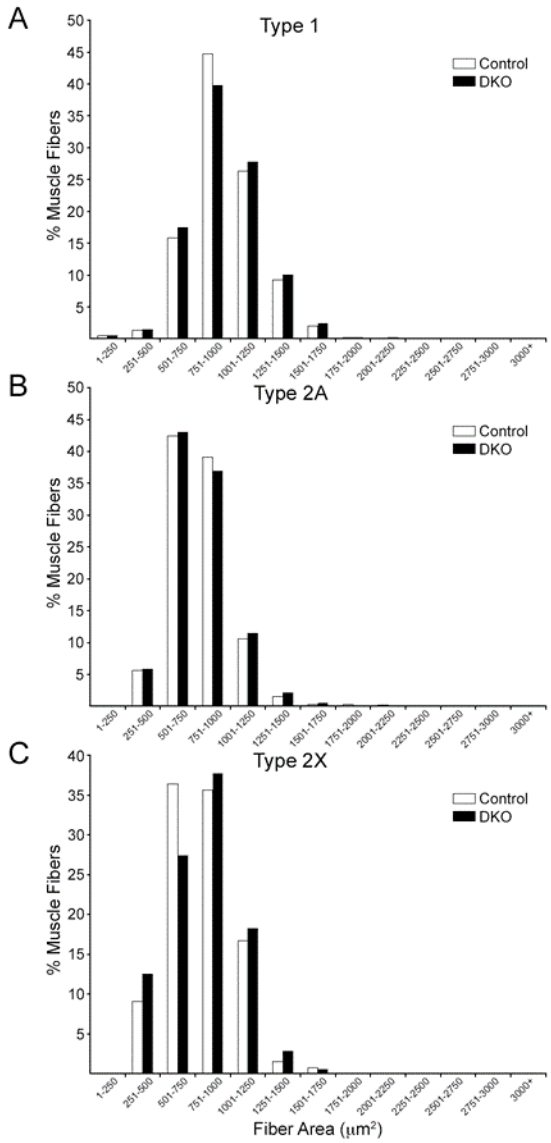

Figure 2.10. (Supplementary Figure 1) Distribution of fiber cross-sectional area by fiber type in the whole soleus muscle at 3 week of age.
Fiber area data for 3-week-old animals are grouped in 250 μm^2 bins along the X axis and the percentages of fibers in those bins are plotted on the Y axis. Fiber area distribution was similar between control and DKO muscles for all fiber types at this age. N=2 control and DKO male muscles. (**a**) Type 1 fibers scored: 457 control, 417 DKO. (**b**) Type 2A fibers scored: 653 control, 802 DKO. (**c**) Type 2X fibers scored: 185 control, 175 DKO. No statistical difference was detected between control and DKO distributions by the Wilconox rank sum test.

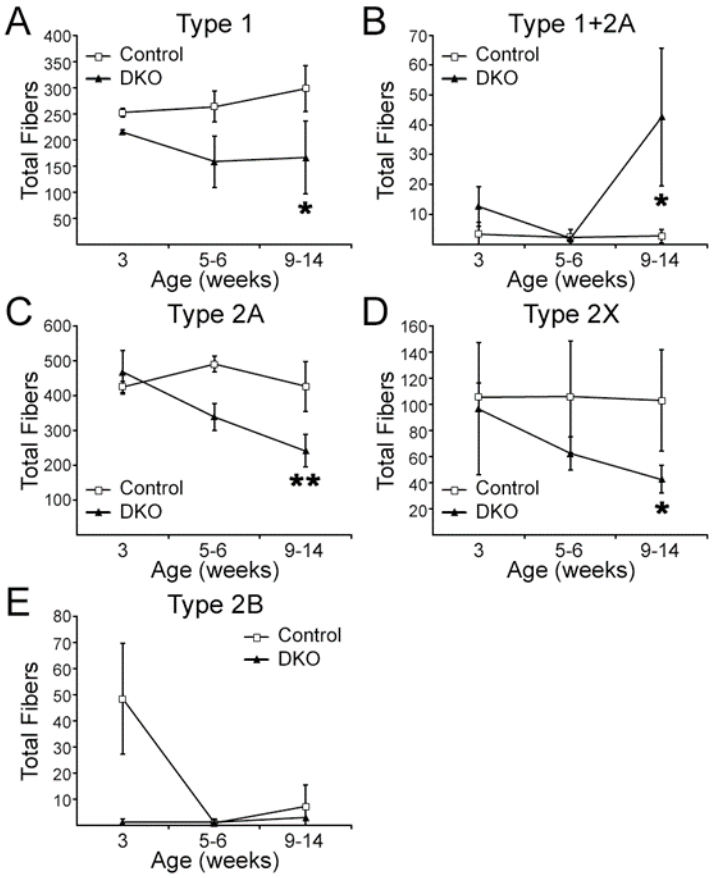

Figure 2.11. (Supplementary Figure 2) Fiber counts by fiber type at different postnatal times.

In young adult DKO SOL (9-14 weeks), type 1+2A hybrids were increased while type 1, 2A and 2X fibers were reduced relative to age-matched controls. Values are mean ± SD. N at 3 weeks: 3 Control, 3 DKO; n at 5-6 weeks: 3 Control, 2 DKO; n at 9 weeks: 2 Control, 2 DKO; n at 14 weeks: 2 control, 3 DKO. Data for 9 and 14 weeks were pooled. **, $p<0.01$; *, $p<0.05$; t-test v. control. P values: 0.013 (**a**); 0.012 (**b**); 0.002 (**c**); 0.012 (**d**).

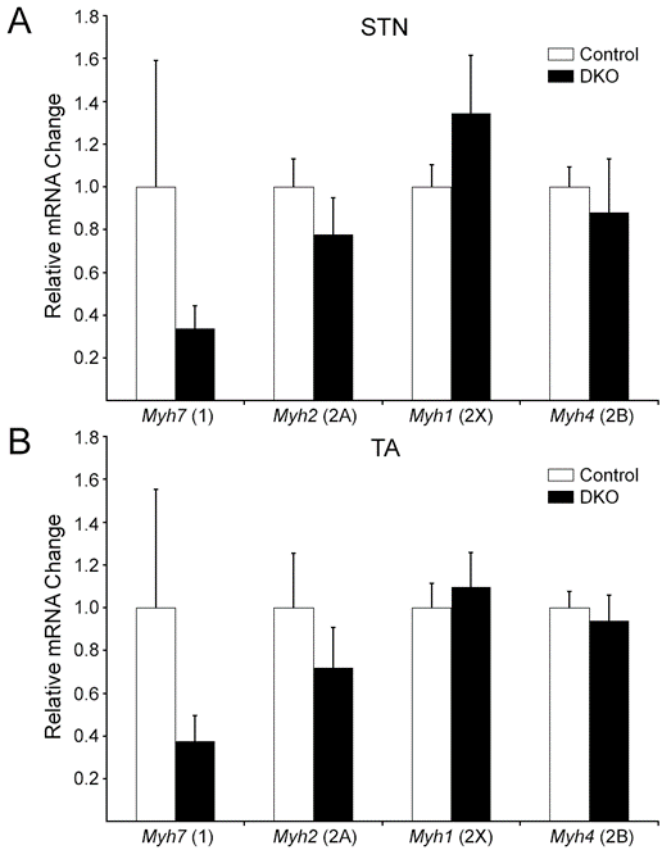

Figure 2.12. (Supplementary Figure 3) Relative *Myh* mRNA expression in young adult STN (a) and TA (b).

Real time PCR for MyHC genes at 9 weeks. N=6 per genotype/muscle. Values are mean + SEM. No statistically significant changes were detected. *Myh7* mRNA levels in control SOL are ~30-fold higher than in either control TA or STN. (**c**) ΔCt data (Ct_{Myh7}-Ct_{18S}) for control SOL, STN and TA. Note that the higher ΔCt the lower the expression level. (**d**) Normalized *Myh7* mRNA expression relative to levels incontrol SOL. N=6 per genotype/muscle. Values are mean + SEM. **, $p<0.01$; t-test vs. SOL.

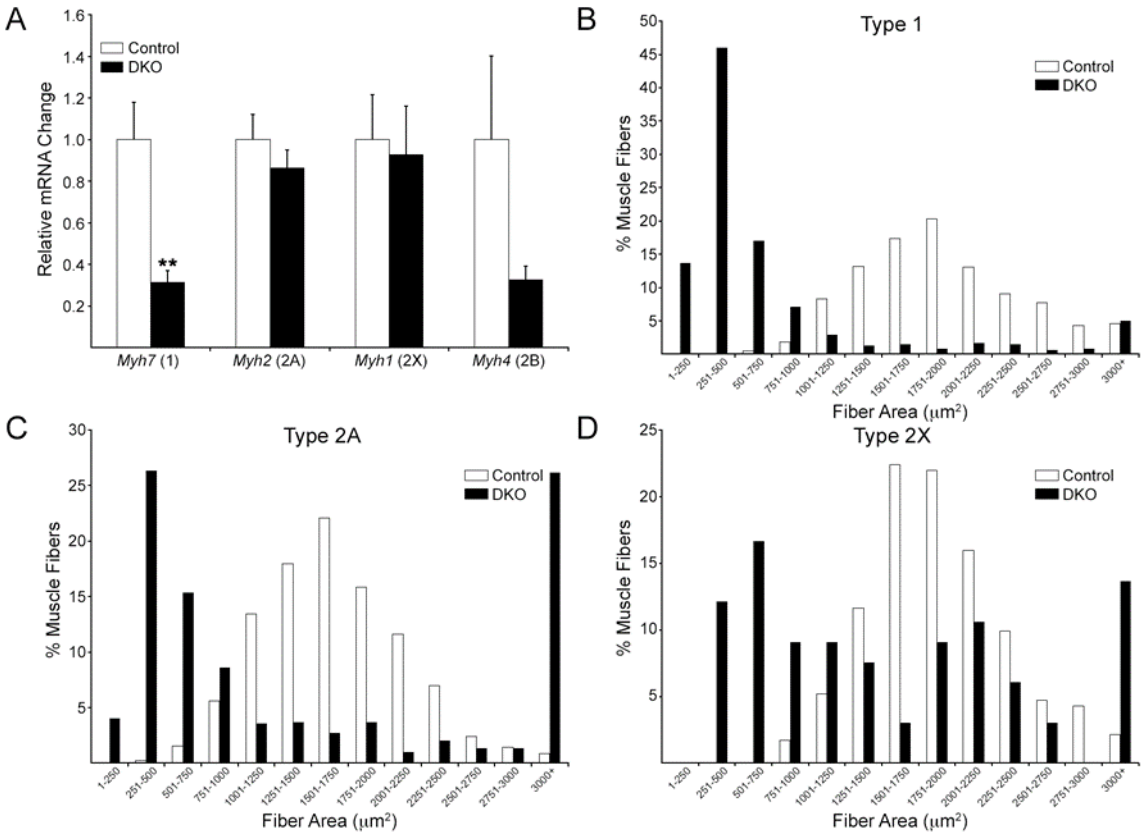

Figure 2.3. Relative *Myh* mRNA expression and area distribution by fiber type. (**a**) Analysis of real-time PCR for MyHC genes at 9 weeks. N = 6 per genotype. Values are mean + SEM. **p < 0.01, t-test v. control. (**b,c,d**) Fiber area data for 14-week-old animals were grouped in 250 μ m^2 bins along the X axis and the percentages of fibers in those bins were plotted on the Y axis. In the DKO SOL, type 1 fibers atrophied, while types 2A and 2X both atrophied and hypertrophied. N = 2, control muscles; 3, DKO muscles. Type 1 fibers scored: 675 control, 476 DKO. Type 2A fibers scored: 914 control, 592 DKO. Type 2X fibers scored: 232 control, 66 DKO. Distributions were compared statistically using the Wilconox rank sum test. $P < 3.2 \times 10^{-5}$ control v. DKO.

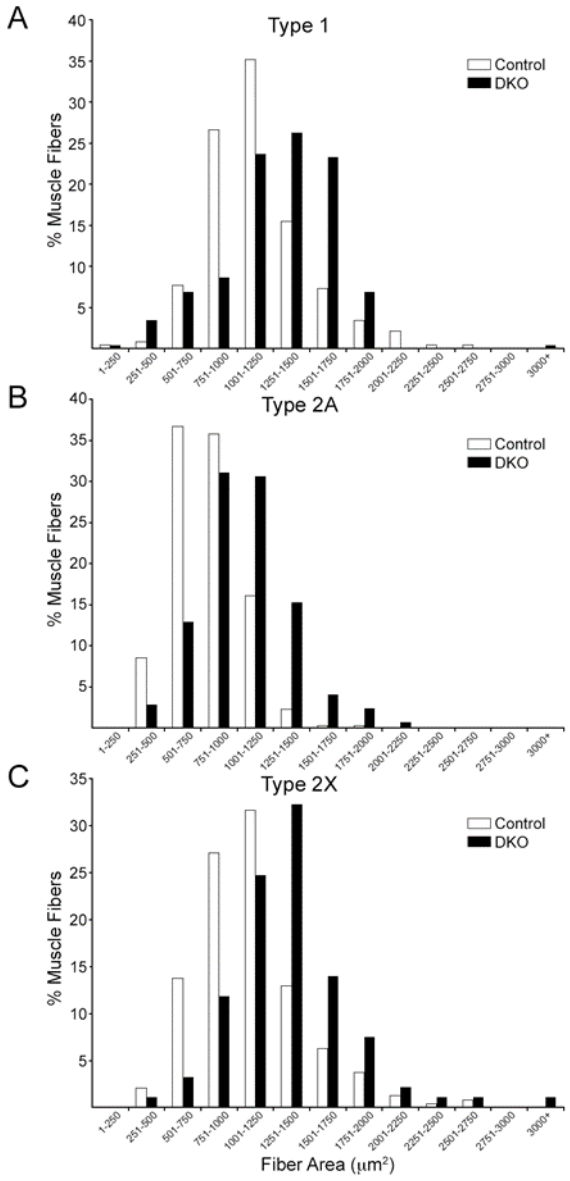

Figure 2.13. (Supplementary Figure 4) Distribution of fiber cross-sectional area by fiber type in the whole soleus muscle at 5-6 week of age.
Fiber area data for 5-6-week-old animals are grouped in 250 μm^2 bins along the X axis and the percentages of fibers in those bins are plotted on the Y axis. Fiber area shifted towards larger sizes for all fiber types at this age. N=2 control and DKO male muscles. (**a**) Type 1 fibers scored: 233 control, 233 DKO. (**b**) Type 2A fibers scored: 314 control, 418 DKO. (**c**) Type 2X fibers scored: 240 control, 91 DKO. Distributions were compared statistically using the Wilconox rank sum test. $P < 2.04 \times 10^{-6}$ control v. DKO.

We also examined type 1 fiber area in two fast-twitch muscles, STN and extensor digitorum longus (EDL) (Supplementary Fig. 5). Type 1 fibers are present at very low numbers in these muscles. Atrophy of type 1 fibers was evident in the 14-week DKO STN as fibers > 300 μ m^2 in area were absent, while present in control. In 14-week DKO EDL, type 1 fiber atrophy was less robust yet statistically present as average fiber area was ~25% lower than control (DKO: 132.17 ± 8.87 μ m2, n = 51 fibers, 4 mice. Control: 178.50 ± 12.18 μ m^2, n = 42 fibers, 4 mice; p = 0.004, t-test; p = 0.008, Wilconox rank sum test). Thus, atrophy of type 1 fibers occurred in all muscles studied.

2.3.2. Effects on Synapse Morphology and Denervation-Related Molecular Markers

As in STN and TA[10], NMJs with signs of fragmentation and diminished AChR expression could be found in young adult DKO SOL (Fig. 2.4**a**, **b**). Using real-time PCR, we found a ~5-fold reduction in AChRε mRNA in DKO SOL relative to control (inset Fig. 2.4**c**; p = 0.000007). There was morphological and molecular evidence of partial denervation in the DKO SOL in young adults (Fig. 2.4). Most notably, there was a ~60-fold increase in mRNA for *Chrng*, the gene encoding the distinctive γ -subunit of the fetal AChR[17] (p = 0.00014), and a ~20-fold induction for *Runx1* mRNA (p = 0.00004), a transcription factor highly induced in skeletal muscle after denervation[18, 19]. Furthermore, the myogenic factor myogenin (*Myog*), the embryonic myosin isoform (*Myh3*), and the agrin-transducing receptor *Musk*, all known markers of denervation[19–21], were also elevated between ~3- and 6-fold over control (p = 0.00003, 0.013, 0.0004, respectively) (Fig. 2.4**c**). Denervation in the adult induces replacement of the AChRε subunit with the AChRγ subunit at synaptic sites[22]. Staining for AChRγ with subunit-

specific antibodies[23] on cross sections of 14 week-old muscle showed that ~90% of BTX-labeled synaptic sites incorporated these fetal receptors in DKO SOL (Fig. 2.5). Absence of co-staining for the presynaptic marker SV2 suggested denervation at ~70% of these sites (Fig. 2.5). Even most of the $SV2^+$ NMJs were also AChRγ^+ (Fig. 2.5**b**). Staining of serial sections with AChRε subunit-specific antibodies[23] was consistent with the AChRγ staining, and directly showed that only ~10% of synaptic sites were AChRε^+ / $SV2^+$ in DKO SOL while over 90% were so in control (Fig. 2.5**b**). Thus, by 14 weeks in DKO SOL, most NMJs appeared denervated and had γ -subunit-containing AChRs. The presence of type 1 + 2A hybrid fibers in DKO SOL of young adults (Fig. 2.2**e**, above), and the selective reduction of Myh7 mRNA (Fig. 2.3**a**) were also consistent with denervation/re-innervation cycles occurring in this muscle[24–26]. Thus, DKO SOL in young adults showed signs of marked NMJ instability that included reduction of AChRε expression and loss of nerve-muscle contact.

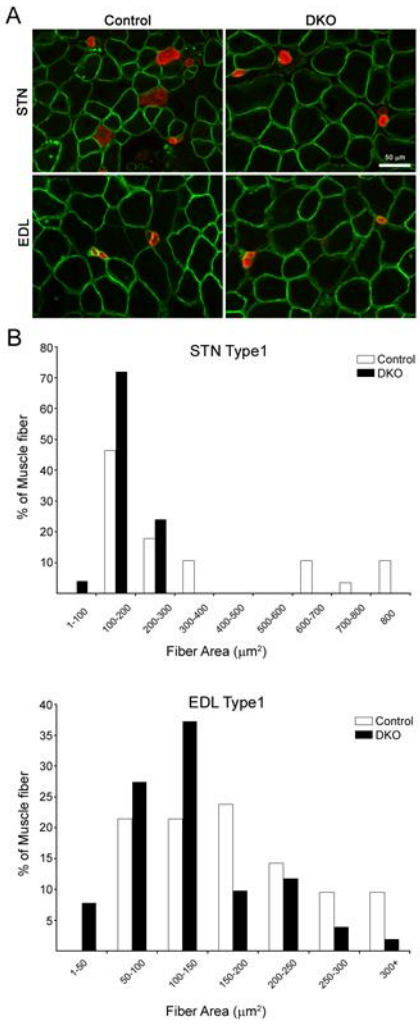

Figure 2.14. (Supplementary Figure 5) Type 1 fibers in DKO mice undergo atrophy in fast twitch STN and EDL.

(**a**) Representative fields from cross sections of 14-week-old control and DKO STN and EDL stained for type 1 MyHC (red) and for laminin (green). Three, larger-area fibers in the control STN are indicated by arrowheads. Five smaller type 1 fibers are also visible in this field. EDL type 1 fibers are typically small regardless of genotype. Scale bar: 50 μm. (**b**) Type 1 fiber area data were grouped in 100- (STN) and 50-μm^2 bins (EDL) along the X axes, respectively, and the percentages of fibers in those bins were plotted on the respective Y axes. In STN, fibers larger than 300 μm^2 were present in control but absent in the DKO. In EDL, fiber size distribution was slightly, but statistically significantly shifted to smaller sizes (p=0.004, t-test; p=0.008, Wilconox rank sum test). STN: n=3 muscles per genotype; 28 fibers, control; 25 fibers, DKO. EDL: n=4 muscles per genotype; 51 fibers, control; 42 fibers, DKO.

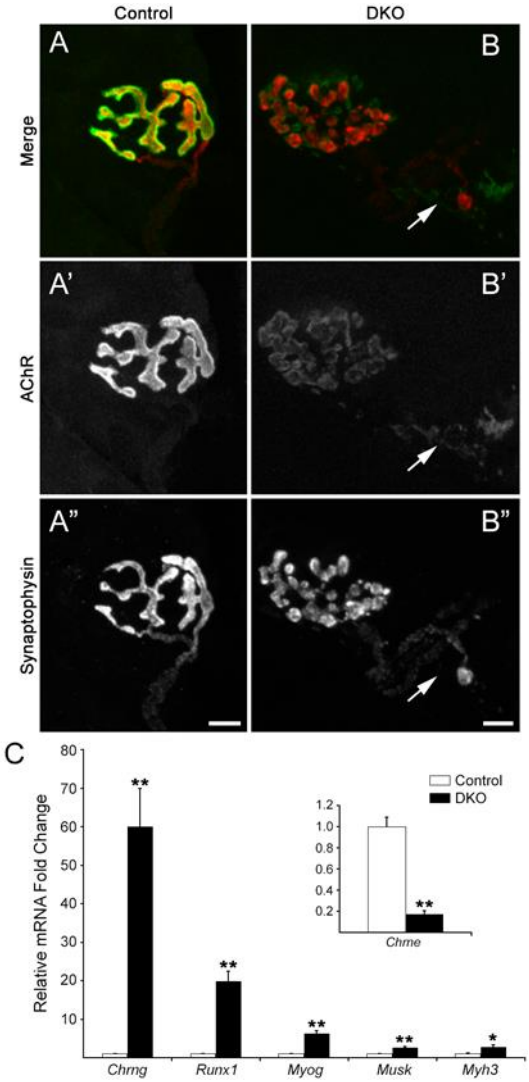

Figure 2.4. Synaptic alterations in young adult DKO SOL.
(**a**) Confocal "en face" view of a 9-week control NMJ labeled with fluorescein-BTX to mark AChRs (**a'**) and with antibodies to synaptophysin, followed by rhodamine-conjugated secondary antibodies, to label nerve terminals (**a"**). Long, continuous AChR domains are tightly apposed by nerve terminals. (**b**) Confocal "en face" view of a fragmented NMJ in 9-week DKO muscle with small, mostly round, dim AChR domains (**b'**) variably apposed by nerve terminal staining (**b"**). Arrow: Side view of an aneural synaptic site with very weak AChR staining and axonal retraction bulb. Scale bar: 10 μ m. (**c**) Real-time PCR of mRNA for denervation and postsynaptic genes at 9 weeks. Chrne was reduced by ~5-fold (inset), while the other mRNAs were increased between 3- and 60-fold. N = 6 per genotype. Values are mean + SEM. **p < 0.01; *p < 0.05; t-test v. control

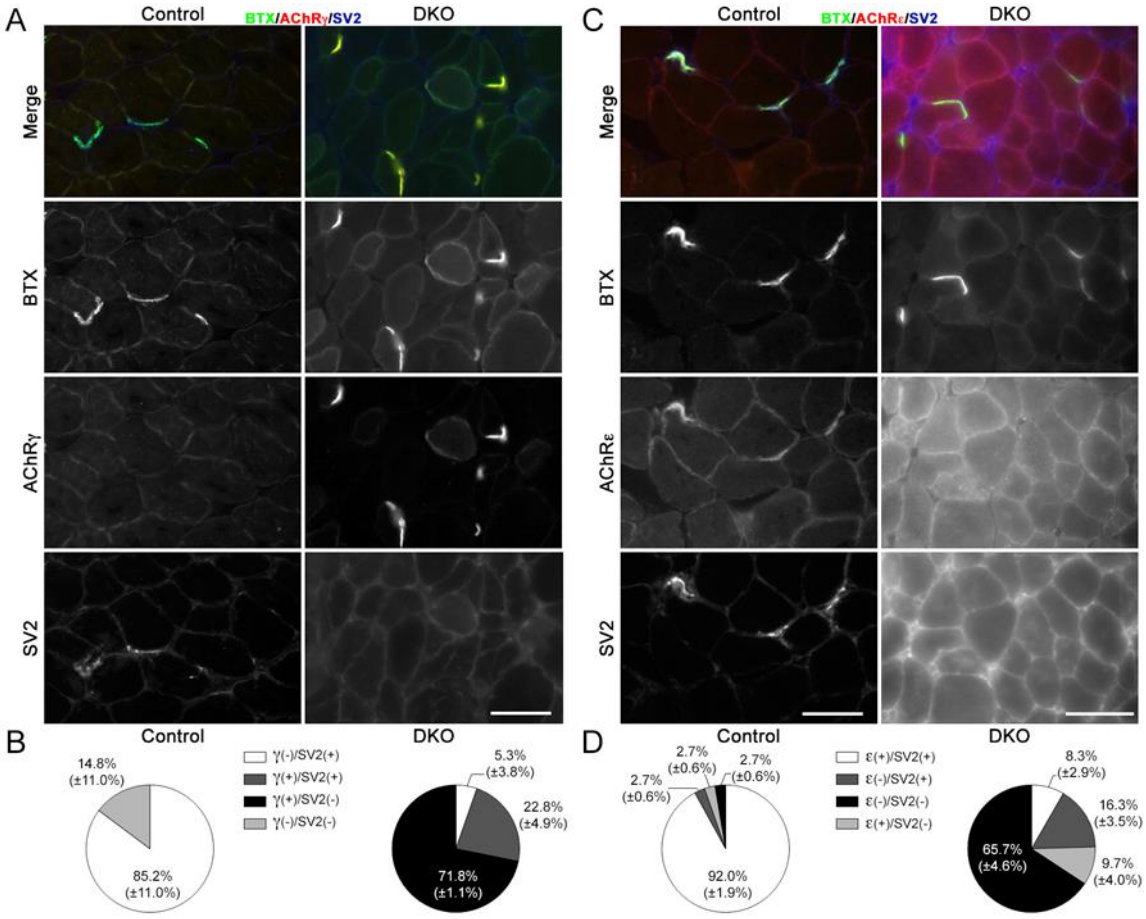

Figure 2.5. AChRγ/ε staining in 14 week SOL cross-sections.
(**a**) Control pictures show 3 innervated NMJs ($SV2^{+}$) that failed to label for AChRγ ($AChR\gamma^{-}$). DKO pictures show 5 $AChR\gamma^{+}$ /$SV2^{-}$ synaptic sites. Scale bar: 50 μ m. (**b**) Quantification for AChRγ /SV2/BTX staining. Values are mean ± (SD). N = 2 control muscles, 74 endplates; 3 DKO muscles, 100 endplates. (**c**) Control pictures show 3 innervated NMJs ($SV2^{+}$) that label for AChRε ($AChR\varepsilon^{+}$). DKO pictures show 5 synaptic sites, two strongly positive for BTX and 3 with weak BTX staining. All 5 sites lack both AChRε and SV2 staining. Scale bars: 50 μ m. (**d**) Quantification for AChRε /SV2/ BTX staining. Values are mean ± (SD). N = 2 control muscles, 77 endplates; 3 DKO muscles, 77 endplates.

2.3.3. Mitochondrial Alterations

Given that over 70% of myofibers in the SOL are metabolically oxidative (type 1

and type 2A), we assessed oxidative capacity on cross sections of 9–14 week-old SOL by cytochemical staining for cytochrome oxidase (COX) and succinate dehydrogenase (SDH)[27]. These enzymes showed much reduced activity in DKO SOL relative to control at this age (Fig. 2.6**a**), consistent with diminished mitochondrial function. Next, we used real-time PCR to measure mRNA levels of the regulators of mitochondrial biogenesis peroxisome proliferator-activated receptor γ coactivator 1α (*PGC-1α*[28]) and *PGC-1β*[29], the mitochondrial fusion/fission markers mitofusin 1 and 2 (*Mfn1, Mfn2*), dynamin-related protein 1 (*Drp1*) [30], and the mitochondrial markers BCL2/Adenovirus E1B 19 kDa interacting protein 3 (*Bnip3*), cytochrome b (*Cytob*), and uncoupling protein 3 (*Ucp3*). While *Ucp3* tended to decrease and *Drp1* did not change, we found statistically significant ~2-fold reductions in mRNA for *PGC-1β*, *Mfn1* and *Mfn2*, *Bnip3*, *Cytob* and *PGC-1α* (p values = 0.005, 0.02, 0.009, 0.001, 0.0003, 0.01, respectively) (Fig. 2.6**b**). A ~3-fold reduction in PGC-1α protein was also detected in the DKO SOL (p = 0.01; Fig. 2.6**c**). In contrast, *PGC-1α* mRNA in the fast twitch STN and TA muscles were not different between mutant and control at the same age (Supplementary Fig. 6). SOD2, a mitochondrial protein that is a direct downstream target of PCG-1α regulation[31], was reduced ~40% in DKO SOL (p = 0.009; Fig. 2.6**c**). Together, these results suggest that absence of muscle ERK1/2 specifically in the SOL leads to reduced mitochondrial biogenesis, which may account, at least in part, for the lower oxidative capacity reflected by the decrease in COX and SDH activities. These mitochondrial alterations were also in keeping with the ample evidence of denervation found in these muscles[26, 32].

2.3.4. Early Events That Precede Fiber Atrophy And Loss

To search for potential mechanisms that drive the phenotype, we analyzed gene expression at 3 weeks. We chose this time point because fiber loss and atrophy were largely absent (Fig. 2.2**b**,**d** and Supplementary Fig. 1). We specifically focused on genes whose expression levels were altered at 9 weeks: *Myh7* (Fig. 2.3**a**), the denervation/synaptic markers (Fig. 2.4**c**) and mitochondrial genes (Fig. 2.6**b**) as well as key genes for autophagy and ubiquitin-proteasome-mediated proteolysis, since these are primary mechanisms mediating muscle atrophy in most muscle wasting situations[33,34]. Only expression of *Chrne* (decreased by ~2-fold; $p = 0.0006$), *Chrng*, and *Runx1* (increased by ~3- and ~1.3-fold, respectively; $p = 0.004$ and 0.02, respectively) were statistically altered at this early time (Fig. 2.7**a**). Neither *Myh7*, or the other MyHC genes (Fig. 2.7**b**), nor the mitochondrial- or muscle atrophy-related genes (Fig. 2.7**c**) exhibited differences at the mRNA level between DKO and control SOL at this early age. These results suggested that synaptic alterations that may lead to denervation preceded all other phenotypic changes in DKO SOL. To further support this conclusion, we co-stained for AChRγ, SV2 and BTX to check for the presence of synapses expressing the fetal form of the AChR (Fig. 2.8). Control muscles at 3 weeks had a very small and variable fraction of AChRγ $^{+}$/SV2^{+} synapses (2.7 ± 3.4%), consistent with previous reports that showed that AChRγ persists in some NMJs about a week longer in normal SOL than in fast-twitch muscles[35]. However, in DKO muscle 38.5 ± 8.1% of NMJs were AChRγ $^{+}$/SV2^{+} at 3 weeks of age (Fig. 2.8**a**, **b**). This ~10-fold difference in AChRγ $^{+}$/SV2^{+} NMJs between DKO and control was statistically significant ($p = 0.002$). Consistent with the

slight but statistically significant increase in Runx1 mRNA (Fig. 2.7) and the presence of a few type1 + 2A hybrid fibers in the DKO SOL at 3 weeks (Fig. 2.2**e**), a small, highly-variable fraction of endplates (3.4 ± 3.7%) appeared denervated as they lacked SV2 staining and were AChRγ $^{+}$ (Fig. 2.8**b**). AChRγ $^{+}$ /SV2^{-} synaptic sites were not detected in control muscles (Fig. 2.8**b**). Staining for AChRε at this early age showed a statistically significant increase in AChRε $^{-}$/SV2^{+} NMJs in DKO muscle relative to control (13.4 ± 2.4% and 4.2 ± 2.2%, respectively; p = 0.008) and a corresponding reduction in AChRε $^{+}$ /SV2^{+} endplates (89.4 ± 4.5% control, 79.6 ± 5.2% DKO) that almost reached statistical significance (p = 0.07) (Fig. 2.8**c**, **d**). Because the fraction of AChRγ $^{+}$ /SV2^{+} NMJs (38.5 ± 8.1%) is larger than the fraction of AChRε $^{-}$/SV2^{+} NMJs (13.4 ± 2.4%), it is likely that many of the AChRε $^{+}$ /SV2^{+} junctions are also AChRγ $^{+}$ in weanling DKO muscles. In this context, it should be mentioned that extrasynaptic background staining tended to be higher, particularly in DKO muscle, when staining for AChRε than when staining for AChRγ (Figs 2.5 and 2.8), which made the quantification more challenging for the former than for the latter. We next stained simultaneously for AChRγ, positively for MyHCs 1 and 2A, negatively for 2X + 2B, and added BTX to try to determine if AChRγ -containing NMJs preferentially localized to a particular fiber type at this early time in DKO SOL. We found that 71% of AChRγ $^{+}$ endplates occurred on type 1 fibers (40/56 endplates, n = 3 muscles), while 25% and 2% of endplates containing this subunit were found on type 2A and 2X/2B fibers, respectively (Fig. 2.9). Thus despite higher proportion of type 2 fibers in SOL (Fig. 2.2**e**), synapses on type 1 fibers were much more susceptible to alteration following ERK1/2 deficiency than those

on type 2 fibers. Taken together, these results strongly suggest that a defective γ /ε - AChR switch and perhaps even loss of synaptic connectivity, particularly on type 1 fibers, are early events in the development of the wasting phenotype in DKO SOL.

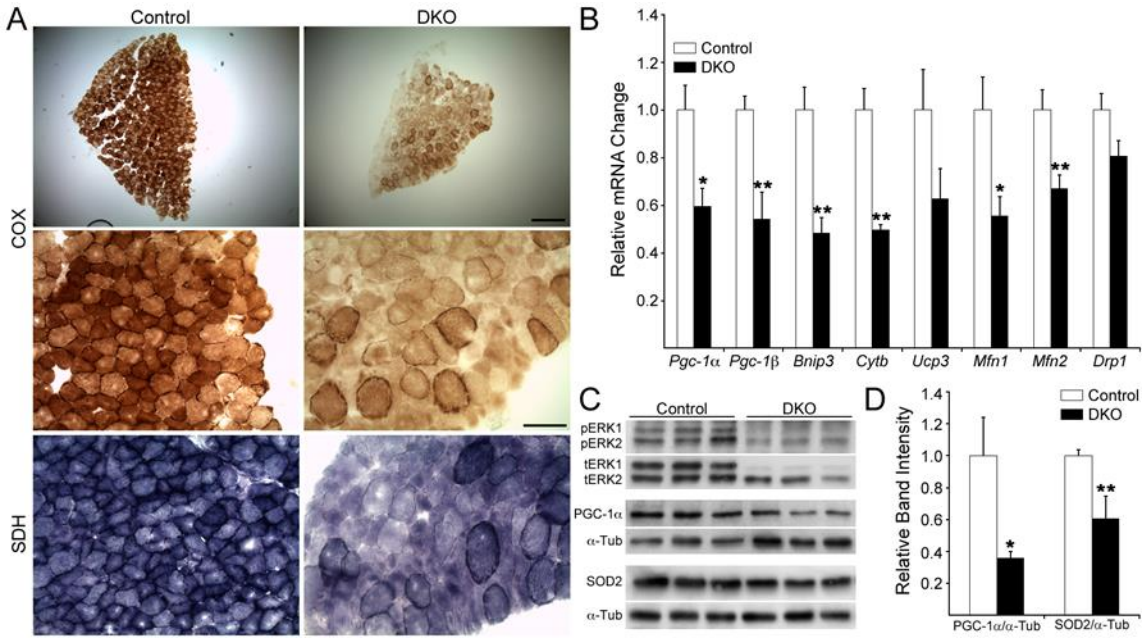

Figure 2.6. Mitochondrial phenotype in young adult DKO SOL.
(**a**) Reduced cytochrome oxidase (COX) and succinate dehydrogenase (SDH) activity on control and DKO SOL cross sections of 9 week mice. Scale bars: Top row pictures 200 μ m; middle and bottom row pictures 50 μ m. N = 2 per genotype. (**b**) Real-time PCR for mRNA of mitochondrial markers on 9 week SOL. N = 6 per genotype. Values are mean + SEM. *p < 0.05; **p < 0.01; t-test v. control. (**c**) Top 2 Western blots illustrate active (pERK1/2) and total (tERK1/2) ERK protein levels in 9-week control and DKO SOL. The same lysates were probed in separate blots for PGC-1α (middle blot) and SOD2 (bottom blot). Loading of PGC-1α and SOD2 blots was assayed with α -tubulin antibody (α -Tub, bottom blot). (d) PCG-1α and SOD2 quantification. N = 3 per genotype. Values are mean + SD. *p < 0.05; **p < 0.01; t-test v. control.

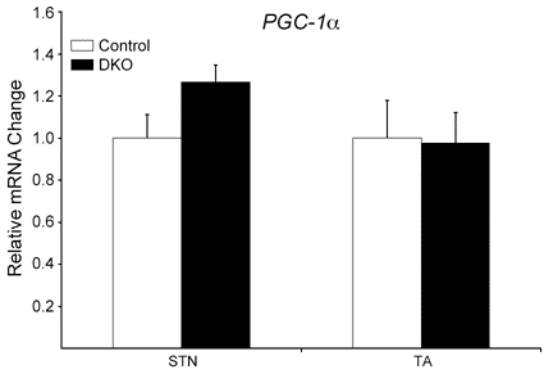

Figure 2.15. (Supplementary Figure 6) Relative *PGC-1α* mRNA expression in young adult STN and TA.
Real time PCR for *PGC-1α* at 9 weeks. N=6 per genotype/muscle. Values are mean + SEM. No statistically significant changes were detected.

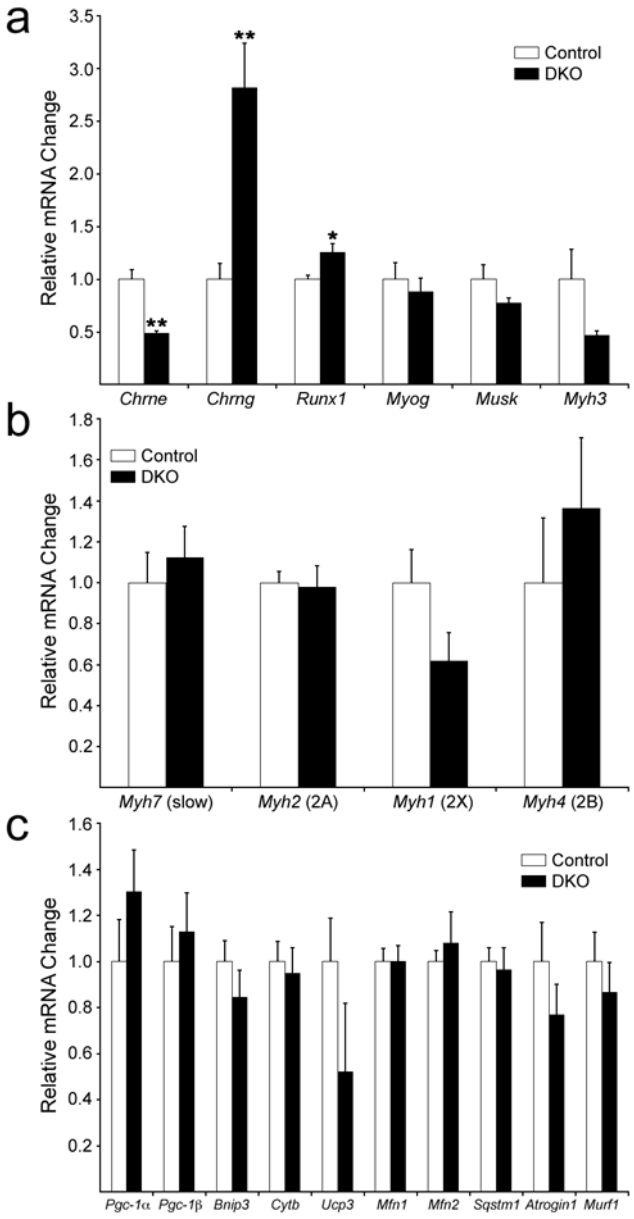

Figure 2.7. Relative mRNA expression at 3 weeks.
(**a**) Real-time PCR of mRNA for denervation and postsynaptic genes at 3 weeks. *Chrne* was reduced by ~2-fold, while *Chrng* and *Runx1* were increased by ~3- and 1.3-fold, respectively. (**b**) Real-time PCR of mRNA for MyHC genes. (**c**) Real-time PCR of mRNA for mitochondrial (*Pgc-1α – Mfn2*) and protein degradation genes (*Sqstm1* (p62), *Atrogin1* and *Murf1*). None of these genes showed any expression changes with genotype at this age. N = 6 control, 5 DKO. Values are mean + SEM. **p < 0.01; *p < 0.05; t-test v. control.

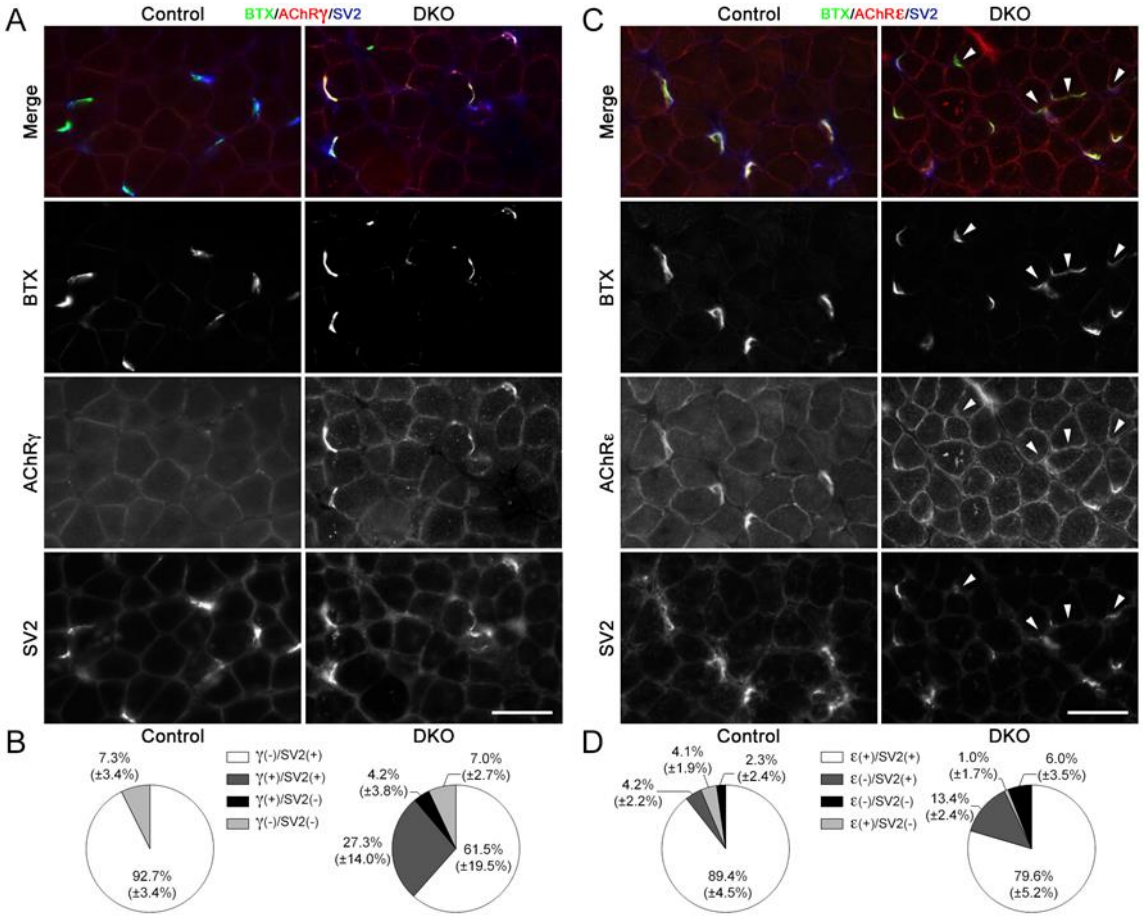

Figure 2.8. AChRγ/ε staining in 3 week SOL cross-sections.
(**a**) Control pictures show 7 innervated NMJs ($SV2^{+}$) that were AChRγ $^{-}$. DKO pictures show 4 AChRγ $^{+}$ /$SV2^{+}$ NMJs in focus. Scale bar: 50 μ m. (**b**) Quantification for AChRγ /SV2/BTX staining. Values are mean ± (SD). N = 3 control muscles, 139 endplates; 3 DKO muscles, 148 endplates. (**c**) Control pictures show 5 innervated NMJs ($SV2^{+}$) that label for AChRε ($AChR\varepsilon^{+}$). DKO pictures show 4 synaptic sites (arrowheads) where AChRε staining is not above extrasynaptic background levels on same fiber (AChRε $^{-}$). The other endplates are AChRε $^{+}$. Scale bar: 50 μ m. (**d**) Quantification for AChRε /SV2/BTX staining. Values are mean ± (SD). N = 3 control muscles, 145 endplates; 3 DKO muscles, 109 endplates.

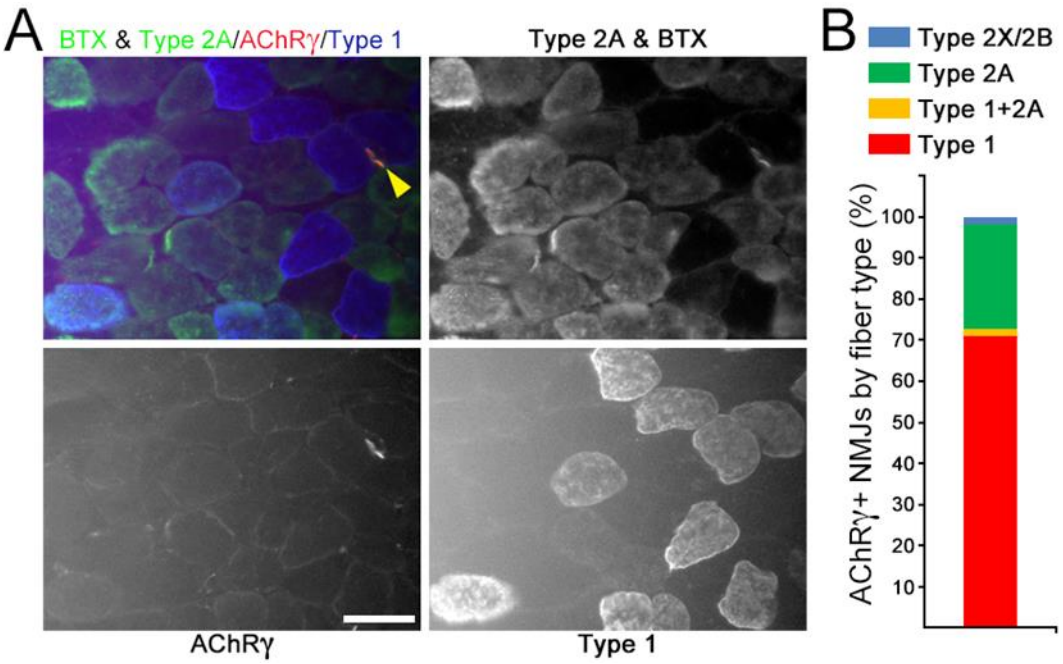

Figure 2.9. AChRγ staining preferentially at NMJs on type 1 fibers in 3-week old DKO SOL.

(**a**) Four NMJs labeled with fluorescein BTX, three on type 2A fibers and one (yellow arrowhead) on a type 1 fiber. Only the latter is AChRγ^{+}. BTX and type 2A staining were visualized in fluorescein channel; AChRγ visualized in rhodamine channel; type 1 visualized in Cy5 (647 nm) channel. Scale bar: 50 μ m. (**b**) Quantification of AChRγ^{+} NMJs by fiber types in DKO SOL. N = 3 muscles; 56 NMJs.

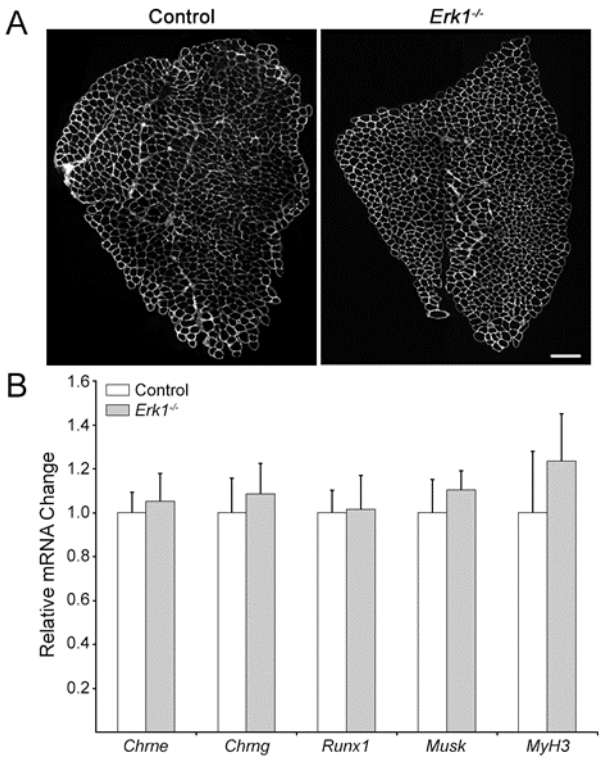

Figure 2.16. (Supplementary Figure 7) Morphological and molecular effects are absent in ERK1-deficient SOL.

(**a**) Cross sections of SOL from 9-week-old control and Erk1$^{-/-}$ stained for laminin to outline individual muscle fibers. Note overall similar morphology between mutant and control muscles. Erk1$^{-/-}$ SOL lacks the dramatic heterogeneity in fiber size found in DKO SOL (Fig 2.5.2**a**). Scale bar: 300 μm. (**b**) Real time PCR for *Chrne*, *Chrng*, *Runx1*, *Musk* and *Myh3* at 9 weeks for control and Erk1$^{-/-}$ SOL. N=6 for control and n=5 for Erk1$^{-/-}$. Values are mean + SEM. No statistically significant changes were detected.

2.4 Discussion

The analysis of the slow-twitch SOL muscles in mice lacking ERK1/2 in myofibers reveals that these kinases critically regulate type 1 fiber size in vivo. This regulation may extend to type 1 fibers in many muscle groups as their atrophy was detected in fast-twitch STN and EDL. ERK1/2 also appears to control the γ /ε -AChR switch at maturing NMJs in SOL, whose impairment precedes any other alterations.

ERK phosphorylation levels in adult rat skeletal muscle fibers are sensitive to the firing pattern of the motoneurons that innervate them. In particular, a low frequency/high amount impulse pattern (20 Hz), typical of slow motoneurons that innervate type 1 fibers, elicited the highest increase in ERK phosphorylation when applied to adult rat SOL muscle[9]. Firing patterns more similar to those for type 2B or type 2A motor units failed to stimulate, or more modestly induced ERK activation, respectively[9]. These results predict that removal of ERK from skeletal muscle fibers should more dramatically affect the type 1 muscle fibers. Our results in mouse SOL are consistent with this prediction and support the notion that ERK1/2 play a critical role in type 1 fibers. Although type 2 fibers are also affected as they undergo both atrophy and hypertrophy (Fig. 2.3), the dramatic myofiber wasting in young adult DKO SOL directly correlates with its higher content of type 1 fibers (~30%, this work and others (e.g.[16])) relative to the previously examined STN and TA[10]. Type 1 fiber atrophy was also detected in fast twitch muscles. In DKO STN there was a clear absence of large type 1 fibers, while in the EDL the atrophy was less robust but present statistically. The difficulty of detecting robust atrophy in EDL might be related to the already small size

of its few slow fibers. Indeed, type 1 fibers in control EDL were on average as small as the most atrophied fibers in the DKO SOL (Fig. 2.3**b**). In addition, it is known that type 1 fibers in the rat EDL, for example, are resistant to denervation-induced atrophy, while they are very sensitive in the SOL[24]. Rat type 1 fibers in SOL are ~3 times larger than in the EDL[16]. Thus, it is possible that small type 1 fibers for some reason are much less sensitive to the lack of ERK1/2 than large type 1 fibers.

Since our DKO mice lack ERK1 in all cells, including motoneurons, it is reasonable to ask whether the absence of ERK1 in motoneurons lowers the threshold for the defects in NMJ maturation we observed. This does not appear to be the case as SOL morphology and relative mRNA levels of synaptic/denervation markers in young adult Erk1$^{-/-}$ mice were similar to control (Supplementary Fig. 7).

A primary role of myofiber ERK1/2 in DKO SOL seems to be synaptic rather than extrasynaptic since a defective γ /ε -AChR subunit switch, largely confined, but not exclusive to NMJs on type 1 fibers, preceded fiber loss and atrophy. *Chrne*$^{-/-}$ mice survive development and go normally through some milestones of postnatal synaptic maturation such as synapse elimination[3, 4]. However, their NMJs, which retain the fetal AChRγ subunit, have a much lower density of AChRs and show structural postnatal abnormalities such as fragmentation[4, 5]. *Chrne*$^{-/-}$ mice also develop muscle atrophy, show a fast-to-slow fiber type transition in both fast- and slow-twitch muscles[36], and fail to live past 14 weeks. These results indicate that ε -containing AChRs play a structural role in the normal maturation of the NMJ, and that a defective γ /ε -switch leads to alterations in the maintenance of muscle fibers. Thus the defective γ /ε -switch may be a

contributor to the striking wasting of the SOL muscle in ERK1/2 deficient mice. A reduction of AChRε expression is common to the STN, TA[10], and SOL (Fig. 2.3**c**) in young adult DKO animals. These reductions are averages for the whole muscle, and it is possible they are larger at some synaptic sites than at others, as suggested by the AChRγ /ε staining (Fig. 2.4). Specific molecular mechanisms by which ERK1/2 upregulate AChRε expression in vivo remain to be determined, although transcriptional regulation is likely one of them[37, 38]. As in the *Chrne*$^{-/-}$ mice, induction of AChRγ expression in ERK1/2-deficient fibers may arise as compensation to the reduction in AChRε and/or after denervation. Alternatively, ERK1/2 may be necessary to repress AChRγ expression, at least in type 1, and perhaps some type 2A fibers. There are some differences between the ERK1/2-deficient and *Chrne*$^{-/-}$ SOL that suggest that processes other than the defective γ /ε -AChR switch also contribute to the phenotype of the former. Neither fiber loss, in general, nor atrophy of type 1 fibers or reduction of *Myh7* expression, in particular, were reported in *Chrne*$^{-/-}$ SOL at least up to 9 weeks of age[36]. Moreover, although physiological evidence[3] and presence of terminal axonal sprouts[4] suggested some degree of paralysis or partial denervation, it is unclear if anatomical denervation actually occurs at AChRε -less NMJs. One could speculate that had the *Chrne*$^{-/-}$ mice survived longer than the 2–3 months of their average lifespan, clearer signs of denervation might have been detected in their SOL. In DKO SOL, denervation extended to ~70% of synaptic sites by 14 weeks of age (Fig. 2.5). This denervation is myogenic, and not neurogenic, in origin, as no changes in activate or total ERK2 levels were detected in spinal cord of DKO mice[10]. This finding is consistent with the lack of

Cre expression in spinal cord for the human α -skeletal actin-Cre driver used to generate these mice (http://www.informatics.jax.org/recombinase/specificity?id= MGI:2447635&systemKey= 4856356). The precise mechanism(s) responsible for denervation is unclear, and it is possible that different mechanisms operate on different fiber types depending on their activity level. Fiber loss, which occurred mainly between 3–6 weeks (Fig. 2.2**d**), and which appeared fiber-type unspecific (Supplementary Fig. 2), may have produced remodeling of motor unit size in the whole mutant SOL. Moreover, the longer open times of the γ -containing AChR2 might lead to increased local postsynaptic Ca^{2+}, which might cause endplate degeneration and induction of slow-channel-like myasthenia[39]. Perhaps in the absence of ERK1/2, the tonic pattern of activity of type1 fibers and certain types of 2A fibers makes them more susceptible to synaptic Ca^{2+} overload than the phasic firing pattern of type 2B fibers. Alternatively or in addition, fiber-wide activity-dependent metabolic damage due to mitochondrial alterations or other general defects in post-weaning maturation may be responsible for the persistent denervation in young adult DKO SOL. Alterations in mitochondrial biogenesis and function were suggested by the reduction in COX and SDH activities and in mitochondrial markers, particularly *PGC1-α* (Fig. 2.6). Lack of PCG-1α reduces mitochondrial biogenesis[40], but it also appears to modulate denervation-induced mitophagy, at least in fast-twitch muscles[41]. Further experiments are required to investigate a possible signaling link between ERK1/2 and PGC-1α, and its potential impact on mitochondrial dynamics. The mitochondrial alterations might trigger and/or increase the severity of denervation-induced wasting in ERK1/2-deficient SOL. To our

knowledge, mitochondrial phenotypes have not been studied in Chrne$^{-/-}$ mice. It will be interesting to do so to compare and contrast with our ERK1/2-deficient mice.

At 3 weeks we also saw a lack of 2B fibers in the DKO SOL (Fig. 2.2). These fibers were a small, very variable minority in control muscle at this age that in any event, were normally reduced to the levels present in DKO muscle by 5–6 weeks. Although this was an early event, it is unlikely that it is a major driver of the wasting of the DKO SOL as these fibers constitute such a minor component of the normal SOL. Furthermore, expression of *Myh4* mRNA (Supplementary Fig. 3) and 2B proportions by immunostaining, even in predominantly fast-twitch STN and TA muscles, are not affected by the lack of myofiber ERK1/2[10]. Induction of AChRγ specifically in type 1 fibers is a common feature of many human neuromuscular disorders[42]. Although simple neurogenic denervation is the presumed main mechanism underlying this effect in most - but not all- cases, it is unclear why it is restricted to type 1 fibers. Given our results in mice, downregulation of myofiber ERK1/2 signaling might be an underappreciated mechanism driving this phenomenon.

2.5 Materials and Methods

Ethics Statement

Care and treatment of all animals followed the National Institutes of Health Guide for the Care and Use of Laboratory Animals, and were approved by the Institutional Animal Care and Use Committee of Texas A&M University under animal use protocols 2012-168 and 2014-060.

Mice and Genotyping

Generation and genotyping of mice were described previously[10]. *Cre* was driven by the human α -skeletal muscle actin (*Hsa*) promoter. Mice deficient in germ line ERK1 and myofiber ERK2 came from the following cross: *Hsa-Cre*$^{+/-}$; *Erk1*$^{+/-}$; *Erk2*$^{f/f}$ x *Hsa-Cre*$^{-/-}$; *Erk1*$^{-/-}$; *Erk2*$^{f/f}$. The genotype of mutant animals (referred in the text as DKO mice) was *Hsa-Cre*$^{+/-}$; *Erk1*$^{-/-}$; *Erk2*$^{f/f}$. The genotype of controls was *Hsa-Cre*$^{-/-}$; *Erk1*$^{+/?}$; *Erk2*$^{f/f}$. Males and females of all genotypes were used in all experiments.

Myofiber Morphological Analysis and Typing

Mice were euthanized by CO2 and muscles were immediately dissected. Muscles were embedded in tissue-tek (OCT, Sakura, Torrance, CA) within a plastic mold, frozen in liquid N2-cooled isopentane and stored at − 80 °C until use. Dystrophin staining of transverse frozen sections was performed essentially as previously described except that sections were not fixed[43]. The same protocol was followed for laminin staining with a chicken polyclonal Ab IgY primary at 1:400, and a goat anti-chicken IgY H + L AlexaFluor 647 secondary at 1:500 (Abcam, Cambridge, MA). Fiber typing was done by multicolor immunofluorescence staining[16] with some modifications. The same primary myosin heavy chain antibodies (Developmental Studies Hybridoma Bank, Iowa City, Iowa) at the previously reported dilutions were used to positively stain for type 1 (BA-F8), type 2A (SC-71), and type 2B (BF-F3). Type 2X fibers were those that remained unstained. Primary antibodies were visualized simultaneously with secondary antibodies (ThermoFisher Scientific/LifeTechnologies, Grand Island, New York) at 1:500 dilution: BA-F8 with Alexa-647 goat anti-mouse IgG2b; SC-71 with Alexa-488 goat anti-mouse

IgG1; BF-F3 with Alexa-568 goat anti-mouse IgM. For fiber typing of individual cross sections, 10X images for each of the three fluorescence channels were taken with a Nikon wide-field E1000 microscope (Nikon Inc., Melville, New York), then merged and pseudocolored in Metamorph (Molecular Devices, Sunnyvale, California). To reconstruct an entire muscle cross section, the above overlapping images were assembled as a montage in Photoshop (Adobe Systems Inc., San Jose, CA). Individual fluorescence channels from these composites were counted to obtain the number of fibers of each type within one entire cross section. All fibers within the composites were counted. These numbers were used to derive the total number of fibers and relative fiber type composition. Fiber area was also derived from these images by first manually drawing a border around stained fibers within a channel using the trace region tool in Metamorph. These regions of interest were thresholded and analyzed with the integrated morphometric analysis tool to determine their area. As these images overlapped to cover the entire cross section, care was taken not to measure the same fibers more than once. At least 60% of fibers per muscle were processed this way for all but the 5–6 week controls, where at least 40% were so measured. Replicates per muscle per genotype were averaged for final quantification.

AChRγ/ε Staining and Quantification

Rabbit antibodies to AChRγ and AChRε were a kind gift of Dr. Norihiro Yumoto (New York University) and were previously characterized[23]. Immunostaining of transverse serial sections was performed as described above with the following modifications: Blocking and antibody incubation for AChRγ experiments were

performed in 10% normal goat serum in PBS + 0.1% Triton X-100, whereas for AChRε experiments they were blocked and incubated in 5% non-fat dry milk in PBS. These antibodies were visualized with rhodamine-goat anti-rabbit IgG (Jackson Immunoresearch Laboratories Inc., West Grove, PA) at 1:400. All AChRs were labeled with fluorescein-α -BTX, LifeTechnologies) at 1:3000. Nerve terminals were labeled with mouse monoclonal antibody to SV2 (Developmental Studies Hybridoma Bank) at 1:10, visualized with Alexa-647 goat anti-mouse IgG (LifeTechnologies) at 1:400. For quantification, 10 images per slide were taken for each separate channel per muscle at 20X magnification with a wide-field microscope (Nikon). BTX-positive synaptic sites were scored for AChR subunit and SV2 staining. Positive staining was that above extrasynaptic background on same fiber. Although we noticed differences in intensity of AChRγ /ε staining among synaptic sites, no efforts were made to quantify these levels separately. For AChRγ and type 1/2A MyHC co-staining, sections remained unfixed throughout. AChRγ , type 1 and type 2A MyHCs were visualized with the same secondary antibodies used above. Fluorescein-BTX was included to mark synaptic sites. Thus type 2A and BTX staining were both observed under fluorescein optics.

Whole Mount Staining and Confocal Microscopy

Visualization of NMJs by whole mount and confocal microscopy was done as described previously[10].

Western Blotting

Muscle lysates were prepared in 25 mM Tris pH 7.4, 95 mM NaCl, 1 mM EDTA, 1 mM EGTA, 1% SDS, 10% Protease Inhibitor Cocktail (P8340, Sigma-Aldrich,

St. Louis, MO), 5 mM NaF, 2 mM Na3VO4, 2.5 mM Na4P2O7. Protein analysis by western blotting was done as described previously[10], except 30 μ g of total lysate per sample was used. The antibody to PGC-1α (NBP1-48320. Novus Biologicals, Littleton, CO) was used at 1:2000. The antibody to SOD2 (SOD-111. Stressgen Biotechnologies, Victoria, BC) was used at 1:10000.

In Situ Mitochondrial Enzyme Activity

Cytochrome oxidase (COX) and succinate dehydrogenase (SDH) activity on unfixed cross sections were performed as described[27]. Cross sections from control and DKO muscles were always run at the same time. Images were acquired with an EC3 camera and software (Leica Microsystems Inc., Buffalo Grove, IL), mounted on an Eclipse E1000 microscope (Nikon).

Real-Time Quantitative PCR

Total RNA extraction, reverse transcription, and real-time PCR were performed essentially as previously reported10. 200 ng of total RNA per sample was used to generate cDNA. Cycle threshold (Ct) values obtained for 18 S rRNA were used to equalize differences in total RNA per sample. Transcript level fold-change was determined by the $2^{-\mathrm{DeltaDeltaCt}}$ method[44] and values were normalized to the Ct values obtained for control muscle for each gene. All Taqman primer sets and probes were from ThermoFisher/ Life Technologies as follows: 18 S rRNA (4333760 F), *Atrogin1* (Mm00499523_m1), *Bnip3* (Mm01275600_g1), *Chrne* (Mm00437411_m1), *Chrng* (Mm00437419_m1), *Cytb* (Mm04225271_g1), *Drp1* (Mm01342903_m1), *Mfn1* (Mm00612599_m1), *Mfn2* (Mm00500120_m1), *Murf1* (Mm01185221_m1), *Musk*

(Mm01346929_m1), *Myh1* (Mm01332489_m1), *Myh2* (Mm01332564_m1), *Myh3* (Mm01332463_m1), *Myh4* (Mm01332518_m1), *Myh7* (Mm01319006_g1), *Myog* (Mm00446194_m1), *Pgc-1α* (Mm01208835_m1), *Pgc-1β* (Mm00504720_m1), *Runx1* (Mm01213404_m1), *Sqstm1* (Mm00448091_m1), *Ucp3* (Mm00494077_m1).

Statistical Analysis

All experiments were done at least in two biological replicas per genotype. Here biological replicas had a $n \leq 3$ numerical data are expressed as mean ± SD. All real-time PCR experiments had at least 5 biological replicas per genotype. Numerical data for these experiments are expressed as mean ± SEM. Two-sample, two-tailed Student t-tests were used to compare means and were computed with Microsoft Excel (Microsoft Corporation, Redmond, WA). Wilcoxon rank sum test probabilities to compare distributions were computed at http://socr.stat.ucla.edu. Significance was set at P values of < 0.05 for* and of < 0.01 for**.

2.6 References

1. Fischbach, G. D., & Schuetze, S. M. (1980). A post-natal decrease in acetylcholine channel open time at rat end-plates. The Journal of Physiology, 303(1), 125-137. doi:10.1113

2. Mishina, M., Takai, T., Imoto, K., Noda, M., Takahashi, T., Numa, S., . . . Sakmann, B. (1986). Molecular distinction between fetal and adult forms of muscle acetylcholine receptor. Nature, 321(6068), 406-411. doi:10.1038/321406a0/jphysiol.1980.sp013275

3. Witzemann, V., Schwarz, H., Koenen, M., Berberich, C., Villarroel, A., Wernig, A., . . . Sakmann, B. (1996). Acetylcholine receptor -subunit deletion causes muscle weakness

and atrophy in juvenile and adult mice. Proceedings of the National Academy of Sciences, 93(23), 13286-13291. doi:10.1073/pnas.93.23.13286

4. Missias, A., Mudd, J., Cunningham, J., Steinbach, J., Merlie, J., & Sanes, J. (1997). Deficient development and maintenance of postsynaptic specializations in mutant mice lacking an 'adult' acetylcholine receptor subunit. Development, 124, 5075-5086.

5. Schwarz, H., Giese, G., Müller, H., Koenen, M., & Witzemann, V. (2000). Different functions of fetal and adult AChR subtypes for the formation and maintenance of neuromuscular synapses revealed in ε-subunit-deficient mice. European Journal of Neuroscience, 12(9), 3107-3116. doi:10.1046/j.1460-9568.2000.00195.x

6. Wortzel, I., & Seger, R. (2011). The ERK Cascade: Distinct Functions within Various Subcellular Organelles. Genes & Cancer, 2(3), 195-209. doi:10.1177/1947601911407328

7. Shi, H., Scheffler, J. M., Zeng, C., Pleitner, J. M., Hannon, K. M., Grant, A. L., & Gerrard, D. E. (2009). Mitogen-activated protein kinase signaling is necessary for the maintenance of skeletal muscle mass. American Journal of Physiology-Cell Physiology, 296(5). doi:10.1152/ajpcell.00475.2008

8. Shi, H., Scheffler, J. M., Pleitner, J. M., Zeng, C., Park, S., Hannon, K. M., . . . Gerrard, D. E. (2008). Modulation of skeletal muscle fiber type by mitogen-activated protein kinase signaling. The FASEB Journal, 22(8), 2990-3000. doi:10.1096/fj.07-097600

9. Murgia, M., Serrano, A. L., Calabria, E., Pallafacchina, G., Lømo, T., & Schiaffino, S. (2000). Ras is involved in nerve-activity-dependent regulation of muscle genes. Nature Cell Biology, 2(3), 142-147. doi:10.1038/35004013

10. Seaberg, B., Henslee, G., Wang, S., Paez-Colasante, X., Landreth, G. E., & Rimer, M. (2015). Muscle-derived extracellular signal-regulated kinases 1 and 2 are required for the maintenance of adult myofibers and Their Neuromuscular Junctions. Molecular and Cellular Biology, 35(7), 1238-1253. doi:10.1128/mcb.01071-14

11. Schiaffino, S., & Reggiani, C. (2011). Fiber types in mammalian skeletal muscles. Physiological Reviews, 91(4), 1447-1531. doi:10.1152/physrev.00031.2010

12. Augusto, Padovani, C., Eduardo, G., & Campos, R. (2004). Skeletal muscle fiber types in c57bl6j mice. Journal of Morphological Science, 21(2), 89-94.

13. Miniou, P. (1999). Gene targeting restricted to mouse striated muscle lineage. Nucleic Acids Research, 27(19). doi:10.1093/nar/27.19.e27

14. Cifuentes-Diaz, C., Frugier, T., Tiziano, F. D., Lacène, E., Roblot, N., Joshi, V., . . . Melki, J. (2001). Deletion of murine SMN exon 7 directed to skeletal muscle leads to severe muscular dystrophy. The Journal of Cell Biology, 152(5), 1107-1114. doi:10.1083/jcb.152.5.1107

15. Nicole, S., Desforges, B., Millet, G., Lesbordes, J., Cifuentes-Diaz, C., Vertes, D., . . . Melki, J. (2003). Intact satellite cells lead to remarkable protection against Smn gene defect in differentiated skeletal muscle. The Journal of Cell Biology, 161(3), 571-582. doi:10.1083/jcb.200210117

16. Bloemberg, D., & Quadrilatero, J. (2012). Rapid determination of myosin heavy chain expression in rat, mouse, and human skeletal muscle using multicolor immunofluorescence analysis. PLoS ONE, 7(4). doi:10.1371/journal.pone.0035273

17. Witzemann, V., Barg, B., Nishikawa, Y., Sakmann, B., & Numa, S. (1987). Differential regulation of muscle acetylcholine receptor γ-and ϵ-subunit mRNAs. FEBS Letters, 223(1), 104-112. doi:10.1016/0014-5793(87)80518-5

18. Zhu, X., Yeadon, J. E., & Burden, S. J. (1994). AML1 is expressed in skeletal muscle and is regulated by innervation. Molecular and Cellular Biology, 14(12), 8051-8057. doi:10.1128/mcb.14.12.8051

19. Wang, X. (2005). Runx1 prevents wasting, myofibrillar disorganization, and autophagy of skeletal muscle. Genes & Development, 19(14), 1715-1722. doi:10.1101/gad.1318305

20. Moresi, V., Williams, A. H., Meadows, E., Flynn, J. M., Potthoff, M. J., Mcanally, J., . . . Olson, E. N. (2010). Myogenin and Class II HDACs Control Neurogenic Muscle Atrophy by Inducing E3 Ubiquitin Ligases. Cell, 143(1), 35-45. doi:10.1016/j.cell.2010.09.004

21. Valenzuela, D. M., Stitt, T. N., Distefano, P. S., Rojas, E., Mattsson, K., Compton, D. L., . . . Yancopoulos, G. D. (1995). Receptor tyrosine kinase specific for the skeletal muscle lineage: Expression in embryonic muscle, at the neuromuscular junction, and after injury. Neuron, 15(3), 573-584. doi:10.1016/0896-6273(95)90146-9

22. GU, Y., & HALL, Z. (1988). Characterization of acetylcholine receptor subunits in Developing. The Journal of Biological Chemistry, 263(26), 12878-85.

23. Yumoto, N., Wakatsuki, S., & Sehara-Fujisawa, A. (2005). The acetylcholine receptor γ-to-ε switch occurs in individual endplates. Biochemical and Biophysical Research Communications, 331(4), 1522-1527. doi:10.1016/j.bbrc.2005.04.081

24. Ciciliot, S., Rossi, A., Dyar, K., Blaauw, B., & Schiaffino, S. (2013). Muscle type and fiber type specificity in muscle wasting. The International Journal of Biochemistry & Cell Biology, 45(10), 2191-2199. doi:10.1016/j.biocel.2013.05.016

25. Patterson, M. F., Stephenson, G. M., & Stephenson, D. G. (2006). Denervation produces different single fiber phenotypes in fast- and slow-twitch hindlimb muscles of the rat. American Journal of Physiology-Cell Physiology, 291(3), 518-528. doi:10.1152/ajpcell.00013.2006

26. Agbulut, O., Vignaud, A., Hourde, C., Mouisel, E., Fougerousse, F., Butler-Browne, G. S., & Ferry, A. (2009). Slow myosin heavy chain expression in the absence of muscle activity. American Journal of Physiology-Cell Physiology, 296(1). doi:10.1152/ajpcell.00408.2008

27. Sciacco, M., & Bonilla, E. (1996). [43] Cytochemistry and immunocytochemistry of mitochondria in tissue sections. Methods in Enzymology Mitochondrial Biogenesis and Genetics Part B, 509-521. doi:10.1016/s0076-6879(96)64045-2

28. Lin, J. et al. Transcriptional co-activator PGC-1 alpha drives the formation of slow-twitch muscle fibres. Nature 418, 797–801. doi: 10.1038/nature00904 (2002).

29. Arany, Z., Lebrasseur, N., Morris, C., Smith, E., Yang, W., Ma, Y., . . . Spiegelman, B. M. (2007). The Transcriptional Coactivator PGC-1β Drives the Formation of

Oxidative Type IIX Fibers in Skeletal Muscle. Cell Metabolism, 5(1), 35-46. doi:10.1016/j.cmet.2006.12.003

30. Elgass, K., Pakay, J., Ryan, M. T., & Palmer, C. S. (2013). Recent advances into the understanding of mitochondrial fission. Biochimica et Biophysica Acta (BBA) - Molecular Cell Research, 1833(1), 150-161. doi:10.1016/j.bbamcr.2012.05.002

31. St-Pierre, J., Drori, S., Uldry, M., Silvaggi, J. M., Rhee, J., Jäger, S., . . . Spiegelman, B. M. (2006). Suppression of reactive oxygen species and neurodegeneration by the PGC-1 transcriptional coactivators. Cell, 127(2), 397-408.

32. Sandri, M., Lin, J., Handschin, C., Yang, W., Arany, Z. P., Lecker, S. H., . . . Spiegelman, B. M. (2006). PGC-1 protects skeletal muscle from atrophy by suppressing FoxO3 action and atrophy-specific gene transcription. Proceedings of the National Academy of Sciences, 103(44), 16260-16265. doi:10.1073/pnas.0607795103

33. Rüegg, M. A., & Glass, D. J. (2011). Molecular Mechanisms and Treatment Options for Muscle Wasting Diseases. Annual Review of Pharmacology and Toxicology, 51(1), 373-395. doi:10.1146/annurev-pharmtox-010510-100537

34. Bonaldo, P., & Sandri, M. (2012). Cellular and molecular mechanisms of muscle atrophy. Disease Models & Mechanisms, 6(1), 25-39. doi:10.1242/dmm.010389

35. Missias, A. C., Chu, G. C., Klocke, B. J., Sanes, J. R., & Merlie, J. P. (1996). Maturation of the Acetylcholine Receptor in Skeletal Muscle: Regulation of the AChR γ-to-ϵ Switch. Developmental Biology, 179(1), 223-238. doi:10.1006/dbio.1996.0253

36. Jin, T., Wernig, A., & Witzemann, V. (2008). Changes in acetylcholine receptor function induce shifts in muscle fiber type composition. FEBS Journal, 275(9), 2042-2054. doi:10.1111/j.1742-4658.2008.06359.x

37. Si, J., & Mei, L. (1999). ERK MAP kinase activation is required for acetylcholine receptor inducing activity-induced increase in all five acetylcholine receptor subunit mRNAs as well as synapse-specific expression of acetylcholine receptor ε-transgene. Molecular Brain Research, 67(1), 18-27. doi:10.1016/s0169-328x(99)00028-5

38. Lacazette, E., Calvez, S. L., Gajendran, N., & Brenner, H. R. (2003). A novel pathway for MuSK to induce key genes in neuromuscular synapse formation. The Journal of Cell Biology, 161(4), 727-736. doi:10.1083/jcb.200210156

39. Gomez, C. M., Maselli, R. A., Groshong, J., Zayas, R., Wollmann, R. L., Cens, T., & Charnet, P. (2002). Active calcium accumulation underlies severe weakness in a panel of mice with slow-channel syndrome. The Journal of Neuroscience, 22(15), 6447-6457. doi:20026643

40. Wu, Z., Puigserver, P., Andersson, U., Zhang, C., Adelmant, G., Mootha, V., . . . Spiegelman, B. M. (1999). Mechanisms controlling mitochondrial biogenesis and respiration through the thermogenic coactivator PGC-1. Cell, 98(1), 115-124. doi:10.1016/s0092-8674(00)80611-x

41. Vainshtein, A., Desjardins, E. M., Armani, A., Sandri, M., & Hood, D. A. (2015). PGC-1α modulates denervation-induced mitophagy in skeletal muscle. Skeletal Muscle, 5(1). doi:10.1186/s13395-015-0033-y

42. Gattenlöhner, S., Schneider, C., Thamer, C., Klein, R., Roggendorf, W., Gohlke, F., . . . Marx, A. (2002). Expression of foetal type acetylcholine receptor is restricted to type 1 muscle fibres in human neuromuscular disorders. Brain, 125(6), 1309-1319. doi:10.1093/brain/awf136

43. Paez-Colasante, X., Seaberg, B., Martinez, T. L., Kong, L., Sumner, C. J., & Rimer, M. (2013). Improvement of neuromuscular synaptic phenotypes without enhanced survival and motor function in severe spinal muscular atrophy mice selectively rescued in motor neurons. PLoS ONE, 8(9). doi:10.1371/journal.pone.0075866

44. Livak, K. J., & Schmittgen, T. D. (2001). Analysis of relative gene expression data using real-time quantitative PCR and the $2^{-\Delta\Delta CT}$ method. Methods, 25(4), 402-408. doi:10.1006/meth.2001.1262

CHAPTER III

MANUSCRIPT#2

3.1 Overview

After muscle denervation, Bone Morphogenetic Protein (BMP) signaling is activated and protects normal skeletal muscle from further atrophy. We found extensive denervation in SOL from young adult *Erk1/2* DKO mice. To test the role of ERK1/2 pathway in BMP mediated muscle mass maintenance, firstly, we measured mRNA expression of several important BMP components and phosphorylation level of Smad1/5/8 (the key regulator for BMP signaling transduction) in ERK1/2 DKO SOL and ERK1/2-inhibited myotubes. We found increased expression of Gdf5 and Gdf 6 (BMPXX and BMPYY, respectively), decreased expression of Bmpr1b, unchanged expression of Id-1, Noggin and Smad6, and unchanged phosphorylation level of Smad1/5/8 in ERK1/2 DKO SOL. These experiments suggest that BMP signaling is not activated in ERK1/2 DKO SOL after denervation. Next, we observed unchanged phosphorylation level of Smad1/5/8 in ERK1/2- inhibited, BMP4-treated myotubes along with unchanged expression of Bmpr1b, suggesting that ERK1/2 regulate BMP signaling in SOL through an indirect mechanism.

3.2 Introduction

Skeletal muscle functionality is a crucial factor that supports normal activities of human beings, such as respiration and locomotion. To achieve this, muscle mass should be well maintained. Loss of muscle mass due to sarcopenia (in normal aging) or cachexia (in the condition of diseases) is actually the signal of unbalanced protein degradation and synthesis. Many signaling pathways participate in balancing muscle protein breakdown and production, such as IGF-1-PI3K-Akt-mTOR axis[1, 2], ubiquitin-proteasome system (UPS) [3] and autophagy-lysosomal pathway[4]

In addition to these classic key regulators, the "cross-talk" with other pathways are also vital to ensure them processing normally. For example, the bone morphogenetic proteins (BMPs)- activated Smad 1/5/8 promote skeletal muscle hypertrophy by controlling activities of Akt –mTOR pathway[5] and inhibiting histone deacetylase 4 (HDAC4)- Myogenin induced muscle atrophy[6]. BMPs, which belong to the transforming growth factor beta (TGFb) superfamily, bind to Type II receptors, such as BMPR2, to facilitate recruitment of type I receptors such as BMPRIA, BMPR1B. Consequently, Smad1/5/8 are phosphorylated, form a complex with Smad4 and eventually translocate into the nucleus to target specific genes[7]. BMP signaling is necessary for skeletal muscle mass maintenance after denervation. Denervation promotes expression of *Gdf5* (encoding BMP14) and *Gdf6* (encoding BMP13) and subsequently induce phosphorylation of Smad1/5/8 so as to activate BMP signaling[7].
Overexpression of BMP-7 is able to significantly mitigate muscle atrophy after denervation[8, 9]. Conversely, inhibition of BMP signaling by removal of GDF5 or increasing *Smad6* expression worsens denervation-induced muscle atrophy[8, 9].

BMP ligands belong to TGF-β superfamily and have different selectivity for specific BMP receptor subtypes to achieve distinct biological functions. As an important member of BMP signaling, GDF5 (Growth/ differentiation factor 5, a.k.a. BMP14) is widely expressed in developing CNS[10] and play roles in skeletal and joint development[11, 12]. GDF5 was proposed to maintain skeletal muscle mass after denervation [5, 8] and thought to promote re-innervation[13]. The increase of *Gdf5* expression is due to the release of inhibitory effect after denervation from two transcriptional co-repressors Dach2-Hdac9[13].

In our previous study[14], we found signs of partial denervation in ERK1/2 DKO SOL at young adult age (see chapter II for details): (1) nerve sprouts at NMJs (2) increased expression of several denervation markers: *Chrng* (encoding AChRγ), *Runx1*, *Myogenin,* and *Myh3* (3) majority of BTX labelled AChRs contain AChRγ subunit and lost their contact to nerve terminals (negative staining for Synaptic Vesicle protein 2). However, we did not see denervation in ERK1/2 DKO TA[15]. In this chapter, we explore the status of BMP signaling in ERK1/2 DKO SOL and normal myotubes. We conclude that: (1) ERK1/ 2 is required for denervation induced- BMP signaling activation in skeletal muscle, at least in SOL; (2) Reduced expression of *Bmpr1b,* unchanged expression of *Noggin* and *Smad6,* are potential factors that account for inefficient BMP activation in ERK1/2 DKO skeletal muscle; (3) ERK1/2 regulated BMP activation probably depends on changes to ERK1/2-regulated downstream genes rather than direct interaction through kinase activity.

3.3 Results

3.3.1 Impaired activation of BMP-signaling in ERK1/2 DKO SOL

Because *Gdf5* and *Gdf6* expression were largely induced after denervation and they seem to be the major ligands to activate BMP signaling[8], we sought to examine the expression of *Gdf5* and *Gdf6* in ERK1/2 DKO SOL at 3 weeks and 9 weeks postnatally, which are the two typical time points we used before[14]. At 3 weeks, we found a slight increased expression of *Gdf5* in ERK1/2 DKO SOL (~1.7-fold higher than control) (Fig.3.1A), which is probably not induced by denervation *per se*, because ERK1/2 DKO TA, which did not have the sign of denervation[15], showed the similar expression level of *Gdf5* when compared to control (~2.1 fold higher than control) (Fig.3.1A). However, 9-week ERK1/2 DKO SOL had a much more increased *Gdf5* level (~132-fold higher than control) (Fig.3.1B). In addition, the *Gdf6* level went up as well (~ 36-fold higher than control) (Fig.3.1B). In contrast, *Gdf5* and *Gdf6* levels were unchanged between ERK1/2 DKO and WT TA at this age (Insert, Fig.3.1B). This finding was consistent with a previous study of nerve transection-induced-denervation model[5, 8], suggesting the initial step of BMP signaling activation, i.e., GDF5/6 induction, was not affected by the loss of ERK1/2 in SOL.

Next, we measured the expression of *Bmpr1a*, *Bmpr1b*, *Bmpr2*, *Acvr2a,* and *Acvr2b*, which are crucial BMP receptors for ligand binding and phosphorylation of Smad1/5/8[16]. Among these receptors, BMPR1B may be more important than others, because it is favored by GDF5[17] and GDF6[18], which are the major ligands for BMP activation after nerve transection-induced denervation[8]. At postnatal 3weeks, *Bmpr1b* expression in ERK1/2 DKO SOL decreased to ~78% of that in WT SOL while *Bmpr1b*

level stayed unchanged in DKO TA compared to WT TA (Fig.3.1C). At postnatal 9weeks, *Bmpr1b* expression in DKO SOL further dropped to ~67% of that in WT SOL and *Bmpr1a* expression in DKO SOL had an increase (~1.5-fold higher than control) (Fig.3.1D). The upregulation of *Bmpr1a* expression at 9weeks suggested a possible compensation effect for the reduction in *Bmpr1b*.

Noggin is a secreted protein that antagonizes BMP signaling by blocking BMPs' ability to bind their receptors[19]. *Noggin* expression is decreased in normal muscle after denervation, but it showed no changes in ERK1/2 DKO SOL and TA at either time points when compared to their controls (Fig.3.1E, F). As mentioned above, Smad4 forms a complex with Smad1/5/8 and translocate to the nucleus. Smad-4 can be phosphorylated by ERK to promote TGF-β induced Smad2/3/4 nucleus translocation[20]. In our ERK1/2 DKO SOL and TA, Smad-4 expression was largely unchanged (Fig.3.1E, F). Smad-6, one of the inhibitory Smads, is known to interact with activated BMP Type I receptors and compete with Smad1/5/8 so that they cannot be phosphorylated[21]. The *Smad-6* expression had no changes in all groups (Fig.3.1E, F).

Next, we sought to examine the expression level of *Id-1*, which belongs to E-protein family and is transcriptionally regulated by Smad1/5/8/4 complex[22]. *Id-1* increases after denervation in normal muscle[8]. However, *Id-1* was unchanged in ERK1/2 DKO SOL when compared to WT SOL (Fig.3.1G), suggesting deactivation of BMP signaling in DKO SOL.

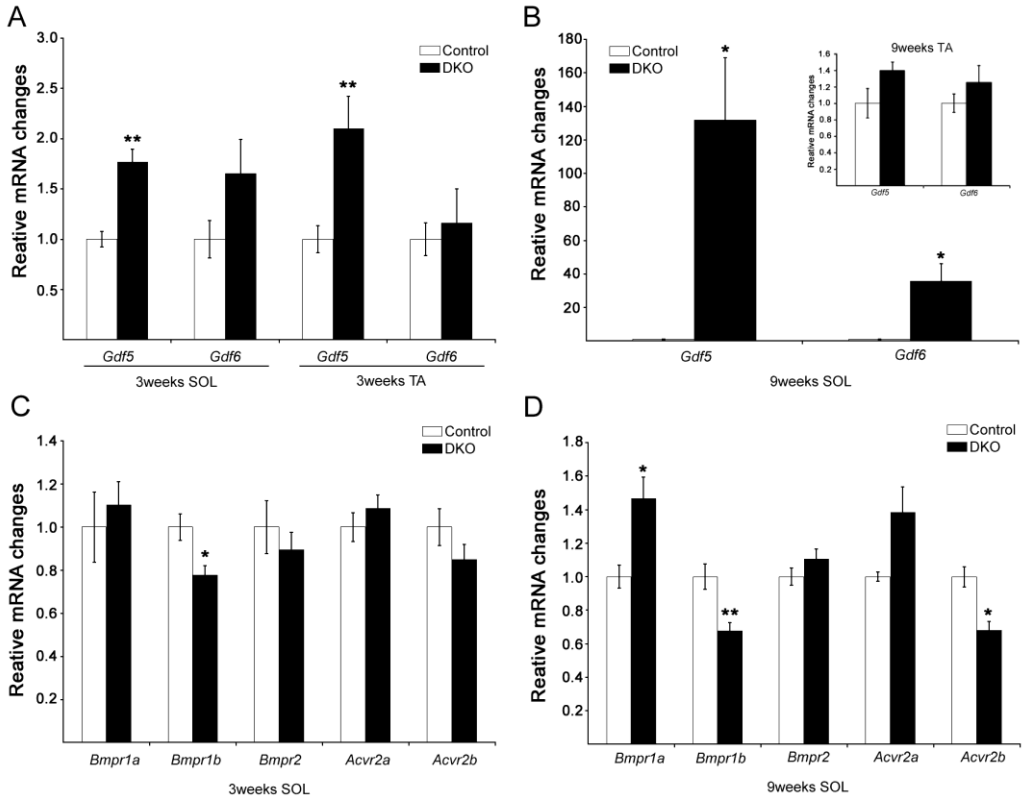

Figure 3.1. Relative mRNA expression of BMP signaling component in ERK1/2DKO muscles at 3 and 9 weeks of age.
(A) Relative mRNA expression for *Gdf5* and *Gdf6* genes in SOL and TA at 3 weeks. *Gdf5* was increased by ~1.8-fold and ~2.1-fold in SOL and TA, respectively. (B) Relative mRNA expression for *Gdf5* and *Gdf6* genes in SOL and TA at 9 weeks. *Gdf5* and *Gdf6* were increased by ~132-fold and ~36-fold, respectively. (C) Relative mRNA expression for *Bmpr1a, Bmpr1b, Bmpr2, Acvr2a* and *Acvr2b* genes in SOL at 3 weeks. *Bmpr1b* was dropped by ~1.3-fold. (D) Relative mRNA expression for *Bmpr1a, Bmpr1b, Bmpr2, Acvr2a* and *Acvr2b* genes in SOL at 9 weeks. *Bmpr1a* was increased by ~1.5-fold while *Bmpr1b* and *Acvr2b* were decreased by ~1.5-fold and ~1.5-fold, respectively. (E) Relative mRNA expression for *Noggin, Smad4* and *Smad6* genes in SOL and TA at 3 weeks. (F) Relative mRNA expression for *Noggin, Smad4* and *Smad6* genes in SOL and TA at 9 weeks. (G) Relative mRNA expression for *Id-1*gene in SOL at 3 and 9 weeks. N = 5 control, 5 DKO. Values are mean + SEM. **p < 0.01; *p < 0.05; t-test v. control.

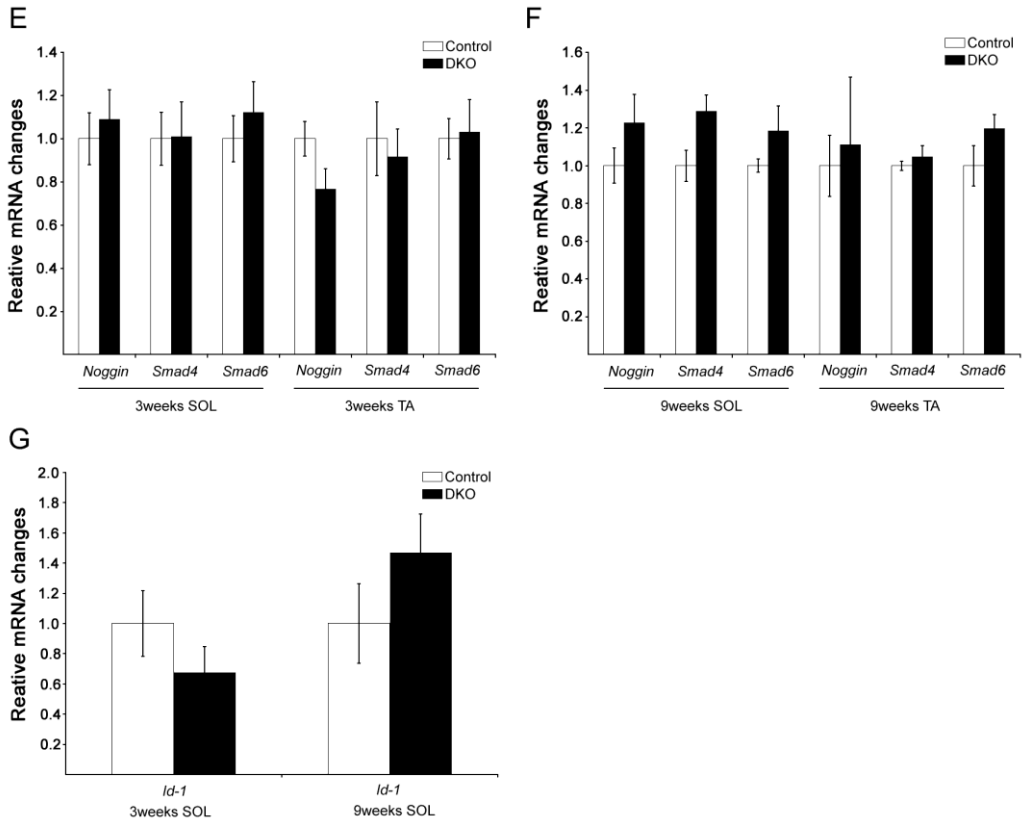

Figure 3.1 Continued.

To look further into the BMP signaling in ERK-deficient skeletal muscle, we sought to measure phosphorylation level of Smad1/5/8, which is crucial for BMP signaling transduction. We first transected the tibial branch of the sciatic nerve of control, wild-type animals and compared the phosphorylation level of Smad1/5/8 in denervated and the contralateral SOL after 1 week. In denervated SOL, as expected, normalized P-Smad1/5/8 to total-Smad1/5/8 (T-Smad1/5/8) and α-tubulin (α-tub) was increased ~1.7 fold and ~1.4 fold, respectively, when compared to their contralateral sides (Fig.3.2C, E, left). In contrast, there was no difference between ERK1/2 DKO and

WT SOL in terms of the normalized P-Smad1/5/8 level to T-smad1/5/8 and α-tub (Fig.3.2C, E, right). These results suggest Smad1/5/8 was not activated in ERK1/2 DKO SOL and are consistent with our inability to detect induction of BMP-signaling regulated genes such as *Id-1* in the same mutant muscles.

3.3.2 ERK1/2 indirectly regulate BMP signaling pathway in vitro

To attempt replicating the results in vivo and to distinguish whether the activation of BMP signaling is induced by ERK1/2's kinase activity or ERK1/2 downstream signaling, we firstly applied BMP4 to cultured myotubes for different times series (10mins, 1hour, 2hours and 4hours) and tested Smad1/5/8 activation by Western blot. Consistent with prior results from others, the normalized P-Smad1/5/8 level was significantly induced in the BMP4-treated group at all time points (Fig3.3B). Next, we pretreated C2C12 myotubes with ERK1/2 inhibitor U0126 and then incubated them in BMP4 for the same time series. The normalized P-Smad1/5/8 level was unchanged between control and U0126 treated group at all time points (10mins, 1hour, 2hours and 4 hours) (Fig3.3D). Blotting for phosphor-ERK showed that U0126 was effective in blocking ERK activation in these experiments (Fig3.3D). Further, we examined the mRNA level of *Bmpr1a*, *Bmpr1b* and *Bmpr2* in either control or U0126 treated C2C12 myotubes. Levels of these BMP receptors stayed unchanged between the control and U0126 treated group (4 hours and 8 hours) (Fig 3.4). Next, to rule out the possibility that ERK1/2 specifically regulate BMP signaling in SOL, we repeated the experiments above using sol8 cells, which are derived from SOL myoblasts and supposed to more closely retain properties of SOL muscle fibers[23]. Again, normalized P-Smad1/5/8 level were

largely unchanged (Fig 3.3F). The unchanged P-Smad1/5/8 in BMP stimulated-c2c12 and sol8 myotubes after treatment of ERK1/2 inhibitor suggests that ERK1/2 are unable to phosphorylate Smad1/5/8 directly. We observed reduced *Bmpr1b* expression in ERK1/2 DKO SOL (Fig 3.1C, D), however, we could not replicate this result by pharmacologically inhibiting ERK1/2 kinase activity in c2c12 cells. Altogether these results suggest ERK1/2 may regulate BMP signaling in an indirect way.

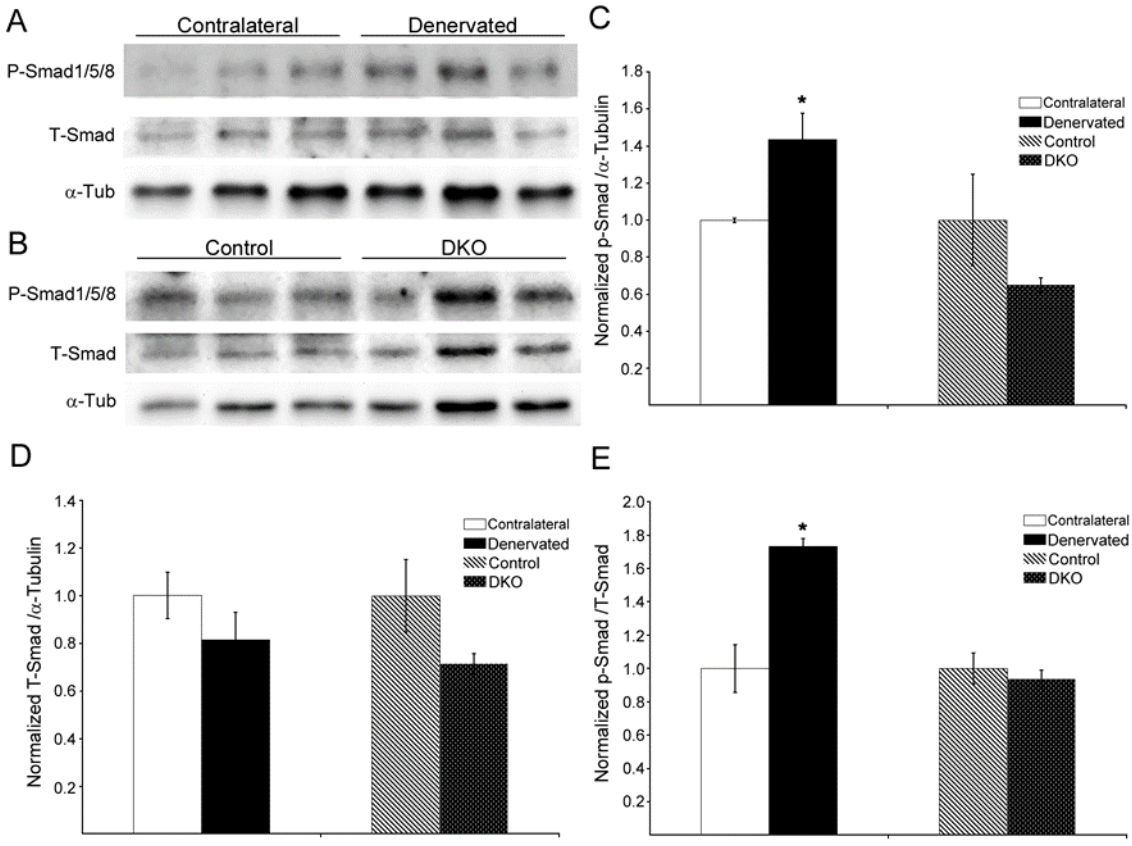

Figure 3.2. The phosphorylation level of Smad/1/5/8 in ERK1/2 DKO SOL at 9 weeks of age.

(A) Western blot for P-smad1/5/8, total Smad-1/5/8(T-Smad) and α –tubulin (α -Tub) in denervated SOL and their contralateral SOL. The tibial branch of the sciatic nerve of control animals was transected and the denervated SOL and their contralateral SOL were collected 1 week later. (B) The western blot for P-Smad1/5/8, T-Smad, and α –Tub in control and ERK1/2 DKO SOL. (C) Normalization of P-Smad1/5/8 to α –Tub showed the P-Smad1/5/8 level in denervated SOL were ~1.4 fold of their contralateral SOL; P-Smad1/5/8 level in ERK1/2 DKO SOL stayed the same as it in control SOL. (D) Normalization of T-Smad1/5/8 to α –Tub in denervated SOL, their contralateral SOL, control, and ERK1/2 DKO SOL. (E) Normalization of P-Smad1/5/8 to α –Tub showed the P-Smad1/5/8 level in denervated SOL were ~1.7 fold of their contralateral SOL; P-Smad1/5/8 level in ERK1/2 DKO SOL stayed the same as it in control SOL. N =3 each group. Values are mean + SEM. *$p < 0.05$; t-test v. control.

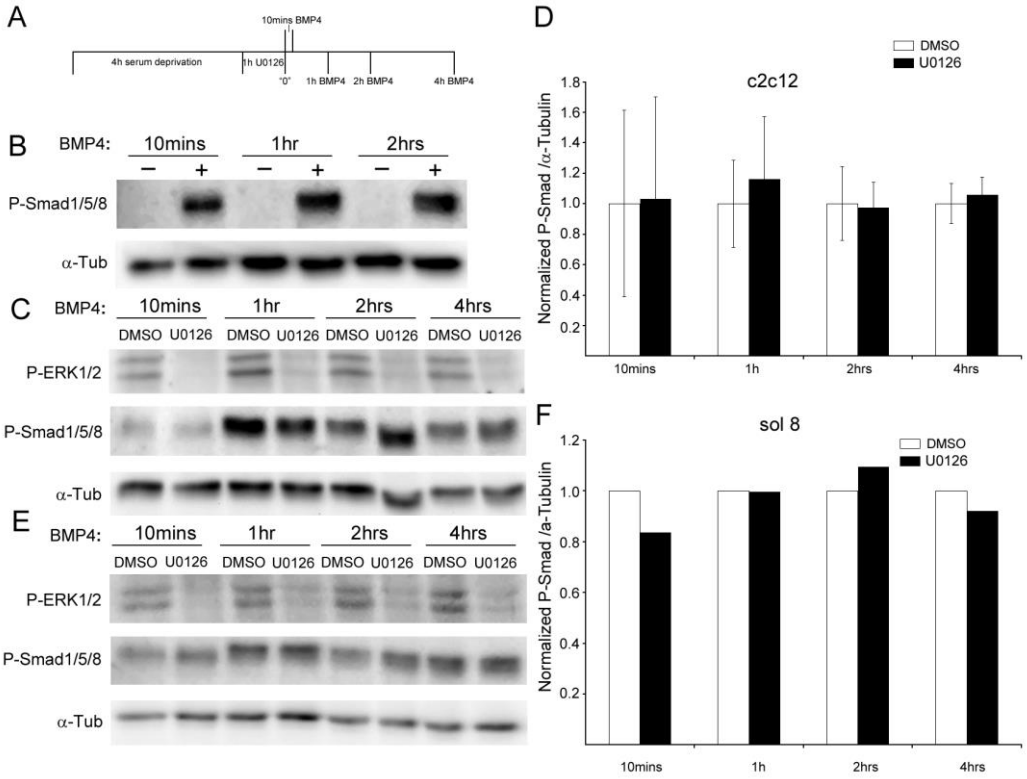

Figure 3.3. The phosphorylation level of Smad/1/5/8 in C2c12 and sol8 myotubes. (A) Schematic panel to show the experimental design. Myotubes were applied BMP4 after the "0" time point. (B) Western blots for P-Smad1/5/8 and α –Tub in control and BMP4 treated c2c12 myotubes. (C) Western blots for P-Smad1/5/8 and α –Tub in control and U0126 treated c2c12 myotubes. C2c12 cells were pre-treated with BMP4. The blots show inhibition of p-ERK1/2 in U0126 treated group and BMP4 induced increase of P-Smad1/5/8 level in all groups (D) Quantification for normalized P-Smad1/5/8 to α –Tub shows there is no significant difference between control and U0126 treated c2c12 myotubes. (E) Western blots for P-Smad1/5/8 and α –Tub in control and U0126 treated sol8 myotubes. Sol8 myotubes were treated the same as c2c12 myotubes. (F) Quantification of normalized P-Smad1/5/8 to α –Tub shows there is no significant difference between control and U0126 treated sol8 myotubes. N= 3 control, 3 U0126 treated in (C); a single experiment in (E). Values are mean + SEM. t-test v. control.

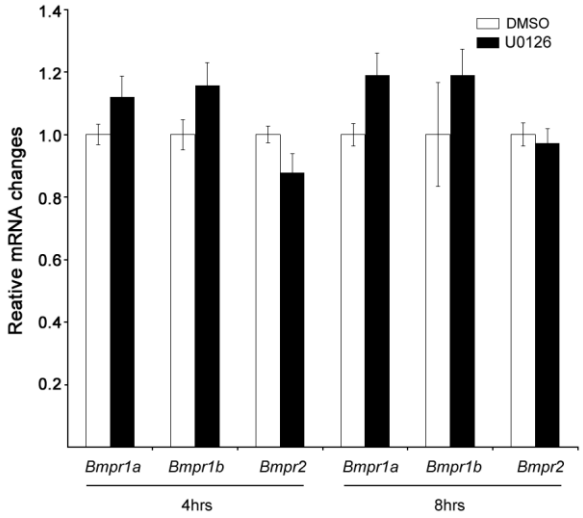

Figure 3.4. Relative *Bmpr* expression in ERK1/2 inhibited c2c12 myotubes. Relative expression of *Bmpr1a*, *Bmpr1b,* and *Bmpr2* in control and U0126 treated c2c12 myotubes at 4 hours and 8 hours. N=5 control, 6 U0126 treated. Values are mean + SEM. t-test v. control.

3.4 Discussion

The huge increase of *Gdf5* expression in ERK1/2 DKO SOL (Fig.3.1B) is consistent with the changes of *Gdf5* in the nerve transection-induced denervation model[8], further confirming denervation in ERK1/2 DKO SOL. The unchanged expression level of *Gdf5* in ERK1/2 DKO TA suggest it is denervation that induces upregulation of *Gdf5* in ERK1/2 DKO SOL, probably through Dach2-Hdac9 signaling. GDF6 (also called BMP13) share ~80-86% identify with GDF5 and GDF7 within the mature C-terminal region[18], suggesting GDF6 has the similar function as GDF5. Nerve cut-induced denervation increased the expression of *Gdf6*, which also happens in the ERK1/2 DKO SOL (Fig.3.5.1B).

BMP receptors include 3 type I receptors, such as BMPRIA (a.k.a. ALK3), BMPRIB (a.k.a. ALK6), and AcvrIA (a.k.a. ALK2) and 3 type II receptors, such as BMPRII, AcvrIIA, and AcvrIIB. BMPR1B is the specific type I receptor favored by GDF5[17] and the expression of *Bmpr1b* went up upon nerve lesion induced denervation[5]. However, we saw downregulation of *Bmpr1b* in ERK1/2 DKO SOL at 3 weeks when the sign of denervation is rare (Fig.3.1C). Further decrease of *Bmpr1b* expression was observed at 9 weeks along with increased expression of *Bmpr1a*, which probably results from compensation effect for loss of *Bmpr1b* (Fig. 3.1D). The downregulation of *Bmpr1b* expression might explain why ERK1/2 DKO SOL still underwent severe muscle atrophy when *Gdf5* was largely induced after denervation. Interestingly, we also found decreased AcvrIIB expression (Fig. 3.1D), which was also seen in nerve lesion induced denervation[5].

Noggin, the BMP signaling antagonist, and the inhibitory Smad6 were reported to have decreased expression after nerve cut-induced denervation of normal muscle[5]. However, the expression of *Noggin* and *Smad6* stayed unchanged in ERK1/2 DKO SOL at all time points examine (Fig.3.1E, F). The lack of downregulation of Noggin and Smad6 may also contribute towards the failure of BMP signaling activation in ERK1/2 DKO SOL.

Id-1 is directly regulated by Smad1/5/8/4 complex and strongly induced after nerve cut-induced denervation[8]. The protein encoded by *Id-1* is able to interact with basic HLH containing-transcription factors so as to inhibit DNA binding and

transcriptional activities[24]. We did not see the increased *Id-1* expression in ERK1/2 DKO SOL at 9weeks (Fig.3.1G), indicating deactivation of BMP signaling.

It has been reported that several Ser/Thr residues in the linker region of Smad1 can be phosphorylated by ERK1/2, facilitating binding of the Smad1/5-specific E3 ubiquitin ligase, Smurf1. Smurf1 degrades Smad1/5/8 through increased ubiquitination and interfere their interactions with the nuclear pore complex, leading to lower P-Smad1/5/8/4 into the nucleus[25]. As a result, BMP signaling can be inhibited by ERK1/2 activation[25, 26]. However, BMP and ERK1/2 pathways can also be synergistic, for example, BMP-4 induces hepatoblast differentiation into biliary epithelial cells in ERK1/2 dependent manner[27]. In our experiment, normalized T-smad1/5/8 to α-tubulin stayed unchanged after ERK1/2 loss in SOL (Fig.3.2D), suggesting ERK1/2 does not suppress BMP pathways through smad1 linker phosphorylation in skeletal muscle. Although, further examination for ERK1/2-induced phosphorylation in linker region may be needed to confirm this result. The unchanged phosphorylation level of Smad1/5/8 in ERK1/2 DKO SOL (Fig.3.2C, E) suggests the function of ERK1/2 on BMP is probably permissive instead of inhibitory.

Based on our *in vivo* experiments, the results below support the idea that ERK1/2 regulate denervation-induced BMP pathway activation in SOL: (1) unchanged expression of smad1/5/8 targeted gene *Id*-1; (2) unchanged phosphorylation level of smad1/5/8; (3) reduced expression of *Bmpr1b*; (4) unchanged expression of *Noggin* and *Smad6*.

Phosphorylation of the C-terminal region of Smad1/5/8 is required for signaling transduction[28] and there was no evidence that ERK1/2 is able to do that. Our *in vitro* experiments showed that pharmacologically inhibition of ERK1/2 could not reduce P-Smad1/5/8 in cultured myotubes, which was induced by BMP4 in both c2c12 and sol8 myotubes at all time points examined (Fig.3.3D, F). In addition, reduced expression of *Bmpr1b* was not seen (Fig.3.4) in c2c12 myotubes while we did observe it in ERK1/2 DKO SOL (Fig.3.1C, D). These two experiments suggest that ERK1/2 regulate BMP signaling probably through an indirect mechanism, that requires long-term inhibition of ERK activity. We could not easily mimic this long-term effect *in vitro* due to the difficulty to maintain myotubes for several days and the rapid turnover of both U0126 and recombinant BMP4. ERK1/2 have numerous downstream targets: They can indirectly regulate transcription activities by phosphorylating other kinases in the cytoplasm (such as 90 kDa Ribosomal Protein S6 Kinases[29]) and nucleus (such as the Mitogen- and Stress-activated Protein Kinases[30]) or directly phosphorylate transcriptional factors (such as c-myc[31]). Among those ERK1/2 targeted transcription factors, c-Jun, c-Fos, and Stat3 are able to bind to the enhancer region of *Bmpr1b*[32] (also see Table 3.1). Furthermore, CCAAT/enhancer binding protein α (C/EBPα), an ERK1/2 phosphorylated transcriptional factor[33], is able to bind the promoter region of *Bmpr1b*[32] (also see Table 3.1). These findings suggest a potential role of these ERK downstream genes in *Bmpr1b* regulation. However, functional experiments are needed to test this hypothesis. In addition, unchanged *Noggin* and *Smad6* expression in ERK1/2 DKO SOL (Fig.3.1E, F) (decreased expression were observed in nerve transection-induced

denervation[5]) suggest their regulation by ERK1/2 (see Table 3.1). Lastly, *Id-1* expression did not go up in ERK1/2 DKO SOL (Fig.3.1G) and it was probably due to low P-Smad1/5/8 level (Fig.3.2C, E). However, we cannot exclude the possibility that the expression of *Id-1* is regulated by ERK1/2 downstream transcription factors (see Table 3.1).

Daniel Goldman's group in 2015 observed that *Gdf5* knockout in skeletal muscle inhibited SOL re-innervation through Dach2-Hdac9 signaling dependent manner[13]. Conversely, Gdf5 over-expression promoted re-innervation. However, whether the better re-innervation is due to retrograde signaling from muscle secreted Gdf5 to nerve terminal or secondary effect on the muscle itself is not clear. Because both motor neuron and muscle express *Bmpr1b*, the Gdf5 binding BMP type I receptor. In our case, muscle-specific ERK1/2 DKO in SOL reduces *Bmpr1b* expression, followed by inactive BMP signaling in SOL. Therefore, it is quite possible that the reason for the severe denervation in ERK1/2 DKO SOL is not only muscle atrophy but also impaired re-innervation. Further investigation is required to test this possibility.

Genes in BMP pathway	ERK1/2 regulated transcriptional factors that bind to its promoter region	ERK1/2 regulated transcriptional factors that bind to its enhancer regions				
		Enhancer1	Enhancer2	Enhancer3	Enhancer4	Enhancer5
Bmpr1b	CEBPB	JUN	JUN, FOS, CEBPB, STAT3	-	-	-
Id-1	FOS, CEBPB, MYC, JUN, ELK1, ETV4, STAT3, SP1, CEBPA	FOS, STAT3, CEBPB, JUN	ELK1, ETV4, SP1, FOS, CEBPB, MYC, ETV1, JUN, CEBPA	ELK1, ETV4, STAT3, SP1, FOS, CEBPB, MYC, JUN, ETV1, CEBPA	CEBPB, MYC, JUN, ETV4	FOS, MYC, ETV1, JUN, ELK1, STAT3
Noggin	CEBPB, CREB, ELK1	FOS, STAT3, CEBPB, MYC, JUN, ETV1	FOS, STAT3, MYC, CEBPB	FOS, STAT3, JUN, CEBPB	FOS	-
Smad-6	MYC, ELK1, ETV4, SP1, CEBPA	MYC, ETV1, ELK1	FOS, ELK1, ETV4, STAT3, CEBPB, MYC, JUN	FOS, CEBPB, JUN	CEBPB, FOS	-

Table 3.1. ERK1/2 regulated transcriptional factors that bind to either promoter or enhancer region of genes in the BMP pathways.

3.5 Materials and Methods

Ethics Statement

Care and treatment of all animals followed the National Institutes of Health Guide for the Care and Use of Laboratory Animals and were approved by the Institutional Animal Care and Use Committee of Texas A&M University under animal use protocols 2012-168 and 2014-060.

Mice and Genotyping

Generation and genotyping of mice were described previously[15]. *Cre* was driven by the human α -skeletal muscle actin (*Hsa*) promoter. Mice deficient in germ line ERK1 and myofiber ERK2 came from the following cross: *Hsa-Cre*$^{+/-}$; *Erk1*$^{+/-}$; *Erk2*$^{f/f}$ x *Hsa-Cre*$^{-/-}$; *Erk1*$^{-/-}$; *Erk2*$^{f/f}$. The genotype of mutant animals (referred in the text as DKO mice) was *Hsa-Cre*$^{+/-}$; *Erk1*$^{-/-}$; *Erk2*$^{f/f}$. The genotype of controls was *Hsa-Cre*$^{-/-}$; Erk1$^{+/?}$; Erk2$^{f/f}$. Males and females of all genotypes were used in all experiments.

Real-Time Quantitative PCR

Total RNA extraction, reverse transcription, and real-time PCR were performed essentially as previously reported[15]. 200 ng of total RNA per sample was used to generate cDNA. Cycle threshold (Ct) values obtained for 18 S rRNA were used to equalize differences in total RNA per sample. Transcript level fold-change was determined by the $2^{-\text{DeltaDeltaCt}}$ method[33] and values were normalized to the Ct values obtained for control muscle for each gene. All Taqman primer sets and probes were from ThermoFisher/ Life Technologies as follows: 18 S rRNA (4333760 F), *Id-1* (Mm00775963_g1), *Gdf5* (Mm00433564_m1), *Gdf6* (Mm01222341_m1), *Bmpr1a* (Mm00477650), *Bmpr1b* (Mm03023971_m1), *Bmpr2* (Mm00432134_m1), *Acvr1a* (Mm00431657_m1), *Acvr1b* (Mm00431664_m1), *Noggin* (Mm01297833_s1), *Smad-4* (Mm03023996_m1), *Smad-6*(Mm00484738_m1).

Western Blotting

Muscle or cell lysates were prepared in 25 mM Tris pH 7.4, 95 mM NaCl, 1 mM EDTA, 1 mM EGTA, 1% SDS, 10% Protease Inhibitor Cocktail (P8340, Sigma-Aldrich,

St. Louis, MO), 5 mM NaF, 2 mM Na_3VO_4, 2.5 mM $Na_4P_2O_7$. Protein analysis by western blotting was done as described previously[10], except 40 μg of total lysate per sample was used. The antibody to p-Smad1/5/8 (13820S, Cell Signaling Technology, MA) was used at 1:1000. The antibody to T-Smad1/5/8 (NB100-56656SS, Novus Biologicals, CO) was used at 1:1000.

Cell culture, ERK1/2 inhibition and BMP activation

C2C12 myoblasts were grown on Matrigel in DMEM, 10% FBS, 0.5% chick embryo extract, and 50 μg/ml of gentamicin. Sol8 myoblasts were often grown with the above medium but using 15% FBS. At confluence, myoblasts were switched into differentiation medium (C2DM) containing DMEM, 2.5% horse serum, and 50 μg/ml of gentamicin. C2c12 or Sol8 cells were grown and differentiated in a humidified incubator at 37 °C, 5%CO_2. Myotubes were used for experiments after full differentiation in C2DM. For inhibition of ERK1/2 and activation of BMP signaling, myotubes were serum-deprived for 4 hours with DMEM containing 0.1% BSA (serum deprivation medium, SDM) and then incubated in 20ng/ml of BMP4 (314-BP R&D systems, MN), which was dissolved in SDM, for 1 hour. Next, ERK1/2 inhibitor, U0126 (U120, Millipore Sigma, MO) was diluted with DMSO and added to reach the concentration of 10 μM for a time series (10mins, 1h, 2hs and 4 hs) until cells were subject to protein extraction.

3.6 References

1. Cassano, M., Quattrocelli, M., Crippa, S., Perini, I., Ronzoni, F., & Sampaolesi, M. (2009). Cellular mechanisms and local progenitor activation to regulate skeletal muscle

mass. Journal of Muscle Research and Cell Motility, 30(7-8), 243-253. doi:10.1007/s10974-010-9204-y

2. Sacheck, J. M. (2004). IGF-I stimulates muscle growth by suppressing protein breakdown and expression of atrophy-related ubiquitin ligases, atrogin-1 and MuRF1. AJP: Endocrinology and Metabolism, 287(4). doi:10.1152/ajpendo.00073.2004

3. Kitajima, Y., & Suzuki, N. (2017). Role of the ubiquitin-proteasome pathway in skeletal muscle. The Plasticity of Skeletal Muscle, 37-54. doi:10.1007/978-981-10-3292-9_2

4. Bonaldo, P., & Sandri, M. (2012). Cellular and molecular mechanisms of muscle atrophy. Disease Models & Mechanisms, 6(1), 25-39. doi:10.1242/dmm.010389

5. Winbanks, C. E., Chen, J. L., Qian, H., Liu, Y., Bernardo, B. C., Beyer, C., . . . Gregorevic, P. (2013). The bone morphogenetic protein axis is a positive regulator of skeletal muscle mass. The Journal of Experimental Medicine, 210(12). doi:10.1084/jem.21012oia54

6. Moresi, V., Williams, A. H., Meadows, E., Flynn, J. M., Potthoff, M. J., Mcanally, J., . . . Olson, E. N. (2010). Myogenin and class II HDACs control neurogenic muscle atrophy by inducing E3 ubiquitin ligases. Cell, 143(1), 35-45. doi:10.1016/j.cell.2010.09.004

7. Massague, J. (2005). Smad transcription factors. Genes & Development, 19(23), 2783-2810. doi:10.1101/gad.1350705

8. Sartori, R., Schirwis, E., Blaauw, B., Bortolanza, S., Zhao, J., Enzo, E., . . . Sandri, M. (2013). BMP signaling controls muscle mass. Nature Genetics, 45(11), 1309-1318. doi:10.1038/ng.2772

9. Winbanks, C. E., Chen, J. L., Qian, H., Liu, Y., Bernardo, B. C., Beyer, C., . . . Gregorevic, P. (2013). The bone morphogenetic protein axis is a positive regulator of skeletal muscle mass. The Journal of Cell Biology, 203(2), 345-357. doi:10.1083/jcb.201211134

10. O'Keeffe, G. W., Dockery, P., & Sullivan, A. M. (2004). Effects of growth/differentiation factor 5 on the survival and morphology of embryonic rat midbrain dopaminergic neurones in vitro. Journal of Neurocytology, 33(5), 479-488. doi:10.1007/s11068-004-0511-y

11. Buxton, P., Edwards, C., Archer, C. W., & Francis-West, P. (2001). Growth/differentiation Factor-5 (GDF-5) and skeletal development. The Journal of Bone and Joint Surgery-American Volume, 83. doi:10.2106/00004623-200100001-00004

12. Francis-West, P. H., Parish, J., Lee, K., & Archer, C. W. (1999). BMP/GDF-signalling interactions during synovial joint development. Cell and Tissue Research, 296(1), 111-119. doi:10.1007/s004410051272

13. Macpherson, P. C., Farshi, P., & Goldman, D. (2015). Dach2-Hdac9 signaling regulates reinnervation of muscle endplates. Development, 142(23), 4038-4048. doi:10.1242/dev.12567

14. Wang, S., Seaberg, B., Paez-Colasante, X., & Rimer, M. (2016). Defective acetylcholine receptor subunit switch precedes atrophy of slow-twitch skeletal muscle

fibers lacking ERK1/2 kinases in soleus muscle. Scientific Reports, 6(1). doi:10.1038/srep3874515.

15. Seaberg, B., Henslee, G., Wang, S., Paez-Colasante, X., Landreth, G. E., & Rimer, M. (2015). Muscle-derived extracellular signal-regulated kinases 1 and 2 are required for the maintenance of adult myofibers and their Neuromuscular Junctions. Molecular and Cellular Biology, 35(7), 1238-1253. doi:10.1128/mcb.01071-14

16. Massague, J. (2005). Smad transcription factors. Genes & Development, 19(23), 2783-2810. doi:10.1101/gad.1350705

17. Nickel, J., Kotzsch, A., Sebald, W., & Mueller, T. D. (2005). A single residue of GDF-5 defines binding specificity to BMP receptor IB. Journal of Molecular Biology, 349(5), 933-947. doi:10.1016/j.jmb.2005.04.015

18. Storm, E. E., Huynh, T. V., Copeland, N. G., Jenkins, N. A., Kingsley, D. M., & Lee, S. (1994). Limb alterations in brachypodism mice due to mutations in a new member of the TGFβ-superfamily. Nature, 368(6472), 639-643. doi:10.1038/368639a0

19. Krause, C., Guzman, A., & Knaus, P. (2011). Noggin. The International Journal of Biochemistry & Cell Biology, 43(4), 478-481. doi:10.1016/j.biocel.2011.01.007

20. Roelen, B. A., Cohen, O. S., Raychowdhury, M. K., Chadee, D. N., Zhang, Y., Kyriakis, J. M., . . . Lin, H. Y. (2003). Phosphorylation of threonine 276 in Smad4 is involved in transforming growth factor- -induced nuclear accumulation. AJP: Cell Physiology, 285(4). doi:10.1152/ajpcell.00053.2003

21. Hayashi, Hidetoshi, et al. “The MAD-related protein Smad7 associates with the TGFβ receptor and functions as an antagonist of TGFβ signaling.” Cell, vol. 89, no. 7, 1997, pp. 1165–1173., doi:10.1016/s0092-8674(00)80303-7.

22. Miyazono, K., and K. Miyazawa. “Id: a target of BMP signaling.” Science Signaling, vol. 2002, no. 151, 2002, doi:10.1126/scisignal.1512002pe40.

23. Daubas, P., Klarsfeld, A., Garner, I., Pinset, C., Cox, R., & Buckingham, M. (1988). Functional activity of the two promoters of the myosin alkali light chain gene in primary muscle cell cultures: comparison with other muscle gene promoters and other culture systems. Nucleic Acids Research, 16(4), 1251-1271. doi:10.1093/nar/16.4.1251

24. The protein Id: a negative regulator of helix-loop-helix DNA binding proteins. (1990). Trends in Genetics, 6, 174. doi:10.1016/0168-9525(90)90161-x

25. Sapkota, G., Alarcón, C., Spagnoli, F. M., Brivanlou, A. H., & Massagué, J. (2007). Balancing BMP signaling through integrated inputs into the Smad1 linker. Molecular Cell, 25(3), 441-454. doi:10.1016/j.molcel.2007.01.006

26. Eivers, E., Fuentealba, L. C., & Robertis, E. D. (2008). Integrating positional information at the level of Smad1/5/8. Current Opinion in Genetics & Development, 18(4), 304-310. doi:10.1016/j.gde.2008.06.001

27. Massagu, J., Kretzschmar, M., & Doody, J. (1997). Opposing BMP and EGF signalling pathways converge on. Nature, 389(6651), 618-622. doi:10.1038/39348

28. Wang, L., Liu, Y., Hao, R., Chen, L., Chang, Z., Wang, H., . . . Wu, J. (2011). Molecular mechanism of the negative regulation of Smad1/5 protein by carboxyl

terminus of Hsc70-interacting protein (CHIP). Journal of Biological Chemistry, 286(18), 15883-15894. doi:10.1074/jbc.m110.201814

29. Blenis, J. (1993). Signal transduction via the MAP kinases: proceed at your own RSK. Proceedings of the National Academy of Sciences, 90(13), 5889-5892. doi:10.1073/pnas.90.13.5889

30. Deak, M. (1998). Mitogen- and stress-activated protein kinase-1 (MSK1) is directly activated by MAPK and SAPK2/p38, and may mediate activationofCREB. The EMBO Journal, 17(15), 4426-4441. doi:10.1093/emboj/17.15.4426

31. Noguchi, K., Kitanaka, C., Yamana, H., Kokubu, A., Mochizuki, T., & Kuchino, Y. (1999). Regulation of c-Myc through Phosphorylation at Ser-62 and Ser-71 by c-Jun N-Terminal Kinase. Journal of Biological Chemistry, 274(46), 32580-32587. doi:10.1074/jbc.274.46.32580

32. Database, G. H. (n.d.). BMPR1B Gene (Protein Coding). Retrieved February 07, 2018, from http://www.genecards.org/cgi-bin/carddisp.pl?gene=BMPR1B

33. Radomska, H. S., Bassères, D. S., Zheng, R., Zhang, P., Dayaram, T., Yamamoto, Y., . . . Tenen, D. G. (2006). Block of C/EBPα function by phosphorylation in acute myeloid leukemia with FLT3 activating mutations. The Journal of Experimental Medicine, 203(2), 371-381. doi:10.1084/jem.20052242

34. Livak, K. J., & Schmittgen, T. D. (2001). Analysis of relative gene expression data using real-time quantitative PCR and the $2^{-\Delta\Delta CT}$ Method. Methods, 25(4), 402-408. doi:10.1006/meth.2001.1262

CHAPTER IV

CONCLUSION AND FUTURE STUDY

4.1 Contents

In this chapter, I list some conclusions that result from a previous study[1] and from chapters II and III. I also propose potential future experiments to further test these conclusions.

It has been reported that ERK1/2 phosphorylation level in myofibers is quite sensitive to the firing pattern of motor neurons[2]. Schiaffino and colleagues showed that a 20Hz low-frequency stimulation, which mimics the firing pattern of slow motor neurons, could induce the highest ERK1/2 phosphorylation level in denervated rat SOL[3]. This significantly increased ERK activity is thought to promote the transition of fast twitch fibers to slow twitch fibers[3]. In chapter II, we observed that the synaptic AchR γ/ε subunit switch was somehow delayed (AChRγ should disappear by 3 weeks after birth in SOL[2]), mostly on type 1 muscle fibers. According to these observations, I may propose that increased ERK phosphorylation in slow fibers is also required for meeting the needs of higher transcriptional activity of AChRε. However, we still do not know whether this increase of ERK phosphorylation occur in the entire fiber or mainly in a specific location (e.g. sub-synaptic region). High resolution microscopy might be used to visualize and localize ERK1/2 phosphorylation when the denervated SOL is given low frequency stimulation. Why slow fibers require higher expression of AChRε than fast fibers? Perhaps, the expression of AChRγ is sustained in slow fibers, therefore, higher AChRε expression is needed to complete the replacement of AChRγ for AChRε. This

viewpoint is supported by three facts: (1) The myogenic factor Myogenin has been shown to regulate AChRγ expression through E-box[4]. (2) Myogenin is selectively expressed in slow-twitch muscles[5]. (3) AChRγ was still visible at NMJ in 3-week-old SOL while AChRγ was totally disappeared as early as postnatal 17 days in EDL, TA, and STN[2]. The γ-containing AChR has longer open time and may increase local calcium influx, possibly leading to endplate degeneration and slow-channel-like myasthenia[6]. In addition, the γ-containing AChR is less stable than the ε-containing AChR[7]. This delayed AchR γ/ε subunit switch might lead to type1 myofiber denervation in mutant SOL after postnatal 3 weeks. This hypothesis is a little bit controversial to the observation in *Chrne*$^{-/-}$ mice in which only very mild sign of partial denervation was found[8, 9]. Therefore, processes other than the defective γ /ε -AChR switch also contribute to denervation of DKO SOL. We observed significantly lower number of fibers between 3-6 weeks. This huge muscle fiber loss may cause the remodeling of motor unit size, together with the defective γ /ε -AChR switch, eventually leading to denervation of the whole muscle. The fiber loss does not seem to be the reason for the severe atrophic phenotype in type 1 fibers, because fiber loss is not fiber-type specific. The dysregulation of the mitochondrial function, especially the reduced expression of PGC1-α (the key regulator of mitochondrial biogenesis[10]) in SOL but not in TA, could partially explain why SOL undergo more severe atrophy than TA. Further experiments need focus on the signaling that links ERK1/2 and PGC1-α. Those experiments are critical, because no ERK muscle specific-substrate has been identified until now[11]. After denervation, BMP ligands, Gdf5 and 6, are largely induced[12] through Dach2-Hdac9 signaling[13]. The

subsequently increased Smad1/5/8 translocate into the nucleus to regulate BMP signaling targeted genes. The regulation of these genes will eventually lead to an anti-atrophic effect by interacting with Akt-PI3K pathway and inhibiting atrogenes, including atrogin1 and MuRF1[14]. In ERK1/2 mutant SOL, expression of GDF5 and 6 was still induced as that has been observed in nerve-cut induced denervation of normal muscle[14]. However, the phosphorylation level of Smad1/5/8 did not change perhaps because GDF5/6-favored BMP type 1 receptor had reduced expression. In addition, ERK1/2 deletion prevented the expression of the negative regulators *Noggin* and *Smad-6* from decreasing, leading to even less active BMP signaling. Therefore, BMP signaling cannot protect DKO muscle from atrophy. In 2016, Yilmaz et al. reported that the muscle-specific kinase, Musk is able to promote BMP4 induced-BMP type I activation in a Musk kinase activity independent manner[15]. In addition, in myotubes, Musk stimulated the BMP4-induced expression of a large set of genes, including the slow muscle-enriched genes myosin heavy chain 15 (Myh15). This experiment suggests the transcription of fiber type-specific genes can be regulated through BMP signaling. Indeed, the ERK1/2 dependent transcription of a specific type of *myh* gene is regulated by BMP signaling in smooth muscle[16]. Although deletion of GDF5 alone is sufficient to drive worse muscle atrophy in TA and EDL[12] (they have very few type 1 fibers), it is possible that ERK1/2 regulate the expression of some specific BMP components in type 1 fibers. Our Real-Time PCR samples were collected from the entire SOL. If the hypothesis above is true, samples collected from type 1 fibers might yield a larger

reduction of *bmpr1b*. These two hypotheses suggest deactivation of BMP signaling in mutant SOL could potentially contribute to the severe wasting of type 1 fibers.

Since a defective AChR γ/ε subunit switch was observed in our ERK1/2 DKO SOL, one of the future studies is to research for molecules that regulate AChR γ/ε–expression at NMJ. Although the hypothesis of the Neuregulin-ERK-GABP-AchRε axis[17-19] has been proposed, several pieces of evidence argue against a major role for GABP in the regulation of AChRε. Firstly, GABP is expressed broadly throughout muscle fibers with only a minor enrichment in the sub-synaptic sites[20]. Secondly, conditional knockout of GABPα in skeletal muscles did not lead to significant muscle weakness and atrophy[21, 22]. In addition, no changes of sub-synaptic gene expression were detected in these animals[21]. Lastly, only minor morphological abnormality of AChR clusters was observed[22]. These recent findings suggest that other ETS transcription factors function in the regulation of sub-synaptic gene expression in skeletal muscles. It has been reported that Etv-5 (a.k.a. Erm), an ETS-related transcriptional factor, is selectively expressed in sub-synaptic nuclei and required for transcriptional regulation of many genes normally expressed sub-synaptically, including *Chrne* [23]. Genetic knockout of Etv-5 in mice induces muscle weakness, neuromuscular transmission deficits and fragmentation at NMJs, and short lifespan, which resemble the genotype of ERK1/2 DKO mice. In addition, ERK 1/2 phosphorylation is required for Etv-5 expression in non-muscle cells[24]. Our preliminary data showed that inhibition of ERK1/2's kinase activity in C2C12 cells decreased the mRNA level of Etv-5 (A1.). Besides, the mRNA level of Etv-5 was reduced in ERK1/2 DKO SOL at 9 weeks (A2.). These two

experiments suggest ERK1/2's kinase activity is required for Etv-5 transcriptional regulation in skeletal myofibers. Moreover, it has been reported ERK1/2 is able to phosphorylate Etv-5 directly and regulate its DNA binding activity in other systems[25-27]. However, it is still unknown whether this is true in skeletal muscle, especially for the expression of *Chrne*. Future studies need to focus on how ERK1/2 regulate *Evt-5* transcription and whether direct phosphorylation of Etv-5 by ERK1/2 is necessary for transcription of *Chrne* in skeletal muscle.

For the BMP part, one unaddressed question is whether ERK1/2-regulated BMP activation after denervation only occurs in SOL. To test this, we could denervate ERK1/2 DKO TA by transecting the sciatic nerve and measure levels and activity of BMP signaling components. The reduced *Bmpr1b* expression and unchanged *Noggin* and *Smad6* expressions seem the main reason for inactive BMP signaling, however, further experiments need to investigate whether overexpression of these genes could rescue the phenotype in mutant SOL.

4.2 References

1. Seaberg, B., Henslee, G., Wang, S., Paez-Colasante, X., Landreth, G. E., & Rimer, M. (2015). Muscle-derived extracellular signal-regulated kinases 1 and 2 are required for the maintenance of adult myofibers and their neuromuscular junctions. Molecular and Cellular Biology, 35(7), 1238-1253. doi:10.1128/mcb.01071-14

2. Missias, A. C., Chu, G. C., Klocke, B. J., Sanes, J. R., & Merlie, J. P. (1996). Maturation of the acetylcholine receptor in skeletal muscle: regulation of the AChR γ-to-ϵ switch. Developmental Biology, 179(1), 223-238. doi:10.1006/dbio.1996.0253

3. Murgia, M., Serrano, A. L., Calabria, E., Pallafacchina, G., Lømo, T., & Schiaffino, S. (2000). Ras is involved in nerve-activity-dependent regulation of muscle genes. Nature Cell Biology, 2(3), 142-147. doi:10.1038/35004013

4. Jia, H., Tsay, H., & Schmidt, J. (1992). Analysis of binding and activating functions of the chick muscle acetylcholine receptor γ-subunit upstream sequence. Cellular and Molecular Neurobiology, 12(3), 241-258. doi:10.1007/bf00712929

5. Nicolas, N., Gallien, C. L., & Chanoine, C. (1996). Analysis of MyoD, myogenin, and muscle-specific gene mRNAs in regenerating Xenopus skeletal muscle. Developmental Dynamics, 207(1), 100-108. doi:10.1002/(sici)1097-0177(199609)207:1<100::aid-aja9>3.0.co;2-m

6. Mishina, M., Takai, T., Imoto, K., Noda, M., Takahashi, T., Numa, S., . . . Sakmann, B. (1986). Molecular distinction between fetal and adult forms of muscle acetylcholine receptor. Nature, 321(6068), 406-411. doi:10.1038/321406a0

7. Salpeter, M. (1985). Nicotinic acetylcholine receptors in vertebrate muscle: Properties, distribution and neural control. Progress in Neurobiology, 25(4), 297-325. doi:10.1016/0301-0082(85)90018-8

8. Witzemann, V., Schwarz, H., Koenen, M., Berberich, C., Villarroel, A., Wernig, A., . . . Sakmann, B. (1996). Acetylcholine receptor -subunit deletion causes muscle weakness and atrophy in juvenile and adult mice. Proceedings of the National Academy of Sciences, 93(23), 13286-13291. doi:10.1073/pnas.93.23.13286

9. Missias, A., Mudd, J., Cunningham, J., Steinbach, J., Merlie, J., & Sanes, J. (1997). Deficient development and maintenance of postsynaptic specializations in mutant mice lacking an ‘adult’ acetylcholine receptor subunit. Development, 124, 5075-5086.

10. Wu, Z., Puigserver, P., Andersson, U., Zhang, C., Adelmant, G., Mootha, V., . . . Spiegelman, B. M. (1999). Mechanisms controlling mitochondrial biogenesis and respiration through the thermogenic coactivator PGC-1. Cell, 98(1), 115-124. doi:10.1016/s0092-8674(00)80611-x

11. Knight, J. D., & Kothary, R. (2011). The myogenic kinome: protein kinases critical to mammalian skeletal myogenesis. Skeletal Muscle, 1(1), 29. doi:10.1186/2044-5040-1-29

12. Sartori, R., Schirwis, E., Blaauw, B., Bortolanza, S., Zhao, J., Enzo, E., . . . Sandri, M. (2013). BMP signaling controls muscle mass. Nature Genetics, 45(11), 1309-1318. doi:10.1038/ng.2772

13. Macpherson, P. C., Farshi, P., & Goldman, D. (2015). Dach2-Hdac9 signaling regulates reinnervation of muscle endplates. Development, 142(23), 4038-4048. doi:10.1242/dev.125674

14. Sartori, R., Gregorevic, P., & Sandri, M. (2014). TGFβ and BMP signaling in skeletal muscle: potential significance for muscle-related disease. Trends in Endocrinology & Metabolism, 25(9), 464-471. doi:10.1016/j.tem.2014.06.002

15. Yilmaz, A., Kattamuri, C., Ozdeslik, R. N., Schmiedel, C., Mentzer, S., Schorl, C., . . . Fallon, J. R. (2016). MuSK is a BMP co-receptor that shapes BMP responses and

calcium signaling in muscle cells. Science Signaling, 9(444). doi:10.1126/scisignal.aaf0890

16. Zhang, M., Yang, M., Liu, L., Lau, W. B., Gao, H., Xin, M., . . . Liu, J. (2014). BMP-2 overexpression augments vascular smooth muscle cell motility by upregulating myosin Va via Erk signaling. Oxidative Medicine and Cellular Longevity, 2014, 1-11. doi:10.1155/2014/294150

17. Fu, A. K., Fu, W., Cheung, J., Tsim, K. W., Ip, F. C., Wang, J. H., & Ip, N. Y. (2001). Cdk5 is involved in neuregulin-induced AChR expression at the neuromuscular junction. Nature Neuroscience, 4(4), 374-381. doi:10.1038/86019

18. Si, J., Wang, Q., & Mei, L. (1999). Essential roles of c-JUN and c-JUN N-terminal kinase (JNK) in neuregulin-increased expression of the acetylcholine receptor epsilon-subunit. The Journal of Neuroscience, 19(19), 8498-8508.

19. Fromm, L., & Burden, S. J. (2001). Neuregulin-1-stimulated phosphorylation of GABP in skeletal muscle cells†. Biochemistry, 40(17), 5306-5312. doi:10.1021/bi002649m

20. Schaeffer, L. (1998). Implication of a multisubunit Ets-related transcription factor in synaptic expression of the nicotinic acetylcholine receptor. The EMBO Journal, 17(11), 3078-3090. doi:10.1093/emboj/17.11.3078

21. Jaworski, A., Smith, C. L., & Burden, S. J. (2007). GA-binding protein is dispensable for neuromuscular synapse formation and synapse-specific gene expression. Molecular and Cellular Biology, 27(13), 5040-5046. doi:10.1128/mcb.02228-06

22. Oleary, D. A., Noakes, P. G., Lavidis, N. A., Kola, I., Hertzog, P. J., & Ristevski, S. (2007). Targeting of the ETS factor GABP disrupts neuromuscular junction synaptic function. Molecular and Cellular Biology, 27(9), 3470-3480. doi:10.1128/mcb.00659-06

23. Hippenmeyer, S., Huber, R. M., Ladle, D. R., Murphy, K., & Arber, S. (2007). ETS transcription factor Erm controls subsynaptic gene expression in skeletal muscles. Neuron, 55(5), 726-740. doi:10.1016/j.neuron.2007.07.028

24. Oh, S., Shin, S., & Janknecht, R. (2012). ETV1, 4 and 5: An oncogenic subfamily of ETS transcription factors. Biochimica et Biophysica Acta (BBA) - Reviews on Cancer, 1826(1), 1-12. doi:10.1016/j.bbcan.2012.02.002

25. Znosko, W. A., Yu, S., Thomas, K., Molina, G. A., Li, C., Tsang, W., . . . Tsang, M. (2010). Overlapping functions of Pea3 ETS transcription factors in FGF signaling during zebrafish development. Developmental Biology, 342(1), 11-25. doi:10.1016/j.ydbio.2010.03.011

26. Janknecht , R., Monté, D., Baert, J. L., & De Launoit, Y. (1996). The ETS-related transcription factor ERM is a nuclear target of signaling cascades involving MAPK and PKA. Oncogene, 13(8), 1745-1754.

27. Li, X., Newbern, J. M., Wu, Y., Morgan-Smith, M., Zhong, J., Charron, J., & Snider, W. D. (2012). MEK is a key regulator of gliogenesis in the developing brain. Neuron, 75(6), 1035-1050. doi:10.1016/j.neuron.2012.08.031

APPENDIX

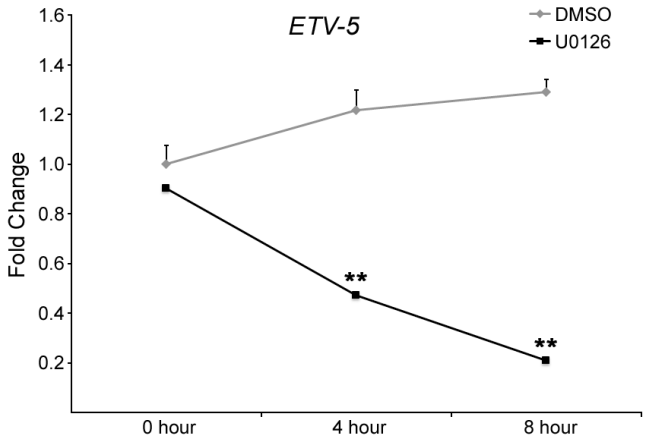

Figure A1. ERK activation regulates *Etv-5* expression *in vitro*. C2C12 myotubes were treated with either 10μm U0126 in DMSO or DMSO alone and total RNA was isolated at the indicated times thereafter. Real-time PCR for Etv-5 mRNA was done as above. Graphed data is normalized to the untreated control at time 0 for each gene. N=5 dishes (time 0), n=4 dishes (4 and 8 h). *, $p < 0.05$; **, $p < 0.01$. (Data generated by Bonnie Seaberg in the Rimer Lab)

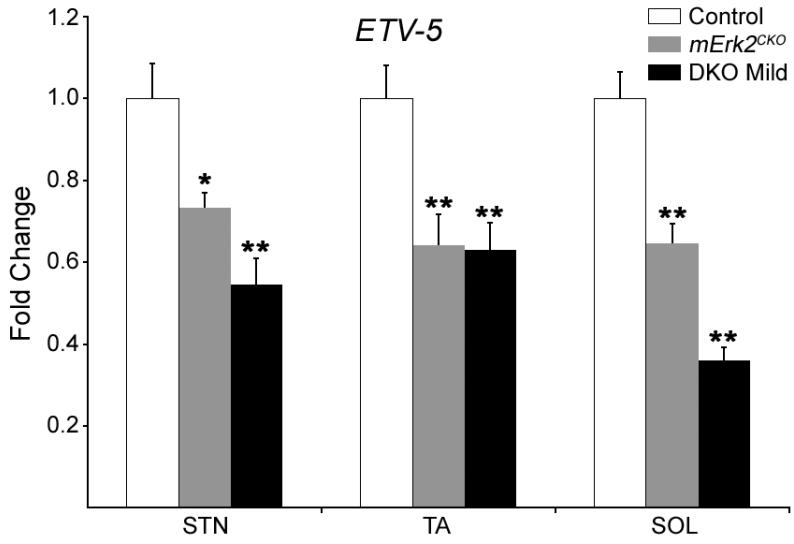

Figure A2. Reduction of *Etv-5* mRNA in mErk2^{CKO} and DKO muscle by real-time PCR. *Chrne* mRNA levels in the mErk2^{CKO} and DKO SOL were 0.62 and 0.18-fold control levels, respectively (data not shown). N= 5-6, per muscle/genotype. *, $p < 0.05$; **, $p < 0.01$. (Data generated by Bonnie Seaberg in the Rimer Lab).